

Electroproduction of $f_0(980)$ and $f_2(1270)$ off the proton with the CLAS detector

Brice Garillon, Ph.D.

1. Introduction and physics motivations
2. Experimental setup
3. Cross sections for $f_0(980)$ and $f_2(1270)$ electroproduction
4. Moments Analysis of 2-pion electroproduction
5. Conclusions

1.Introduction and physics motivations

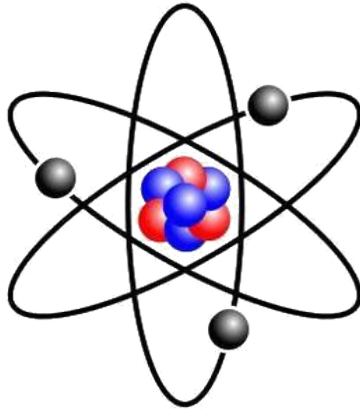
2.Experimental setup

3.Cross section for $f_0(980)$ and $f_2(1270)$

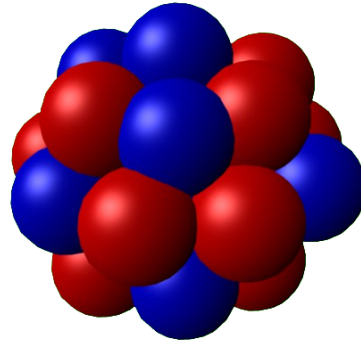
4.Moments Analysis of 2-pion electroproduction

5.Conclusions

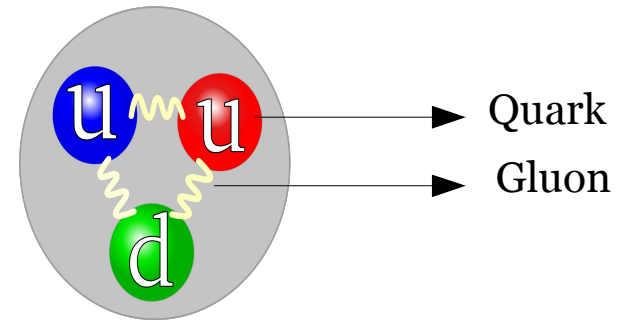
Visible matter at subatomic scale



Atom
 10^{-10} m



Nucleus
 10^{-11} m



Nucleon
 10^{-16} m

Parton
 10^{-18} m

- **Strong interaction** : Interaction between **quarks** and **gluons**.
- In the Standard Model, the strong interaction is described by Quantum Chromodynamics (QCD).
 - Each quark or gluon carry a colour charge (**r,g,b**).
 - **Hadron** : bound state of quarks and gluons, colour singlet.
- To this day , QCD cannot be solved analytically for bound states.
- **Quark model** (Gell-Mann, Zweig 1963-64)
 - One half spin = **Baryon** = qqq
 - Integer spin = **Meson** = **qq**

The $f_0(980)$ and $f_2(1270)$

	$f_0(980)$	$f_2(1270)$
J^{PC}	0^{++} (scalar)	2^{++} (tensor)
Isospin	0	0
Mass (MeV)	990 ± 20	1275 ± 1.2
FWHM (MeV)	40-100	185.1 ± 3
Main decay channel	$\pi^+\pi^-$	$\pi^+\pi^-$

$f_0(980)$

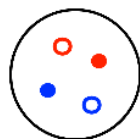
Scalars : 5 observed $I=0$ states vs. 2 predicted (2 nonets) in the quark model.

→ Some states are different from $q\bar{q}$.

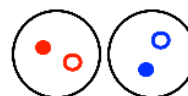
$\Phi \rightarrow \gamma f_0 \rightarrow \gamma \pi^0 \pi^0$: Important strangeness content.

$f_0(980)$: candidate for an **exotic state**¹ :

- Tetraquark² ($q\bar{q}q\bar{q}$)



- $K\bar{K}$ Molecule³



$f_2(1270)$

→ Compatible with quark model predictions.

→ Dynamically generated by vector meson-vector meson interactions⁴ ?



• Studies from πN scattering, e^+e^- and $p\bar{p}$ collisions, photoproduction γp ⁵.

¹ A. Donnachie, Yu.S. Kalashnikova, arXiv:0806.3698v1

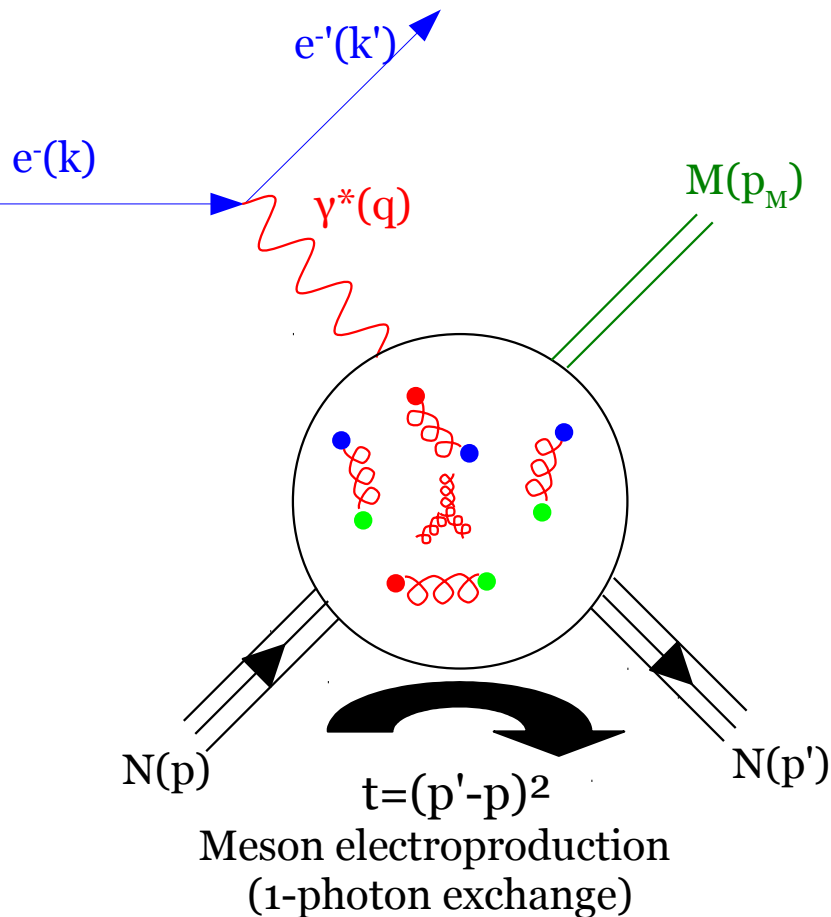
⁴ E. Oset *et al*, Eur. Phys. Journal A, 44, 2, p.305-311

² R.L. Jaffe, Phys. Rev. D 15, 267 (1977)

⁵ M. Battaglieri *et al*, Phys.Rev. D80 (2009) 072005

³ T. Barnes, Phys. Lett. B 165, 434 (1985)

Meson electroproduction



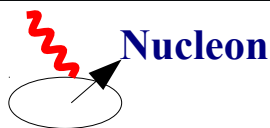
- The electron interacts with the nucleon via an exchange of a **virtual photon γ^***
 → Perturbative QED
 $(\alpha_{EM} = 1/137 \ll 1)$
- **$Q^2 = -(\mathbf{e}' - \mathbf{e})^2$ Virtuality**
 → $Q^2 = 0$: Photoproduction
 → Compton Wavelength : $\lambda \propto 1/\sqrt{Q^2}$
 Spatial resolution on the probed nucleon

**Cross sections for
 exclusive $\gamma^* p \rightarrow p f_0/f_2$
 have never been measured!**

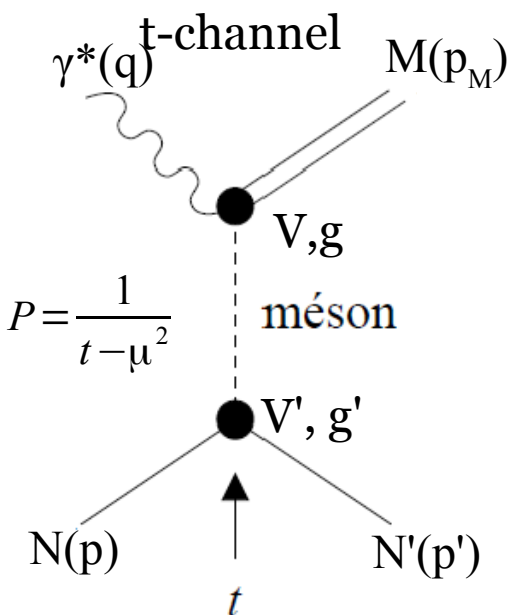
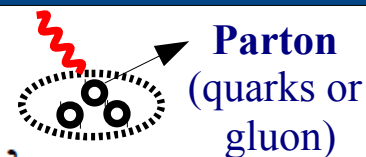
- **Q^2 and t -dependences might give hints on the nature of f_0 and f_2 .**

$\gamma^*N \rightarrow N'M$ mechanisms

Low Q^2
Particle exchange



High Q^2
DVMP

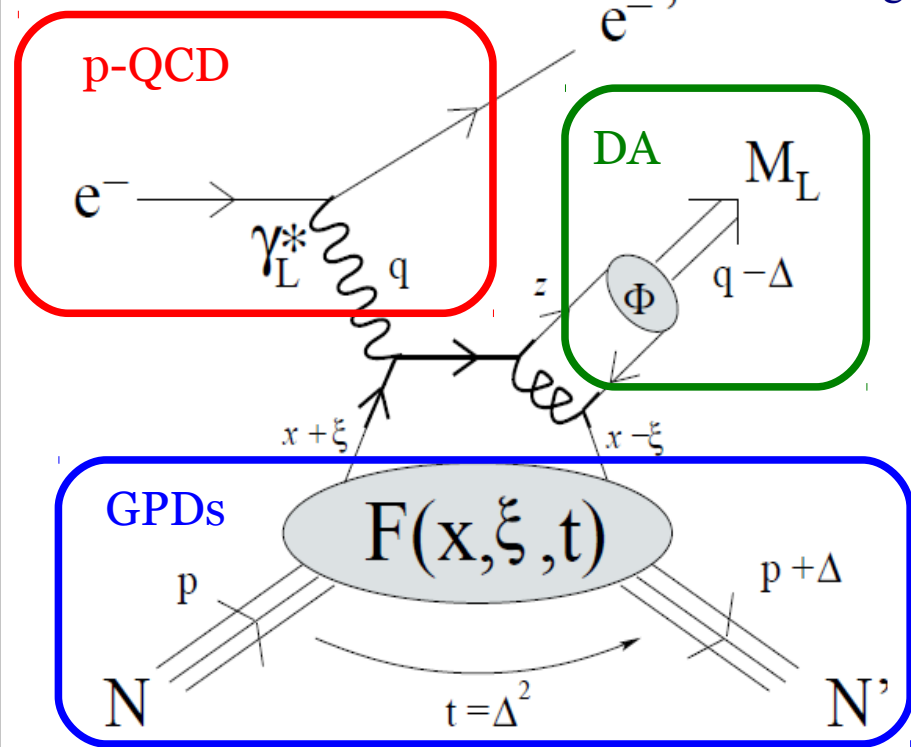


Mandelstam variables

$$t = (q - p_M)^2$$

$$u = (q - p')^2$$

$$s = (q + p)^2$$



($Q^2, v \rightarrow \infty$ et x_B constants), $t \ll Q^2$
Longitudinally polarized photon.

• **t channel exchange dominant** for the f_0 and f_2 production.

• Amplitude :
 $A \sim gVPg'V'$
P : Propagator.
V, V' : Vertices
g, g' : Coupling constants

- **Factorisation theorem :**
 - **“Hard” scattering**
 - **Distribution Amplitude (DA)**
 - **4 Generalized Parton Distributions (GPDs)** H, E, \tilde{H} et $\tilde{E}(x, \xi, t)$
- Correlation between the transverse position of a quark and its longitudinal momentum fraction.

The exclusive $ep \rightarrow ep\pi^+\pi^-$ final state

- The f_0 and f_2 are analysed in their main decay channel :

$f_0 \rightarrow \pi^+\pi^-$ (dominant) and $f_2 \rightarrow \pi^+\pi^-$ (85%)

- The exclusive final state $e'p'\pi^+\pi^-$ comes from several processes :

$ep \rightarrow e'p' M$

└► $\pi^+\pi^-$

$ep \rightarrow e' N^* \pi^{+/-}$

└► $p'\pi^{+/-}$

$ep \rightarrow e'p'\pi^+\pi^-$

The exclusive $ep \rightarrow ep\pi^+\pi^-$ final state

- The f_0 and f_2 are analysed in their main decay channel :

$$f_0 \rightarrow \pi^+\pi^- \text{ (dominant) and } f_2 \rightarrow \pi^+\pi^- \text{ (85\%)}$$

- The exclusive final state $e'p'\pi^+\pi^-$ comes from several processes :

$$ep \rightarrow e'p' M$$

$$\downarrow \pi^+\pi^-$$

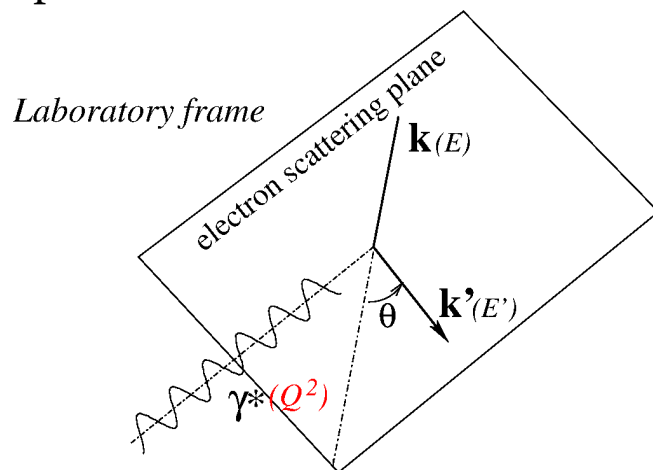
$$ep \rightarrow e' N^* \pi^{+/-}$$

$$\downarrow p'\pi^{+/-}$$

$$ep \rightarrow e'p'\pi^+\pi^-$$

The unpolarized cross section is described by 7 independent kinematic variables :

- Q^2 Virtuality of the virtual photon (γ^*).
 $\mathbf{v} = (\mathbf{E} - \mathbf{E}')$



The exclusive $ep \rightarrow ep\pi^+\pi^-$ final state

- The f_0 and f_2 are analysed in their main decay channel :

$$f_0 \rightarrow \pi^+\pi^- \text{ (dominant) and } f_2 \rightarrow \pi^+\pi^- \text{ (85\%)}$$

- The exclusive final state $e'p'\pi^+\pi^-$ comes from several processes :

$$ep \rightarrow e'p' M$$

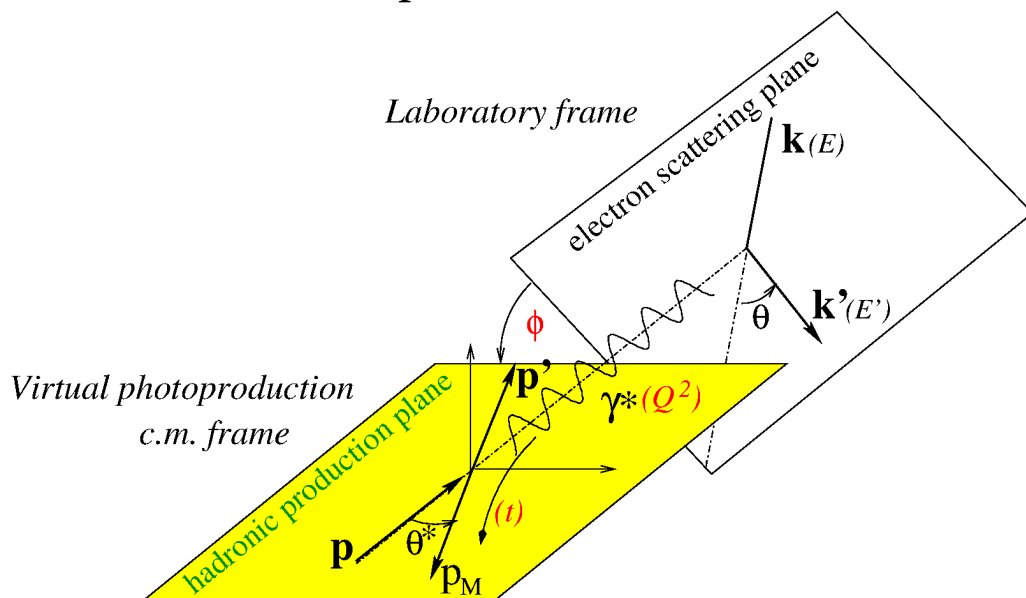
$$\downarrow \pi^+\pi^-$$

$$ep \rightarrow e' N^* \pi^{+/-}$$

$$\downarrow p'\pi^{+/-}$$

$$ep \rightarrow e'p'\pi^+\pi^-$$

The unpolarized cross section is described by 7 independent kinematic variables :



Q^2 Virtuality of the virtual photon (γ^*).
 $\mathbf{v} = (\mathbf{E} - \mathbf{E}')$

$\mathbf{x}_B = Q^2 / 2M_p \mathbf{v}$ Bjorken variable
 ($\sim 1/W$, energy of (γ^*, p) center of mass frame)

\mathbf{t} Momentum transfer to the nucleon

Φ Azimuthal angle between the leptonic plane (γ^*, e') and the hadronic plane (γ^*, p').

The exclusive $ep \rightarrow ep\pi^+\pi^-$ final state

- The f_0 and f_2 are analysed in their main decay channel :

$$f_0 \rightarrow \pi^+\pi^- \text{ (dominant) and } f_2 \rightarrow \pi^+\pi^- \text{ (85\%)}$$

- The exclusive final state $e'p'\pi^+\pi^-$ comes from several processes :

$$ep \rightarrow e'p' M$$

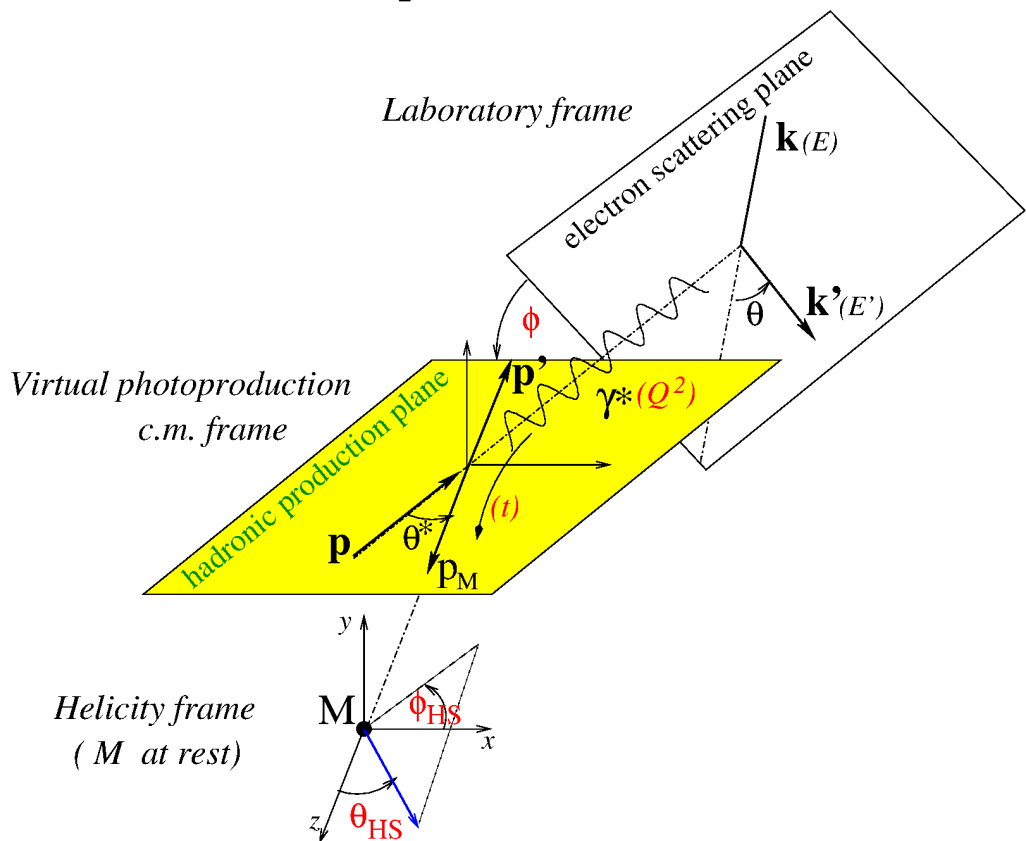
$$\downarrow \pi^+\pi^-$$

$$ep \rightarrow e' N^* \pi^{+/-}$$

$$\downarrow p'\pi^{+/-}$$

$$ep \rightarrow e'p'\pi^+\pi^-$$

The unpolarized cross section is described by 7 independent kinematic variables :



Q^2 Virtuality of the virtual photon (γ^*).
 $\mathbf{v} = (\mathbf{E} - \mathbf{E}')$

$\mathbf{x}_B = Q^2 / 2M_p \mathbf{v}$ Bjorken variable
 ($\sim 1/W$, energy of (γ^*, p) center of mass frame)

\mathbf{t} Momentum transfer to the nucleon

Φ Azimuthal angle between the leptonic plane (γ^*, e') and the hadronic plane (γ^*, p').

$\text{Cos}(\theta_{\pi^+}), \Phi_{\pi^+}$ π^+ angles in the helicity rest frame of the meson.

$M_{\pi^+\pi^-}$ $\pi^+\pi^-$ invariant mass

1. Introduction and physics motivations

2. Experimental setup

3. Cross section for $f_0(980)$ and $f_2(1270)$

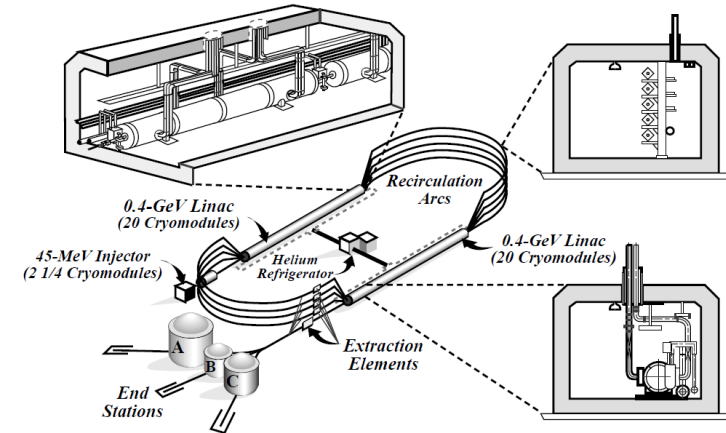
4. Moments Analysis of 2-pion electroproduction

5. Conclusions

The experimental setup

Jefferson Laboratory

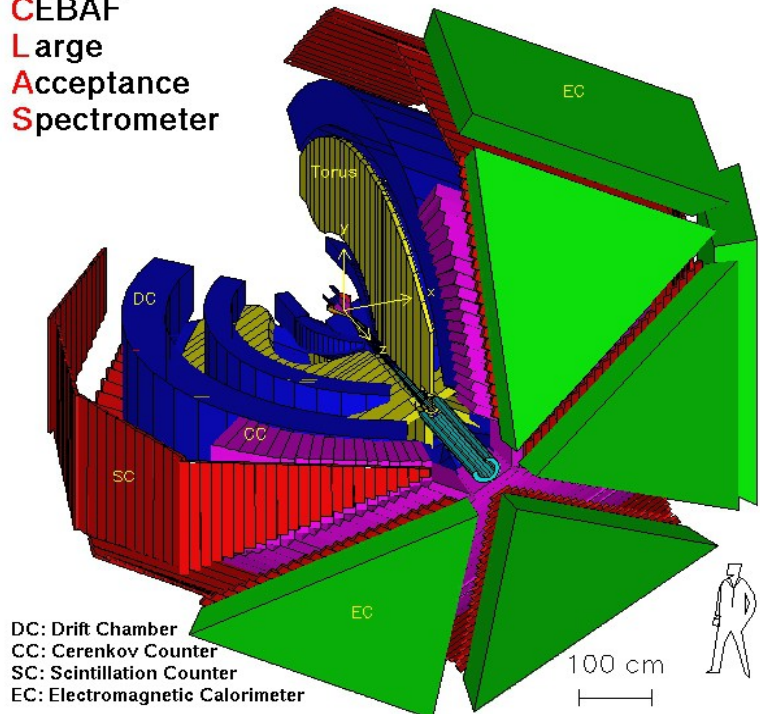
- CEBAF (2012) : $E_{\max} = 6 \text{ GeV}$, $I_{\max} = 200 \mu\text{A}$
- Distributed to 3 experimental Halls A, B and C (2012).



CLAS (Hall B, 1997-2012)

- Large acceptance spectrometer (“ 4π ”).
- Split by the toroidal magnet ($B_{\max} = 2.5\text{T}$) into 6 azimuthal sectors. Each sector included :
 - **3 regions of Drift Chambers (DC)** : Charged particles momenta. ($\Delta p/p < 0.5\%$ for 1 GeV/c)
 - **Cherenkov Counters (CC)** : π/e^- separation up to 2.5 GeV/c. ($8^\circ < \theta < 45^\circ$)
 - **Electromagnetic Calorimeters (EC)** : electron and neutral particle identification.
 - **Scintillator Counters (SC)** : Particle identification by time-of-flight measurement ($8^\circ < \theta < 140^\circ$, $\Delta t = 80$ to 160 ps).

CEBAF
Large
Acceptance
Spectrometer



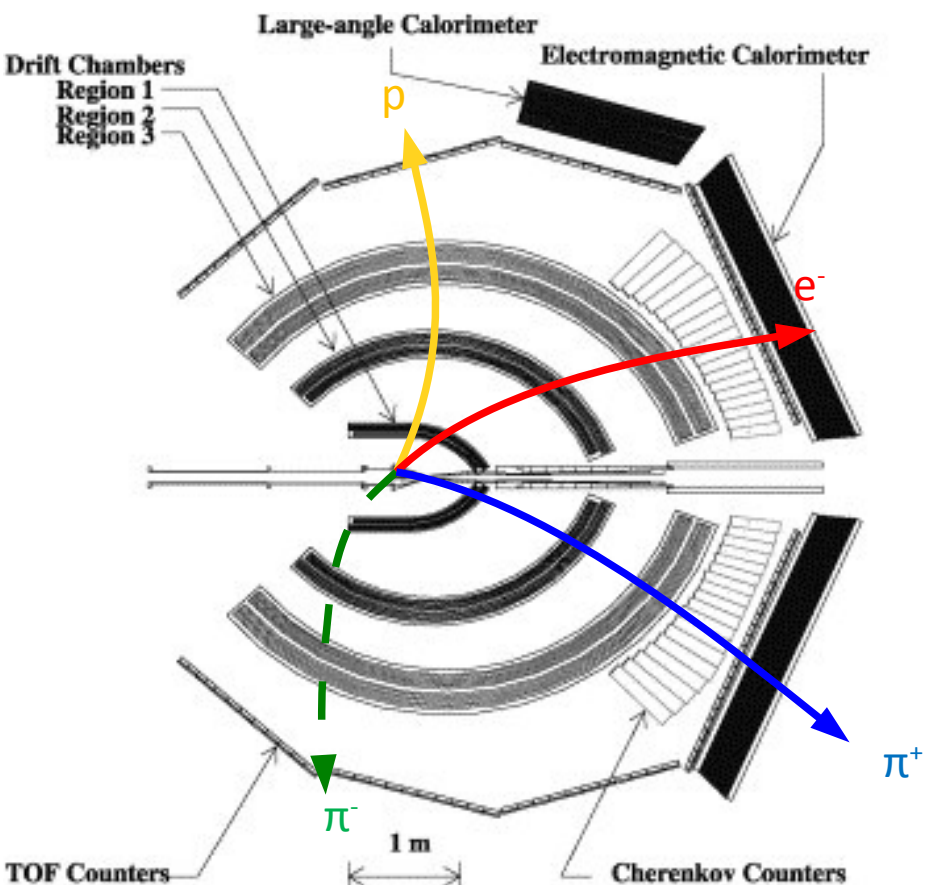
DC: Drift Chamber
CC: Cherenkov Counter
SC: Scintillation Counter
EC: Electromagnetic Calorimeter

e1-6 (2001)

- Electron beam : $E_{\text{mean}} = 5.754 \text{ GeV}$, $I_{\text{mean}} = 7 \text{ nA}$
- Target : LH_2 (length=5 cm, diameter=1.5 cm)

1. Introduction and physics motivations
2. Experimental setup
- 3. Cross section for $f_0(980)$ and $f_2(1270)$**
4. Moments Analysis of 2-pion electroproduction
5. Conclusions

Selection of exclusive $e'p'\pi^+\pi^-$



e^- identification

- $p_{e^-} > 0.8 \text{ GeV}/c$
- Z-Vertex selection within the target volume (DC)
- Fiducial cuts (EC et CC).
- Energy sample fraction (EC)
- Track matching between DC, CC and SC.

p and π^+ identification

- $p_{q>0} > 0.2 \text{ GeV}/c$
- Fiducial cuts (DC)
- Time-of-flight (SC) :

Measured velocity

$$\Delta \beta_m = \beta_{mes} - \beta_{calc}(m) = \frac{l}{ct} - \frac{p}{\sqrt{p^2 + m^2}}$$

SC
DC

SC

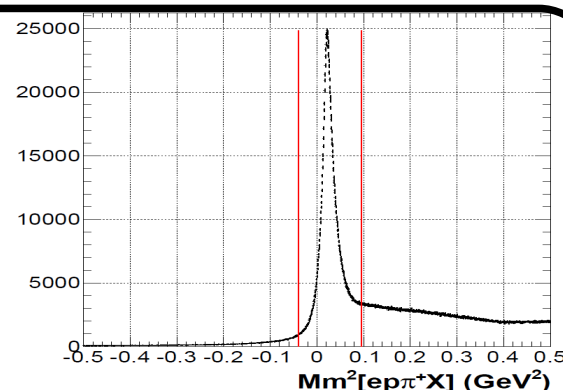
Predicted velocity for a particle with given mass m .

Exclusivity

→ Selection on π peak in missing mass spectrum $Mm[ep\pi^+X]$

$$-0.05 \leq Mm^2[ep\pi^+X] \leq 0.08 \text{ GeV}^2$$

- Z-Vertex selection within the target volume
- Cherenkov noise removed for $p_{e^-} < 1.5 \text{ GeV}/c$



Differential cross sections $\sigma^{\gamma^*p \rightarrow p\pi^+\pi^-}$

Reduced cross section

$$\frac{d^2\sigma^{\gamma^*p \rightarrow p\pi^+\pi^-}}{d\eta dM_{\pi^+\pi^-}} = \frac{1}{\Gamma_V(Q^2, x_B)} \frac{d^4\sigma^{ep \rightarrow p\pi^+\pi^-}}{dQ^2 dx_B d\eta dM_{\pi^+\pi^-}}$$

Γ_V Virtual photon flux factor
 η : A kinematic variable among $(-t, \Phi, \cos\theta_{HS})$, or none.

→ Selection of exclusive $e'p\pi^+\pi^-$ events in experimental data

For each $e'p\pi^+\pi^-$ selected event

Weighing by the factor

$$w_k = \frac{1}{\Gamma_V \text{Acc}_{\text{Corr Rad}} \text{Eff}_{\text{CC}}}$$

Projection onto a $M_{\pi\pi}$ dependent distribution, in a given (Q^2, x_B, η) bin

Each (Q^2, x_B, η, M) normalized by

$$\frac{1}{L_{\text{int}} \cdot \Delta V \cdot F_{\text{Corr Vol}} \cdot F_h}$$

- $\text{Acc}_{\text{Corr Rad}}(Q^2, x_B, t, \Phi, \cos\theta_{HS}, \varphi_{HS}, M_{\pi\pi})$ CLAS acceptance, corrected from radiative effects. Computed with **Monte Carlo simulations**.
- $\text{Eff}_{\text{CC}}(\mathbf{p}_e, Q^2, x_B)$ Loss of good events after electron-ID cut.
- $L_{\text{int}} = 30 \text{ fb}^{-1}$ Integrated luminosity. Integrated beam charge measured with Faraday cup.
- $\Delta V = \Delta Q^2 \Delta x_B \Delta \eta \Delta M_{\pi\pi}$ Bin volume.
- $F_{\text{corrVol}}(Q^2, x_B, \eta)$ Bin volume fraction occupied by $e'p\pi^+\pi^-$ phase space events
- $F_h(Q^2, x_B, \eta, M)$ Correction to the acceptance, in a $(Q^2, x_B, \eta, M_{\pi\pi})$ bin.

Monte Carlo simulations

→ Acceptance correction

Genev
 $e\pi^+\pi^-$ Monte Carlo event generator

Generated $e\pi^+\pi^-$

GSIM
 CLAS simulation package

ADC/TDC

GPP (GSIM Post-Processing)
 Smearing and inefficiencies to reproduce
 real data

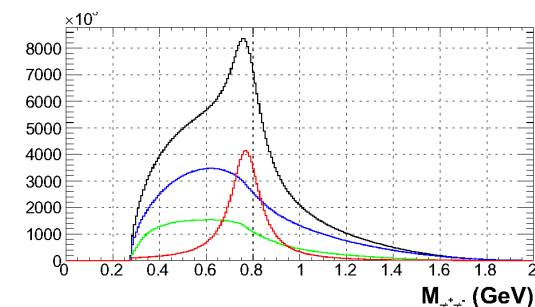
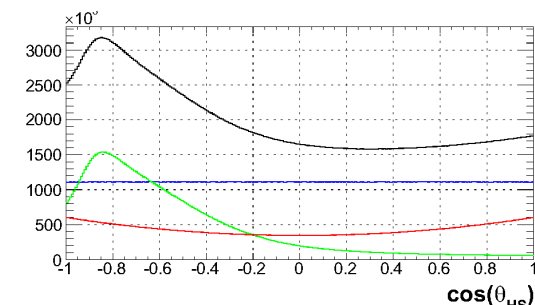
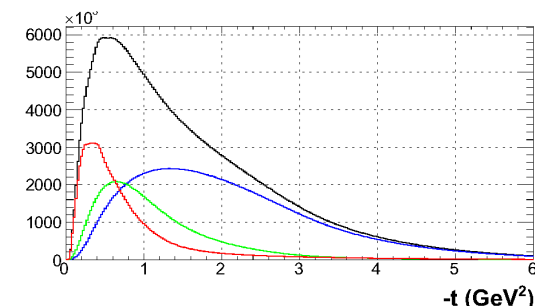
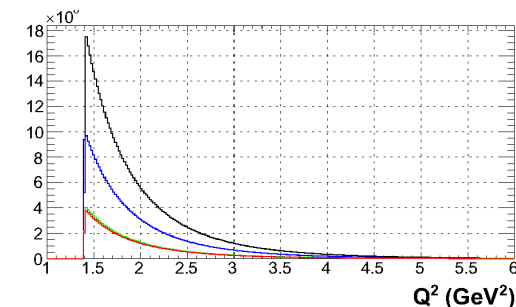
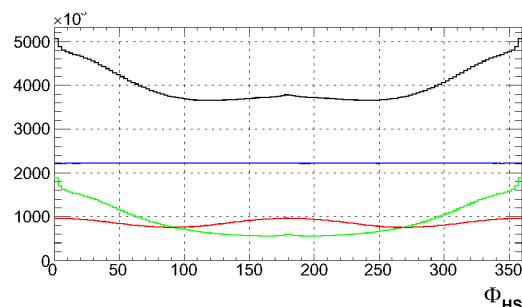
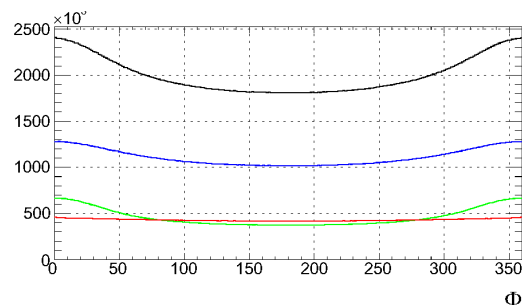
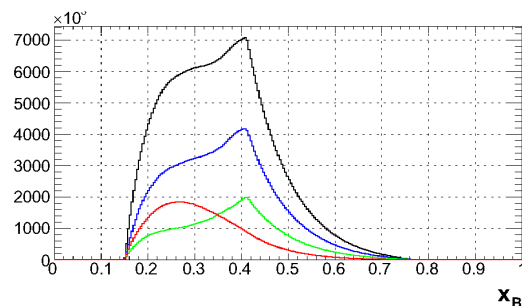
ADC/TDC

Reccis
 Reconstruction
 (ADC/TDC → Physical variables)

$e\pi^+\pi^-$ accepted
 by CLAS

Event selection
 Same algorithm as in the real data
 (except for the CC related cuts)

Generated MC
 – Total (240 M)
 – Non resonant $e\pi^+\pi^-$ (45%)
 – $e\pi \rightarrow e\pi\rho^0$ (25%)
 – $e\pi \rightarrow e\pi\Delta^{++}\pi^-$ (30%)



Monte Carlo simulations

→ Acceptance correction

Genev
 $e\pi^+\pi^-$ Monte Carlo event generator

Generated $e\pi^+\pi^-$

GSIM
 CLAS simulation package

ADC/TDC

GPP (GSIM Post-Processing)
 Smearing and inefficiencies to reproduce real data

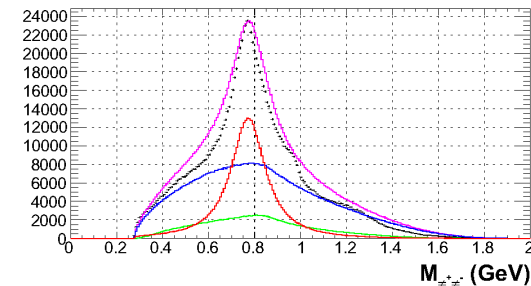
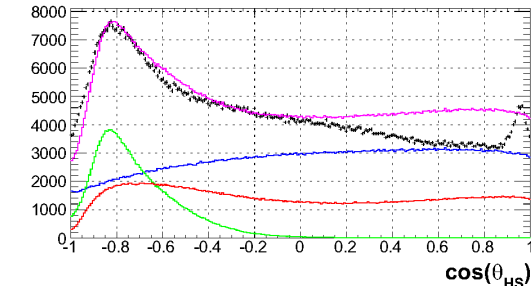
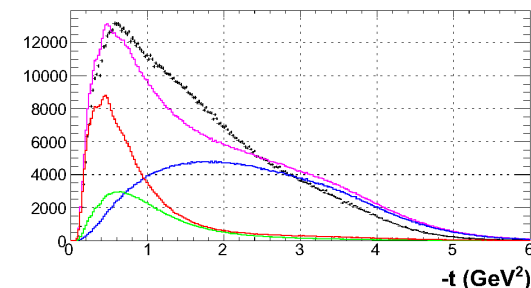
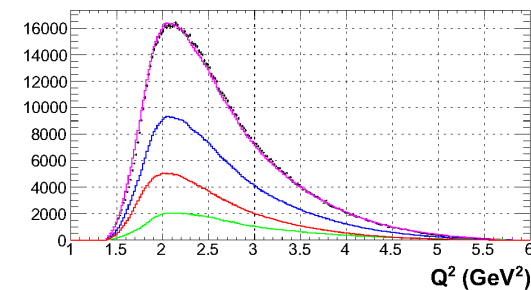
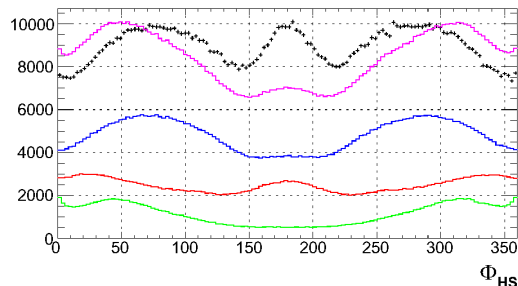
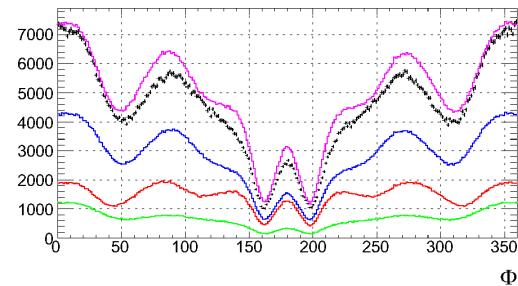
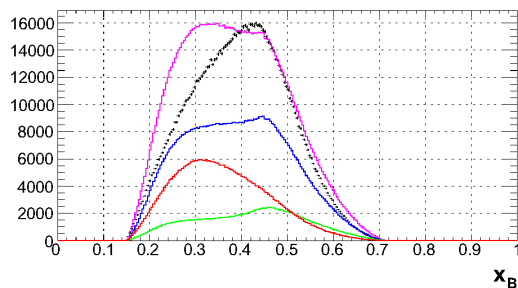
ADC/TDC

Reccis
 Reconstruction
 (ADC/TDC → Physical variables)

$e\pi^+\pi^-$ accepted
 by CLAS

Event selection
 Same algorithm as in the real data
 (except for the CC related cuts)

– **Data**
 – **Reconstructed MC (Normalised to data)**
 – **Non resonant $e\pi^+\pi^-$**
 – **$e\pi \rightarrow e\rho\rho^0$**
 – **$e\pi \rightarrow e\rho\Delta^{++}\pi$**

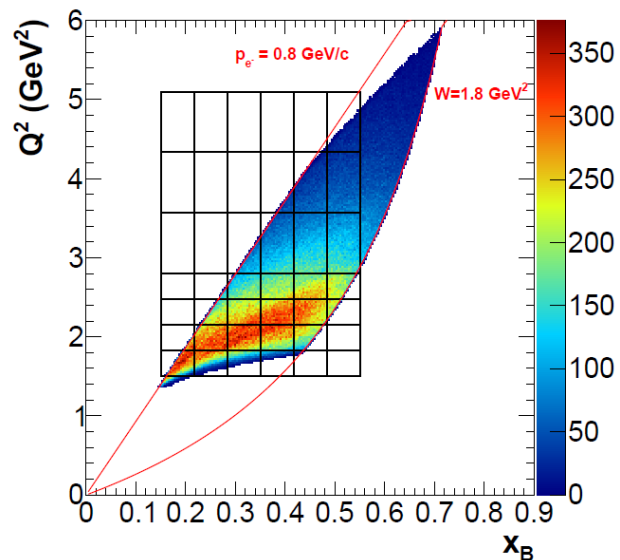
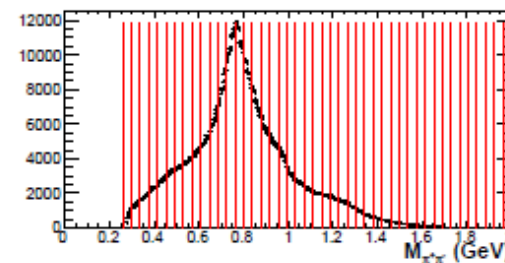
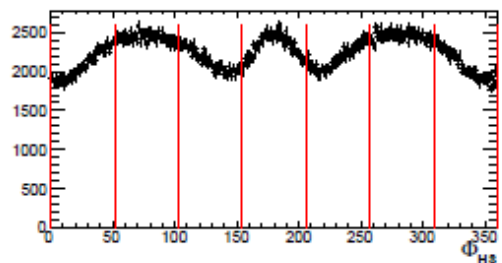
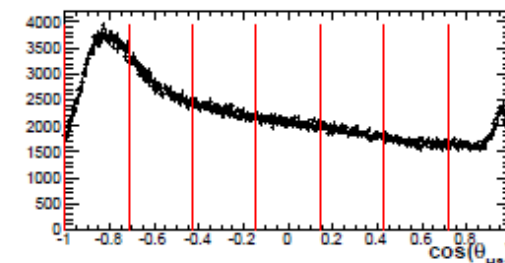
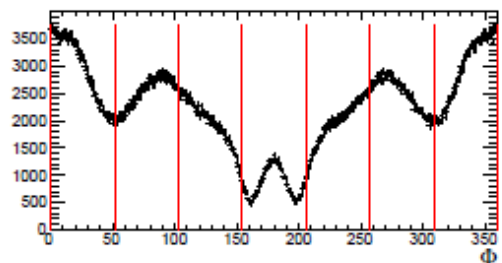
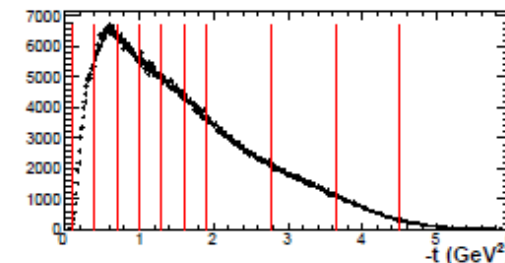
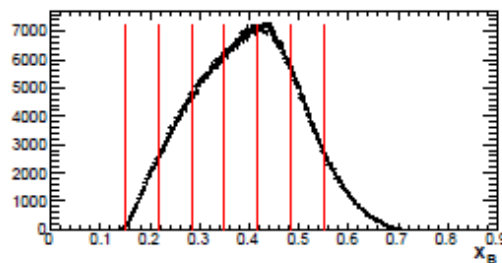
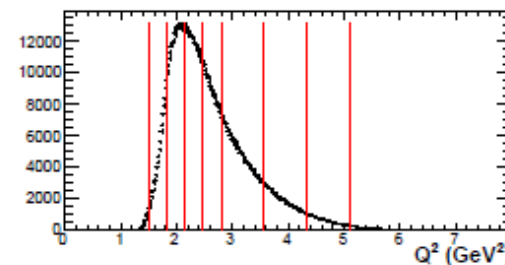


Binning of the phase space

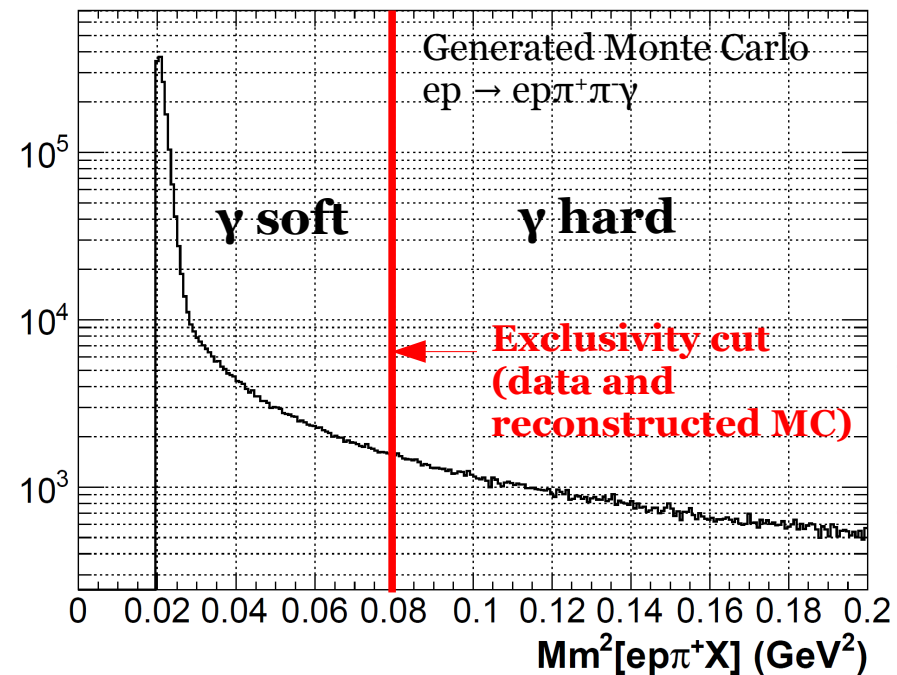
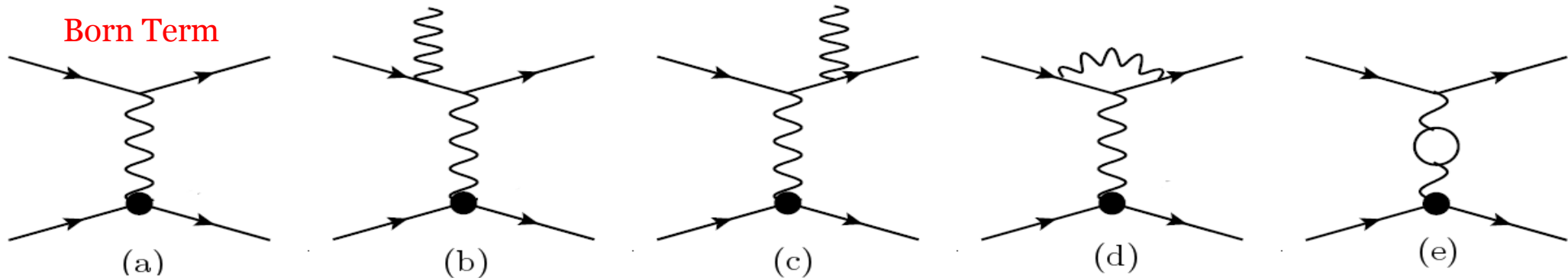
$W > 1.8 \text{ GeV}$,
 $p_{e^-} > 0.8 \text{ GeV}/c$

Variable	Unit	Intervals	Nb. bins	Bin width
Q^2	GeV^2	1.50-2.80	4	0.33
		2.80-5.10	3	0.76
x_B	-	0.15-0.55	6	0.06
$-t$	GeV^2	0.1-1.90	6	0.30
		1.90-4.30	3	0.80
Φ	$^\circ$	0-360	7	51.4
$\cos \theta_{\pi^+}^{\text{HS}}$	-	-1. à 1.	7	0.28
$\Phi_{\pi^+}^{\text{HS}}$	$^\circ$	0-360	7	51.4
$M_{\pi^+\pi^-}$	GeV	0.26-2.00	45	0.04

Experimental data



Radiative corrections



- The e^- radiates photons easily.
- “Hard” photons
“soft” photons : Low energy emissions and/or reabsorbed immediately (**still in data after exclusivity cut**).
- Mo and Tsai. (fig. b) to e)) radiative effects embedded in GENEV, calculated for $ep \rightarrow ep$ process.
- Born cross section : $\sigma_{Born} = F_{Rad} * \sigma_{Born+diagrams\ b)\ to\ e)}$

→ Radiative correction factor:

$$F_{rad} = \frac{Gen_{non\ rad}}{Gen_{rad\ soft}} \quad (\sim 5\ to\ 20\%)$$

Acceptance corrected from radiative effects

- $Acc = \text{Geometrical acceptance} \cdot \text{CLAS detection efficiency}$

Integrated acceptance
(mean : 2.5%)

$$Acc = \frac{Rec_{Rad\ soft}}{Gen_{Rad\ soft}}$$

← Nb. of MC events reconstructed by CLAS in a bin.
← Nb. of MC events generated in a bin.

→ Computed with MC simulations.

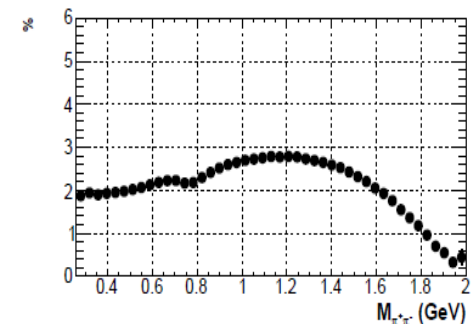
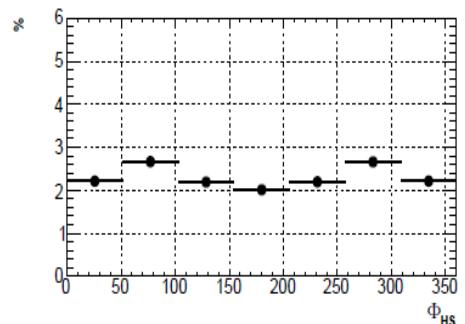
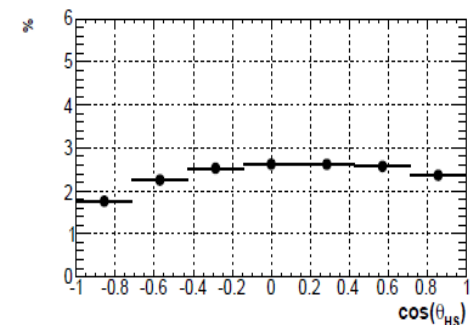
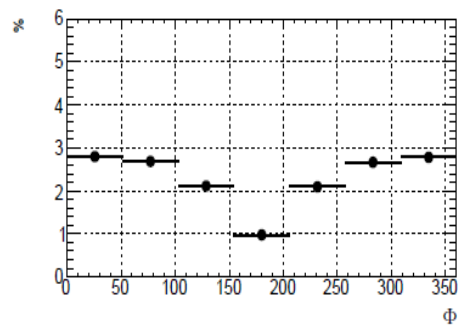
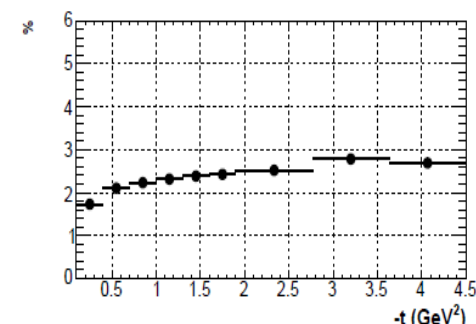
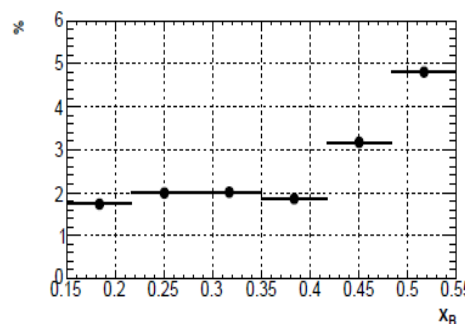
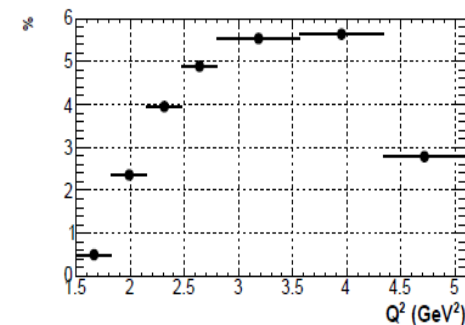
- Acceptance and radiative corrections computed in a single effective term $Acc_{Corr\ Rad}$

$$\sigma_{Born}^{\gamma p \pi^+ \pi^-} = \frac{N_{Rad\ soft}^{\gamma p \pi^+ \pi^-} \cdot F_{RAD}}{L_{int} \cdot Eff_{cuts} \cdot Acc}$$

$$Acc_{Corr\ Rad} = \frac{Rec_{Rad\ soft}}{Gen_{non\ rad}}$$

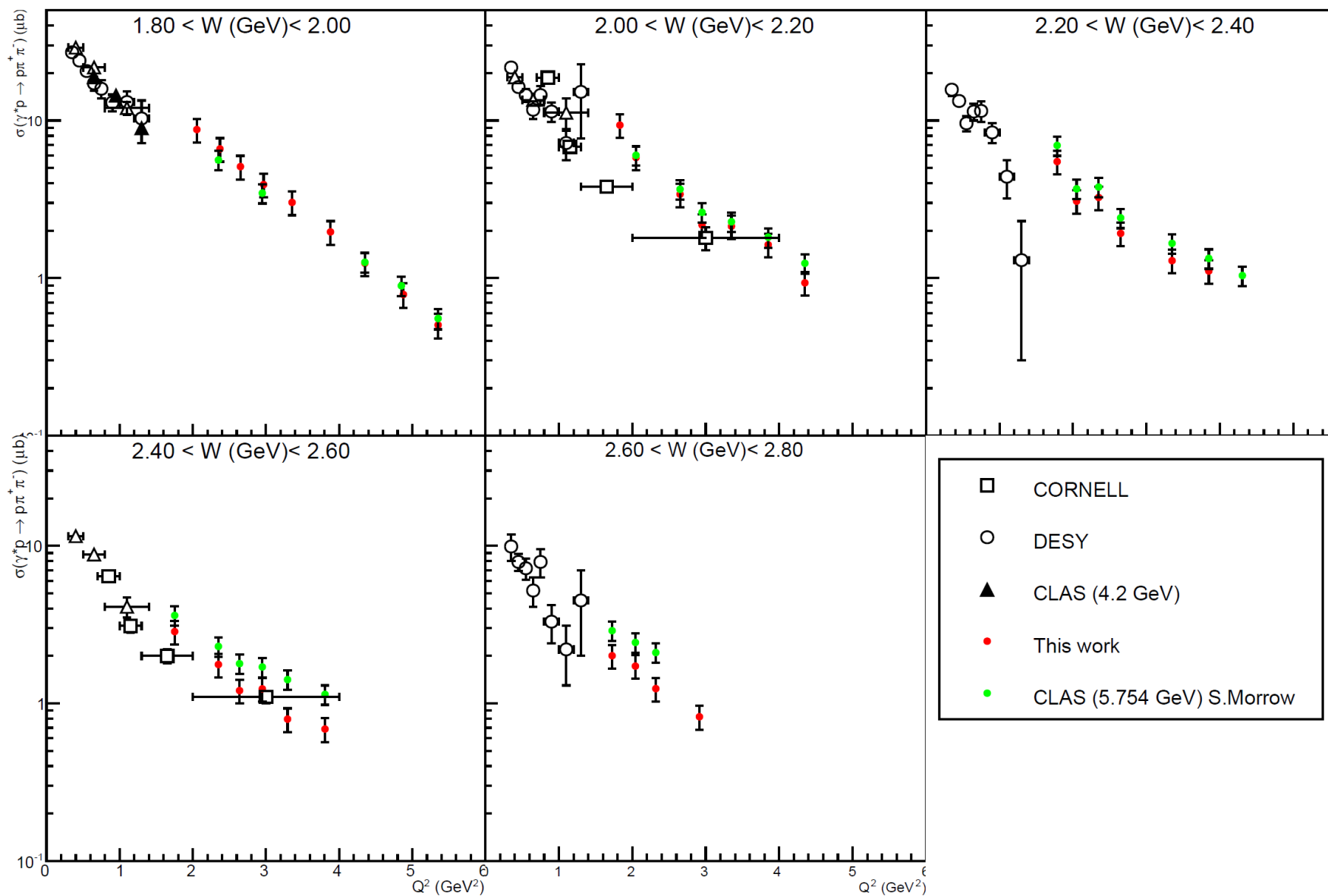
$Rec_{Rad\ soft}$ $e p \pi^+ \pi^- \gamma_{soft}$ reconstructed by CLAS and selected in a bin .

$Gen_{non\ rad}$ $e p \pi^+ \pi^-$ generated without radiative effects in a bin.



- $Acc_{Corr\ Rad}$ computed for each 7D bin
($Q^2, x_B, -t, \Phi, \cos \theta_{HS}, \phi_{HS}, M_{\pi^+ \pi^-}$)

Cross section $\sigma^{\gamma^*p \rightarrow p\pi^+\pi^-}$ in (Q^2, W)

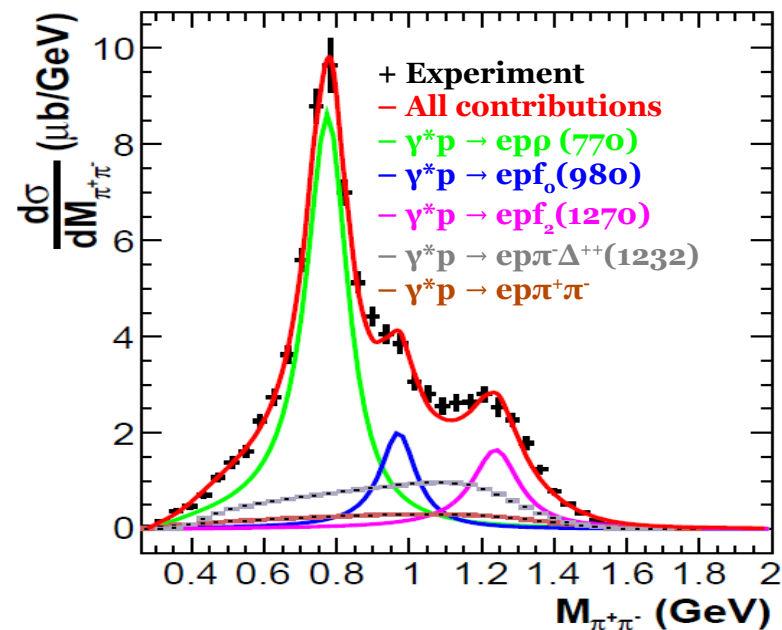


Good agreement with previous CLAS ρ^0 analysis.¹

¹ S.A. Morrow *et al*, Eur. Phys. J. A 39, 5-31 (2009)

Extraction of f_0 and f_2 signals

$1.50 \leq Q^2 < 1.82, 0.22 \leq x_B < 0.28$



- f_0 and f_2 extracted from a fit on **reduced cross section spectrum as a function of $M_{\pi^+\pi^-}$** , in a given (Q^2, x_B, η) bin. $\eta = t, \varphi, \cos \theta_{HS}$ (or nothing).

- Fit model= **incoherent sum of the following contributions** :

→ **3 resonances** :

Skewed Breit Wigner (BW) for ρ, f_0, f_2

→ 4 parameters :

-Intensity

-Centre

-FWHM

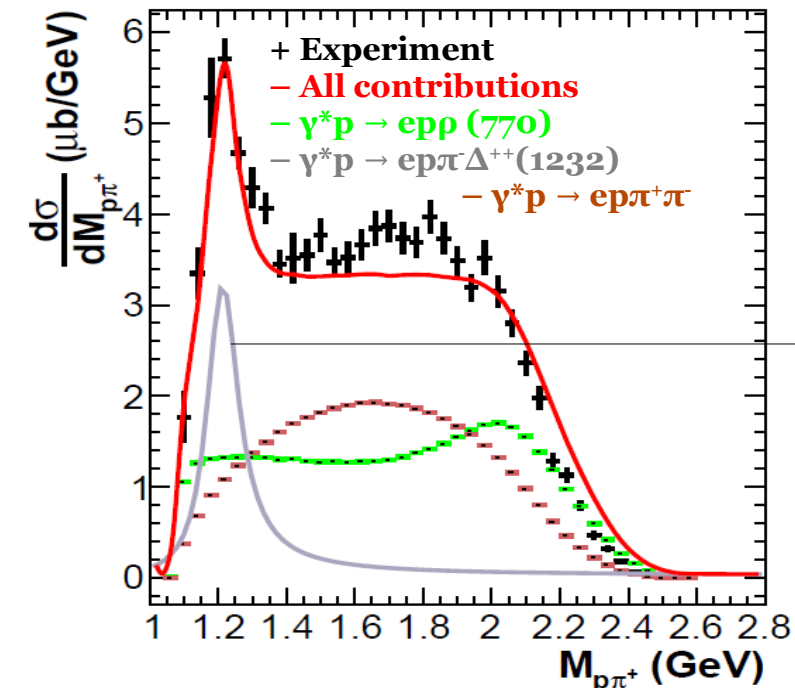
-Skewness toward lower mass region.

→ **2 backgrounds** : **non resonant $\pi^+\pi^-$** and Δ^{++} .

Spectra generated with GENEV (no radiative effects).

→ 2 scale parameters (total spectrum fraction):

$\alpha_{\pi\pi}$ (from 0.01 to 1) et α_{Δ} (<0.2)



Cross section for meson production

$$\sigma_{\gamma^* p \rightarrow p \text{ Meson}} = \frac{\int_0^2 BW_{skew}^{\text{Meson}}(M_{\pi^+\pi^-}) dM_{\pi^+\pi^-}}{BR^{\text{Meson} \rightarrow \pi^+\pi^-}}$$

Branching ratio :
 f_0 : 100 %
 f_2 : 85%

Systematic errors

$$\frac{\Delta\sigma}{\sigma} = \sqrt{\left(\frac{\Delta\sigma_{\text{stat fit}}}{\sigma}\right)^2 + \left(\frac{\Delta\sigma_{\text{syst norm}}}{\sigma}\right)^2 + \left(\frac{\Delta\sigma_{\text{syst fit}}}{\sigma}\right)^2}$$

Acceptance and radiative corrections	15 %	} $\frac{\Delta\sigma_{\text{syst norm}}}{\sigma} = 17\%$
Monte Carlo model	5 %	
Holes in DC	6 %	
CC-cut losses efficiency	1.5 %	
Luminosity	3 %	
Fitting procedure	Bin by bin	

$$\Delta\sigma_{\text{syst fit}} = \sqrt{\frac{1}{4} \sum_{i=1}^4 (\sigma - \sigma_i)^2}$$

4 systematic variations on fitting procedure :

- 1) Free Δ^{++} scale parameter.
- 2) Non resonant background only
- 3) f_0 and f_2 without skewness
- 4) +/- 15 % variation on centre and FWHM of f_2 and ρ^0 .

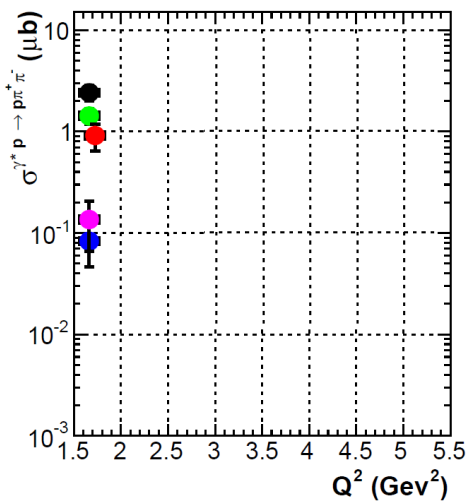
Fitting procedure is the main source of systematic error :

For various (Q^2, x_B) bins, ρ^0 : 17 to 22 % f_0 : 28 to 150 % f_2 : 44 to 85 %

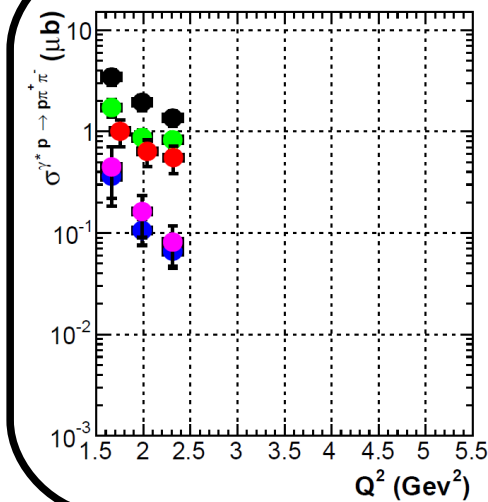
→ Cross section points with $\Delta\sigma/\sigma_{\text{stat}} > 90\%$ rejected.

Cross sections in (Q^2, x_B)

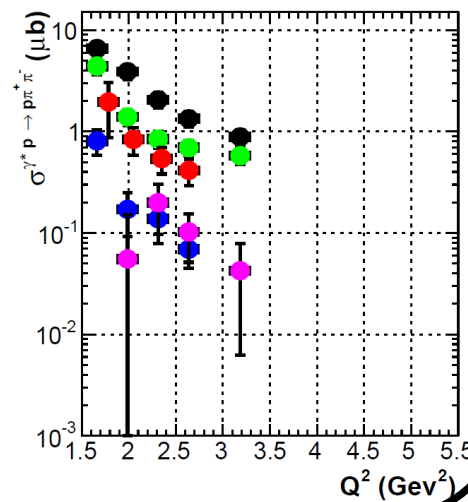
$0.15 < x_B < 0.22$



$0.22 < x_B < 0.28$

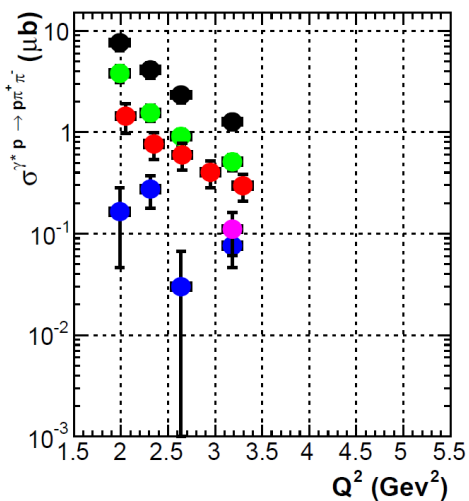


$0.28 < x_B < 0.35$

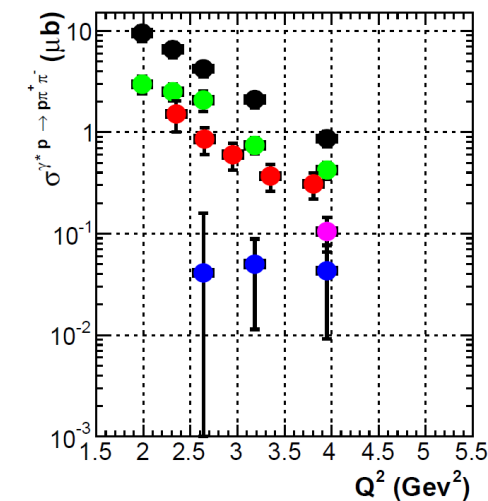


- + $\gamma^* p \rightarrow e p \pi^+ \pi^-$
- + $\gamma^* p \rightarrow e p \rho^0$ (770)
- + $\gamma^* p \rightarrow e p \rho^0$ (2009)
- + $\gamma^* p \rightarrow e p f_0(980)$
- + $\gamma^* p \rightarrow e p f_2(1270)$

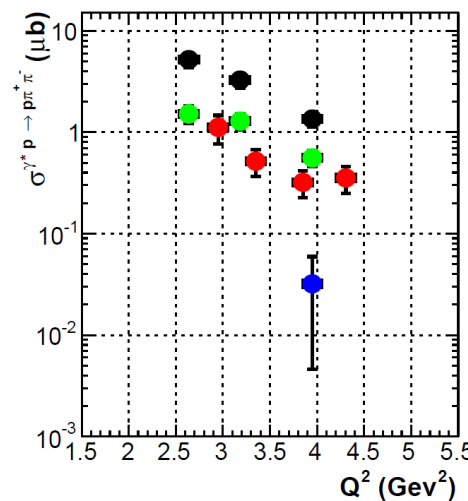
$0.35 < x_B < 0.42$



$0.42 < x_B < 0.48$



$0.48 < x_B < 0.55$



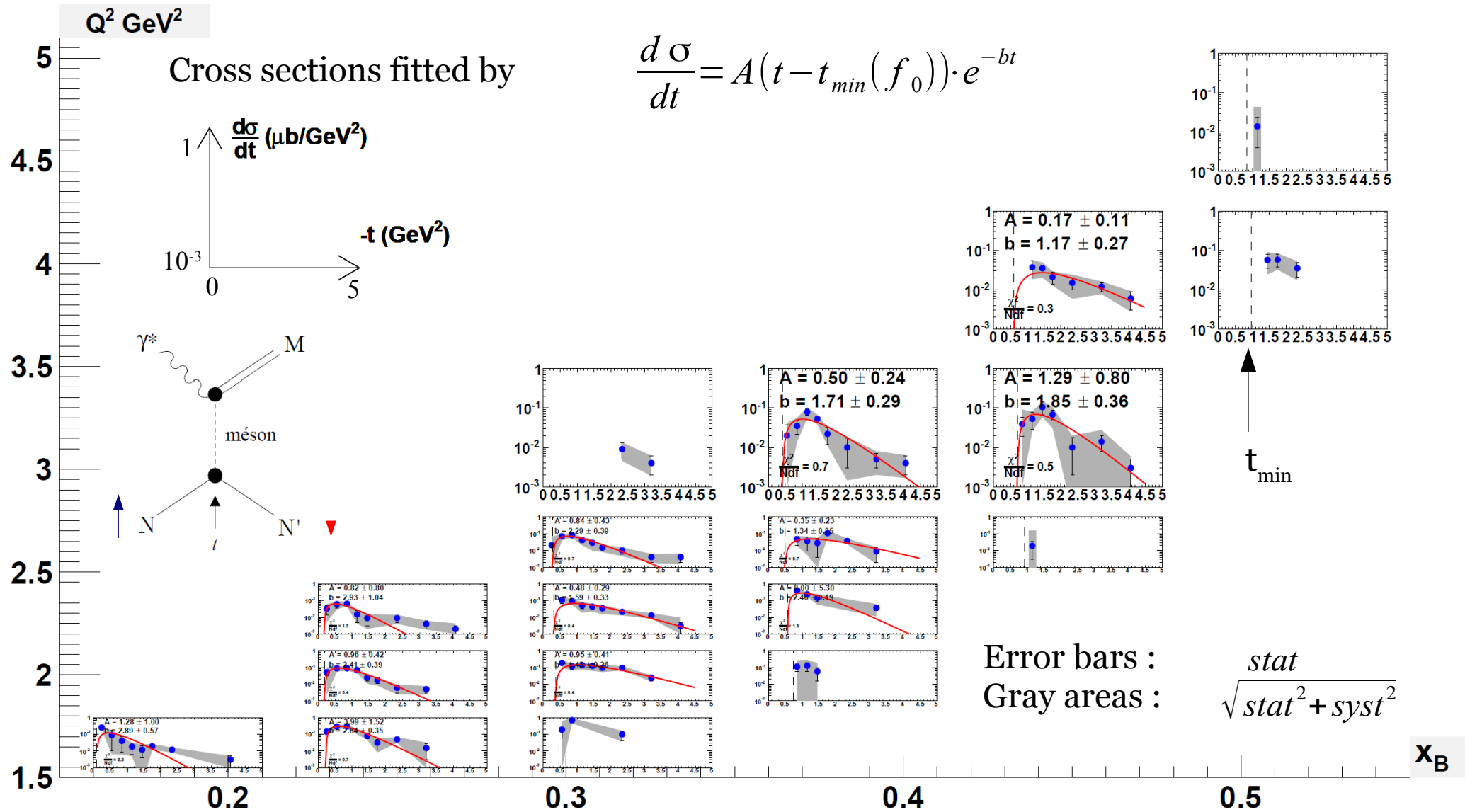
- Q^2 -scaling
- $\rho^0 \sim 1/Q^{6 \pm 1}$
- $f_0 \sim 1/Q^{10 \pm 1.5}$
- $f_2 \sim 1/Q^{10 \pm 1.8}$

DVMP : $\sigma_L \sim 1/Q^6$
 $\sigma_T \sim 1/Q^8$

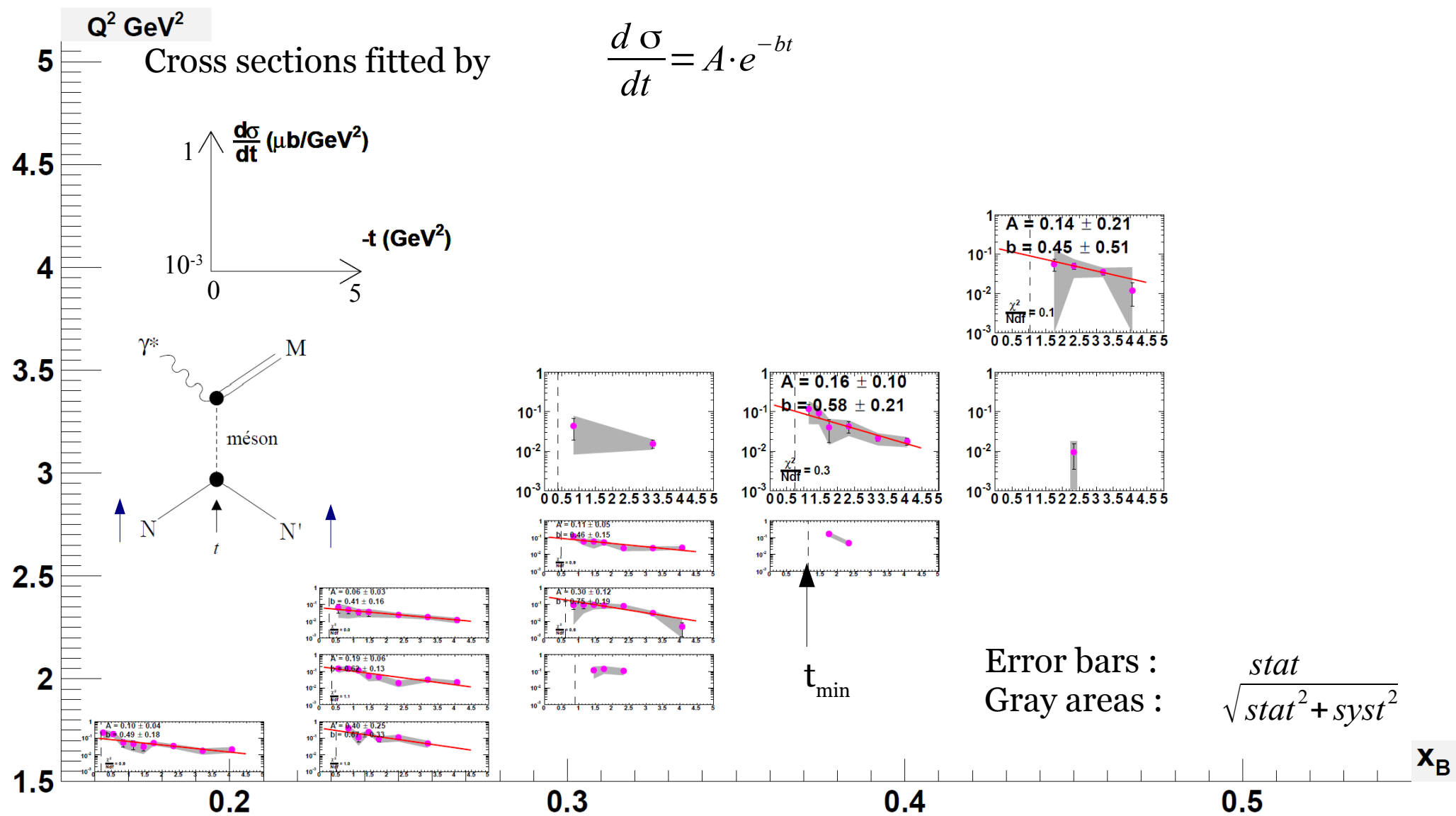
- Good agreement on $\sigma^{\gamma p \rightarrow p \rho}$ with previous CLAS ρ^0 analysis.¹
- f_0 and f_2 seems to follow a different Q^2 -scaling from the DVMP one.

¹ S.A. Morrow *et al*, Eur. Phys. J. A 39, 5-31 (2009)

f_0 differential cross sections in (Q^2, x_B, t)



f_2 differential cross sections in (Q^2, x_B, t)



Impact parameter b

$$\frac{d\sigma}{dt} \propto A e^{-bt}$$

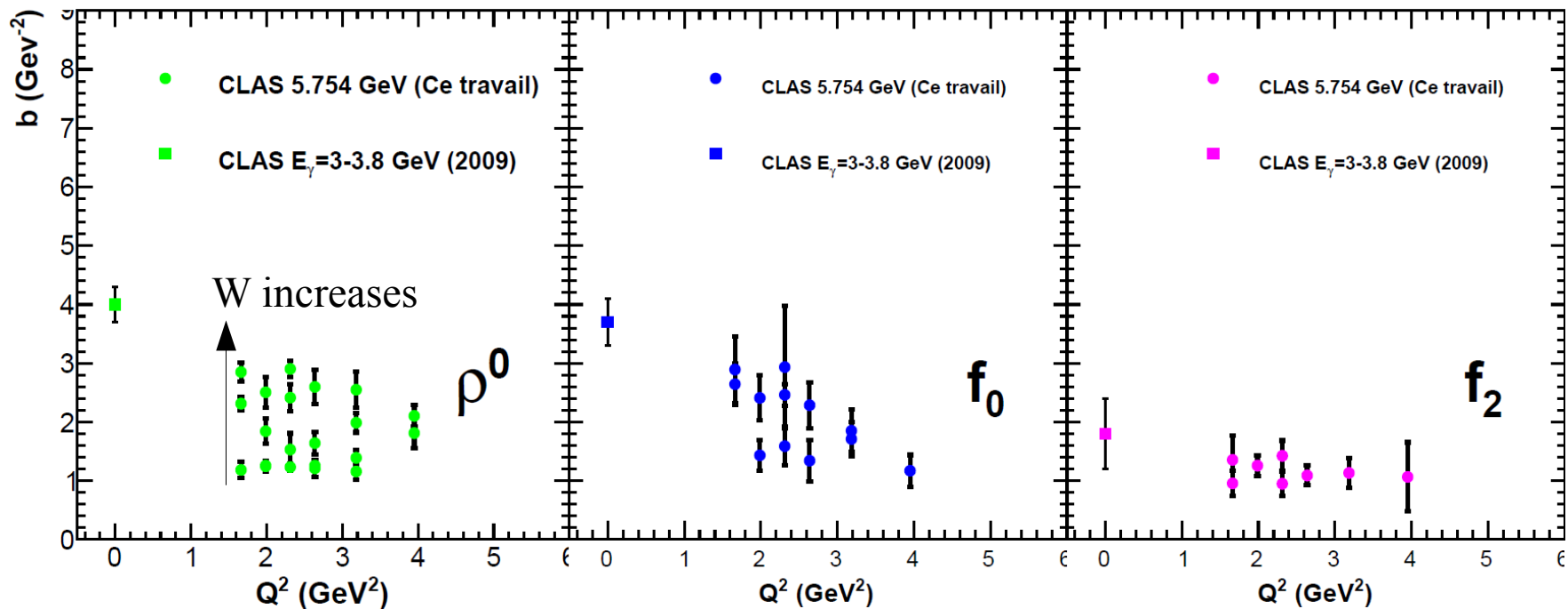
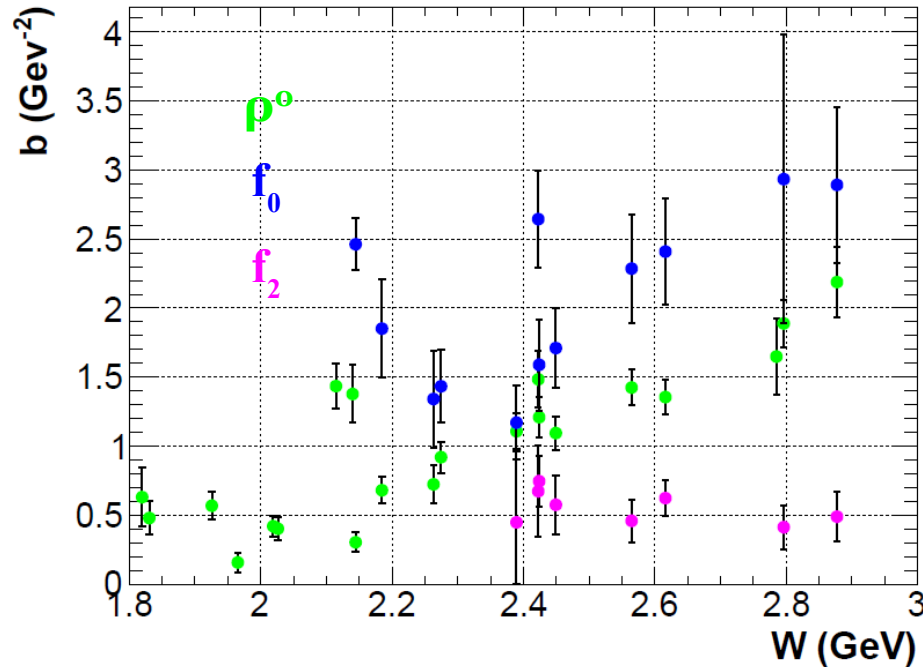
$b \rightarrow$ **Transverse size of γ^*p interaction region.**

b vs W

- f_0 and ρ^0 : Similar behaviour
- f_2 : b constant in the available W region.

b vs Q^2

- b decreases as Q^2 increases.
 \rightarrow Smaller interaction region with a smaller resolution scale.
- f_2 : Flattest b decrease.
 \rightarrow Meson mass acts as a resolution scale. ($b_{f_2}(Q^2=0) \sim b_\rho(Q^2=2-3 \text{ GeV}^2)$)



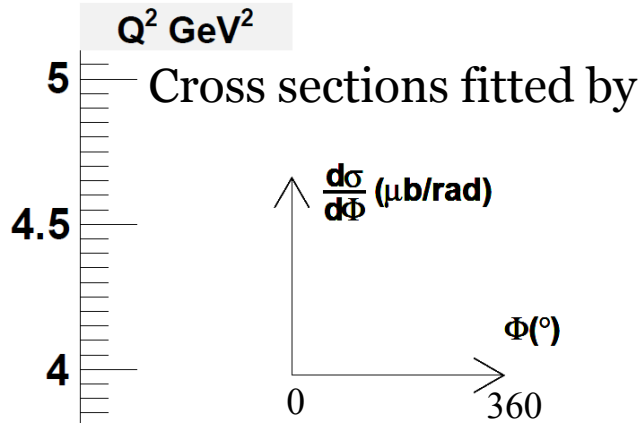
f_0 differential cross sections in (Q^2, x_B, Φ)

Factorisation in terms of GPDs

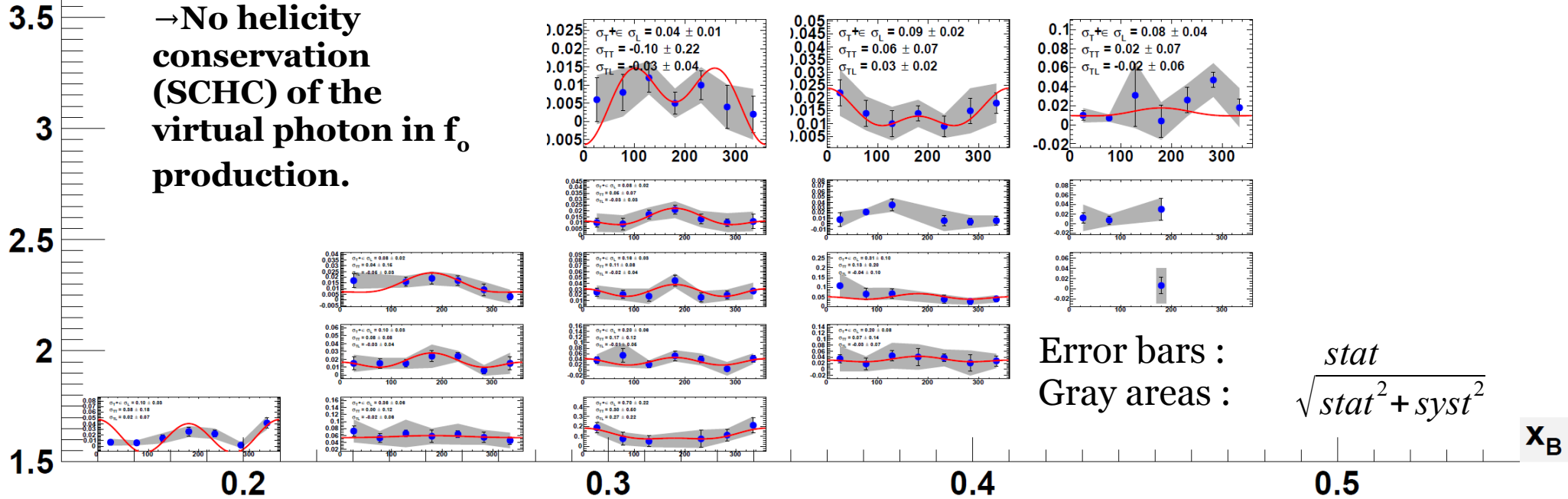
$$\frac{d\sigma}{d\Phi} = \frac{1}{2\pi} (\sigma_T + \epsilon \sigma_L + \epsilon \cos 2\Phi \sigma_{TT} + \sqrt{2\epsilon(1+\epsilon)} \cos \Phi \sigma_{TL})$$

T : Transversely polarised virtual photon ($\lambda=+/-1$).
L: Longitudinally polarised ($\lambda=0$)

$$\epsilon = \frac{1}{1 + 2 \frac{Q^2 + (E - E')^2}{4EE'}}$$



→ No helicity conservation (SCHC) of the virtual photon in f_0 production.

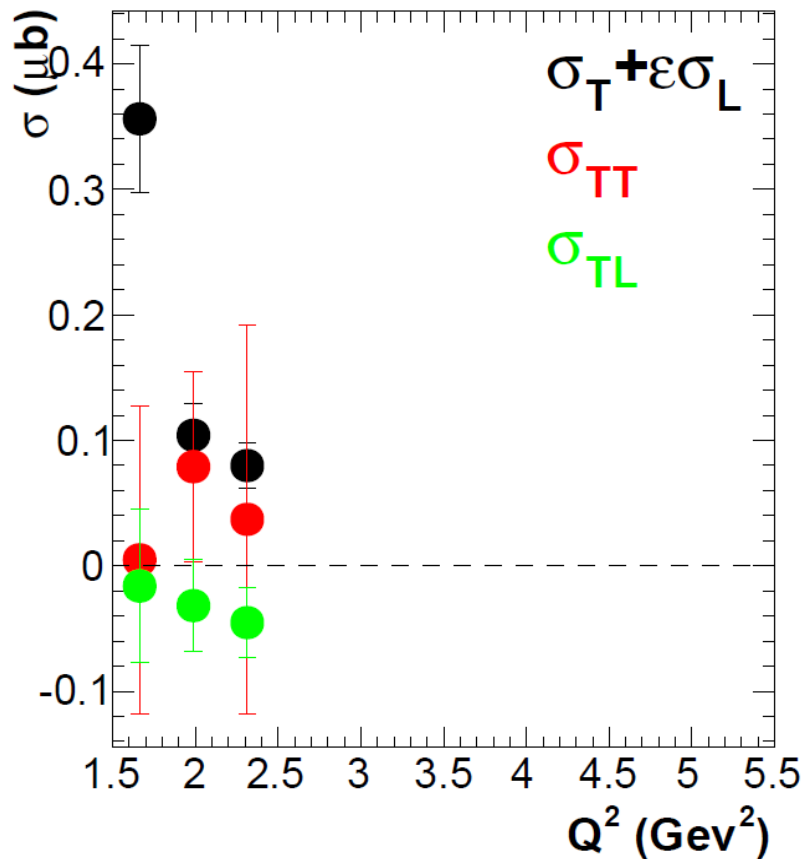


Error bars : $\frac{stat}{\sqrt{stat^2 + syst^2}}$
Gray areas : $\sqrt{stat^2 + syst^2}$

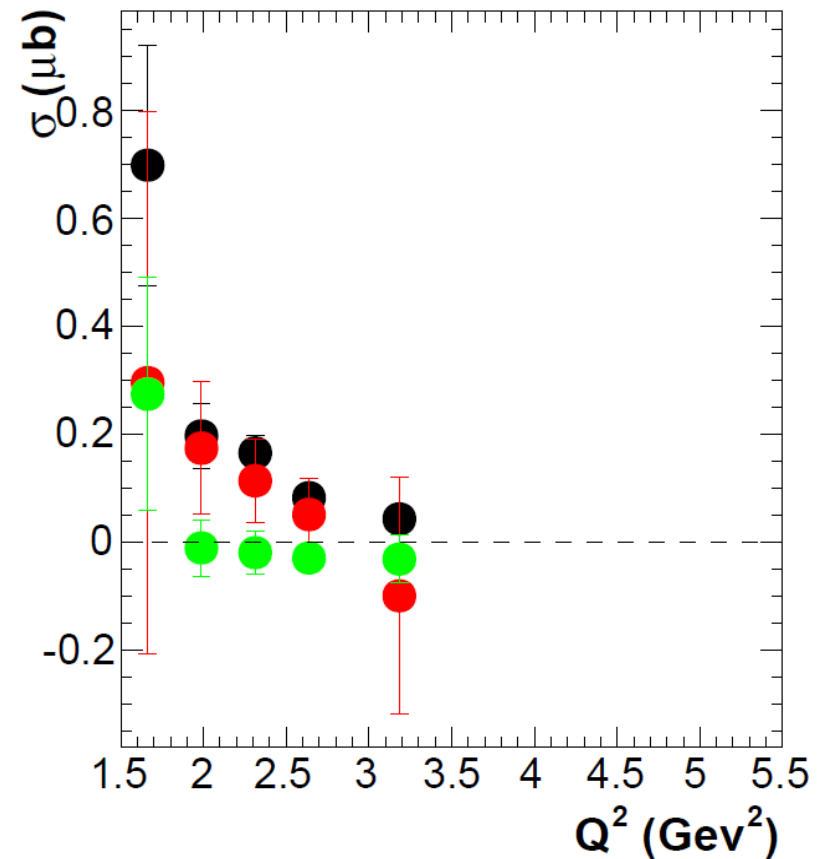
σ_T et σ_L could be extracted by the Rosenbluth technique (measurements at different beam energies, same (Q^2, x_B)).

TT and TL interferences of $\gamma^*p \rightarrow pf_0$

$0.22 < x_B < 0.28$



$0.28 < x_B < 0.35$



- Non negligible contribution from TT response function.
- TT contribution similar to $\gamma^*p \rightarrow p\pi^0$ electroproduction.

¹ I. Bedlinsky et al., Phys. Rev. C 90, 039901 (2014)

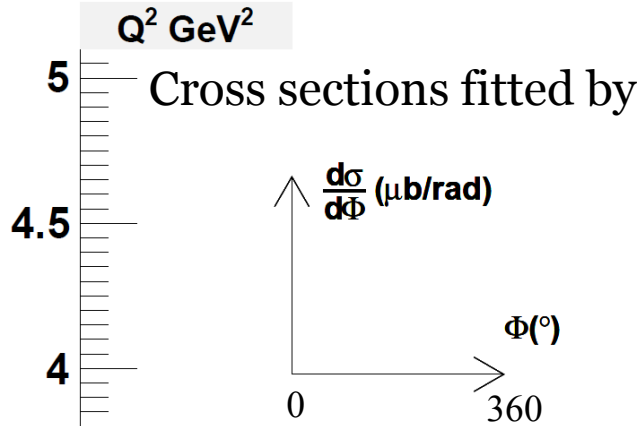
f_2 differential cross sections in (Q^2, x_B, Φ)

Factorisation in terms of GPDs

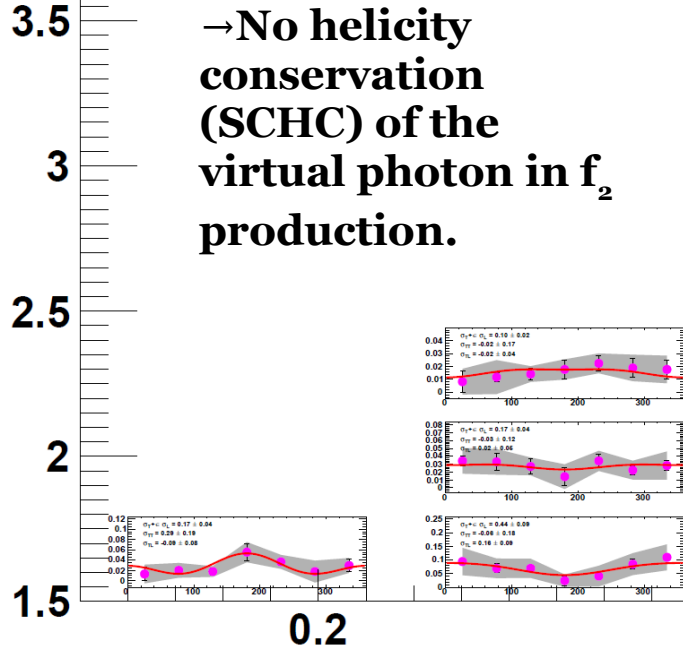
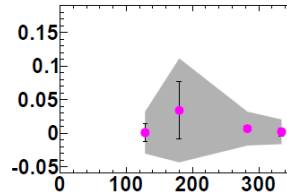
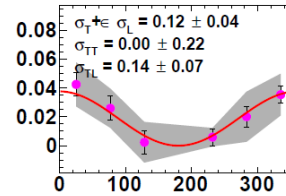
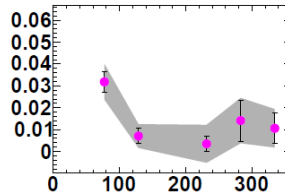
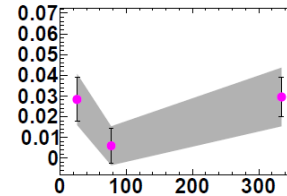
$$\frac{d\sigma}{d\Phi} = \frac{1}{2\pi} (\sigma_T + \epsilon \sigma_L + \epsilon \cos 2\Phi \sigma_{TT} + \sqrt{2\epsilon(1+\epsilon)} \cos\Phi \sigma_{TL})$$

T : Transversely polarised of the virtual photon ($\lambda=+/-1$).
L: Longitudinally polarised ($\lambda=0$)

$$\epsilon = \frac{1}{1 + 2 \frac{Q^2 + (E - E')^2}{4EE'}}$$



→ No helicity conservation (SCHC) of the virtual photon in f_2 production.



Error bars : $\frac{stat}{\sqrt{stat^2 + syst^2}}$
Gray areas : $\sqrt{stat^2 + syst^2}$

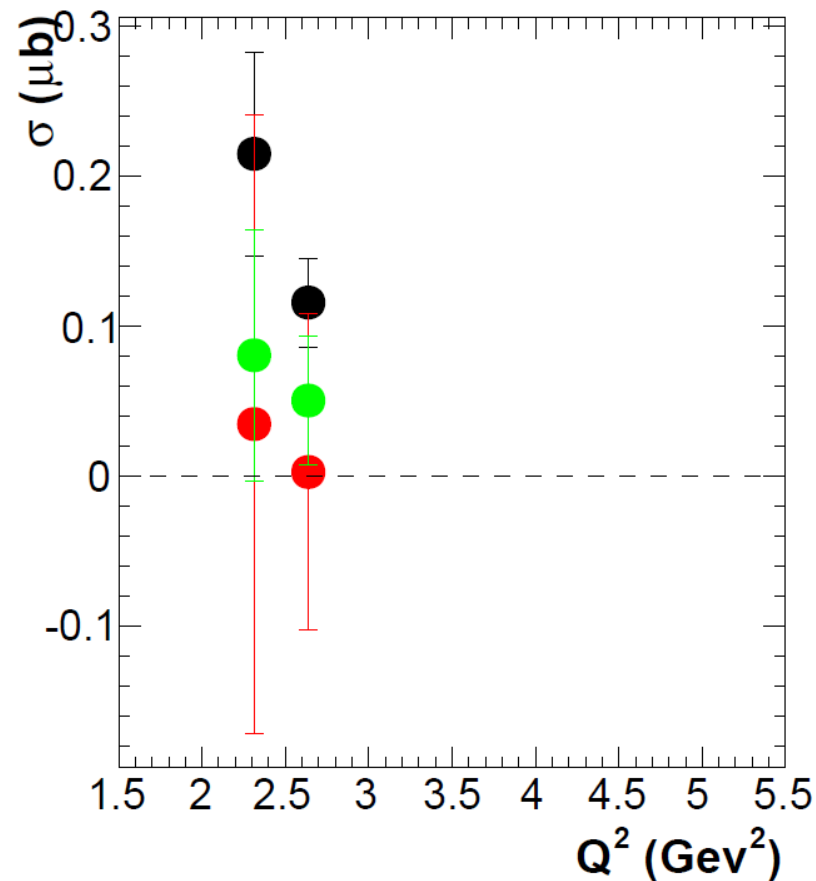
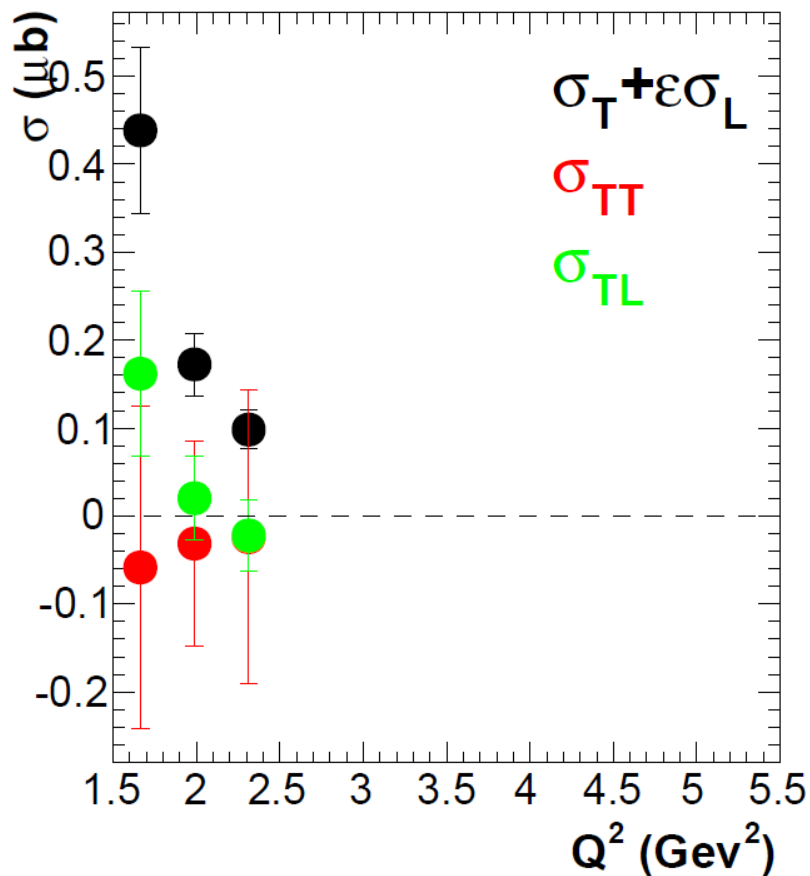
x_B

σ_T et σ_L could be extracted by the Rosenbluth technique.

TT and TL interferences for $\gamma^*p \rightarrow pf_2$

$0.22 < x_B < 0.28$

$0.28 < x_B < 0.35$



- Hint of TL response function.
- TL contributions in f_2 mass region in agreement with Legendre moments analysis at HERMES¹.

¹ Airapetian et al. (Collaboration HERMES) Phys. Lett. B 599, 212 (2004)

1. Introduction and physics motivations

2. Experimental setup

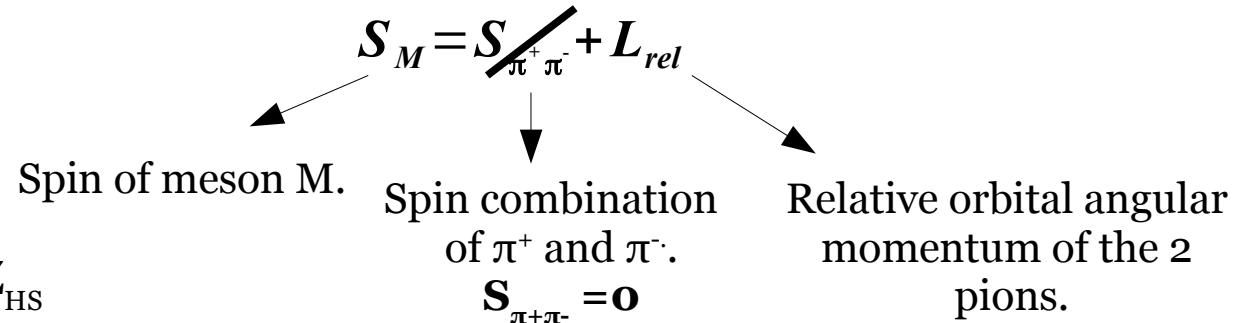
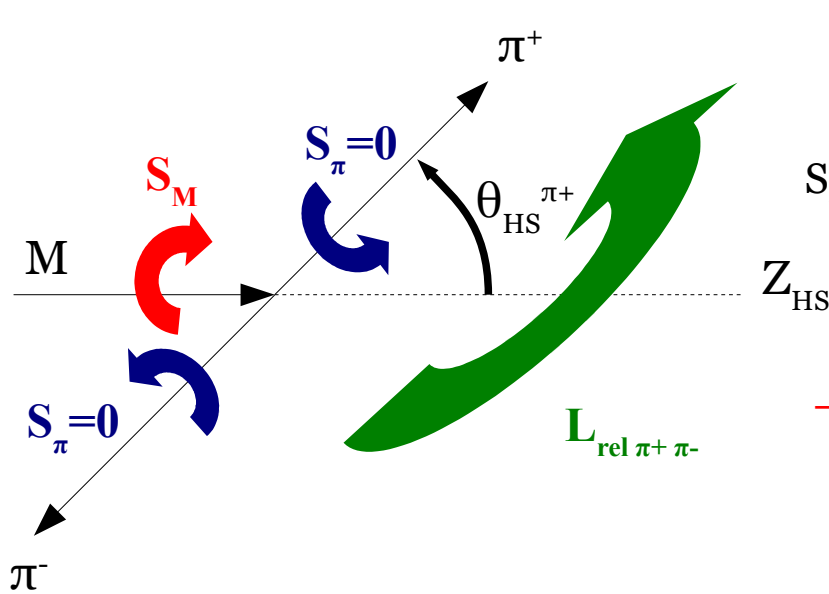
3. Cross section for $f_0(980)$ and $f_2(1270)$

4. Moments Analysis of 2-pion electroproduction

5. Conclusions

Partial Wave Amplitudes

→ f_0 ($J=0$) and f_2 ($J=2$) extracted using their spin.



→ Spin of M determined by analysis the decay angles of π^+ .

- $e p \rightarrow e p \pi \pi$ amplitude decomposed into a **coherent sum of partial wave amplitudes**.

$$\left| A(Q^2, x_B, -t, \Phi, \cos \theta, \varphi, M_{\pi^+ \pi^-}) \right|^2 = \left| \sum_{l=0}^{\infty} \sum_{m=-l}^{m=+l} a_{lm}(Q^2, x_B, -t, \Phi, M_{\pi^+ \pi^-}) \cdot Y_{lm}(\cos \theta, \varphi) \right|^2$$

l : Relative angular orbital momentum
 m : Angular momentum projection along Z_{HS} axis in helicity frame.

Production amplitude

Spherical Harmonics
 Decay amplitude

→ First attempt of PWA on $e p \rightarrow e p \pi \pi$ with mass independent fits.

(in collaboration with M. Battaglieri, A. Celentano, D. Glazier, V. Mathieu, A. Szczepaniak) :

Pseudo-data : Consistent results in simple cases, fails with realistic ρ → **Parity conservation ?**

Real data : Not enough statistics to perform fit in (Q^2, x_B, t, Φ, M) bins.

Moments of angular distributions

→ Amplitudes indirectly determined by analysing moments of the decay angular distributions

Moments decomposition¹

For each $e\pi^+\pi^-$ event,

$$I(\Theta, \Phi) = \sqrt{4\pi} \sum_{L=0}^{L_{max}} \sum_{M=0}^L \langle Y_{LM} \rangle \Re(Y_{LM}(\Theta, \Phi)), \quad L_{max} = 4$$

Intensity

Moment ($0 \leq M \leq L$, free parameter)
→ Interferences between amplitudes

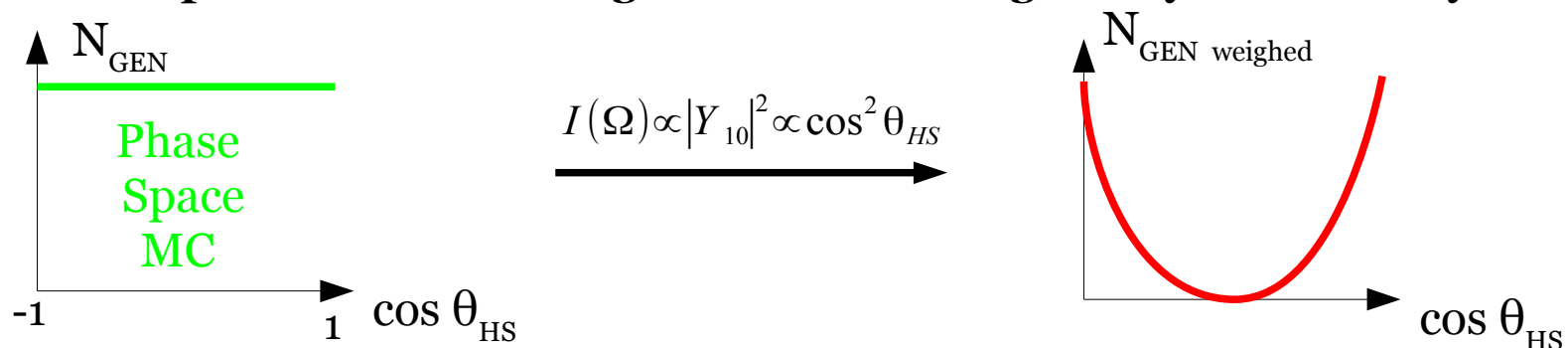
Spherical Harmonics

Fit of the intensity (AmpTools)²

Minimisation of $-\ln L = \underbrace{-\left(\sum_i^n \ln(I(\tau_i, \vec{x}))\right)}_{\text{Experimental data}} + \underbrace{\frac{1}{N^{GEN}} \sum_{k=1}^{NREC} I(\tau_i)}_{\text{e}\pi^+\pi^- \text{ Monte Carlo accepted by CLAS (Acceptance correction term)}}$

$\tau_i = (\theta, \Phi)$
 $\vec{x} = \langle Y_{LM} \rangle$

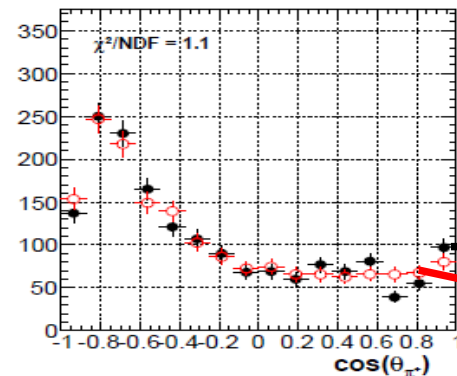
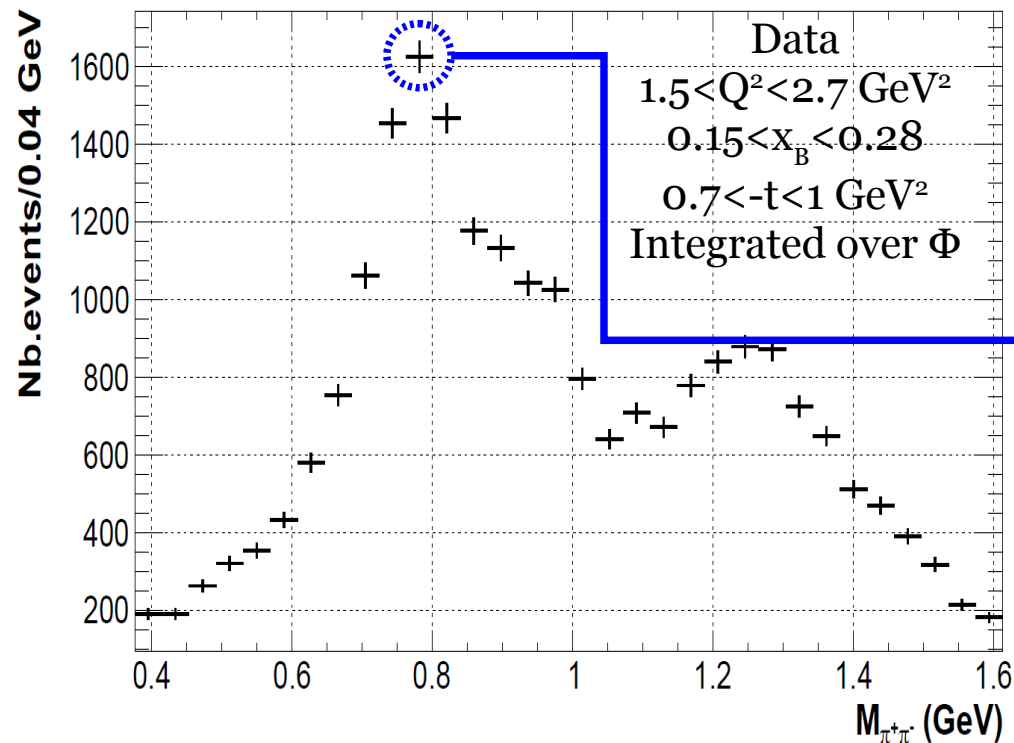
Acceptance corrected angular distribution given by the intensity



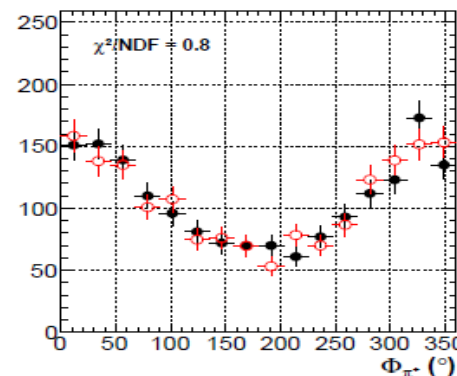
¹ M. Battaglieri *et al*, Phys.Rev. D80 (2009) 072005

² <http://sourceforge.net/projects/amptools/>

Fit of the moments to the data

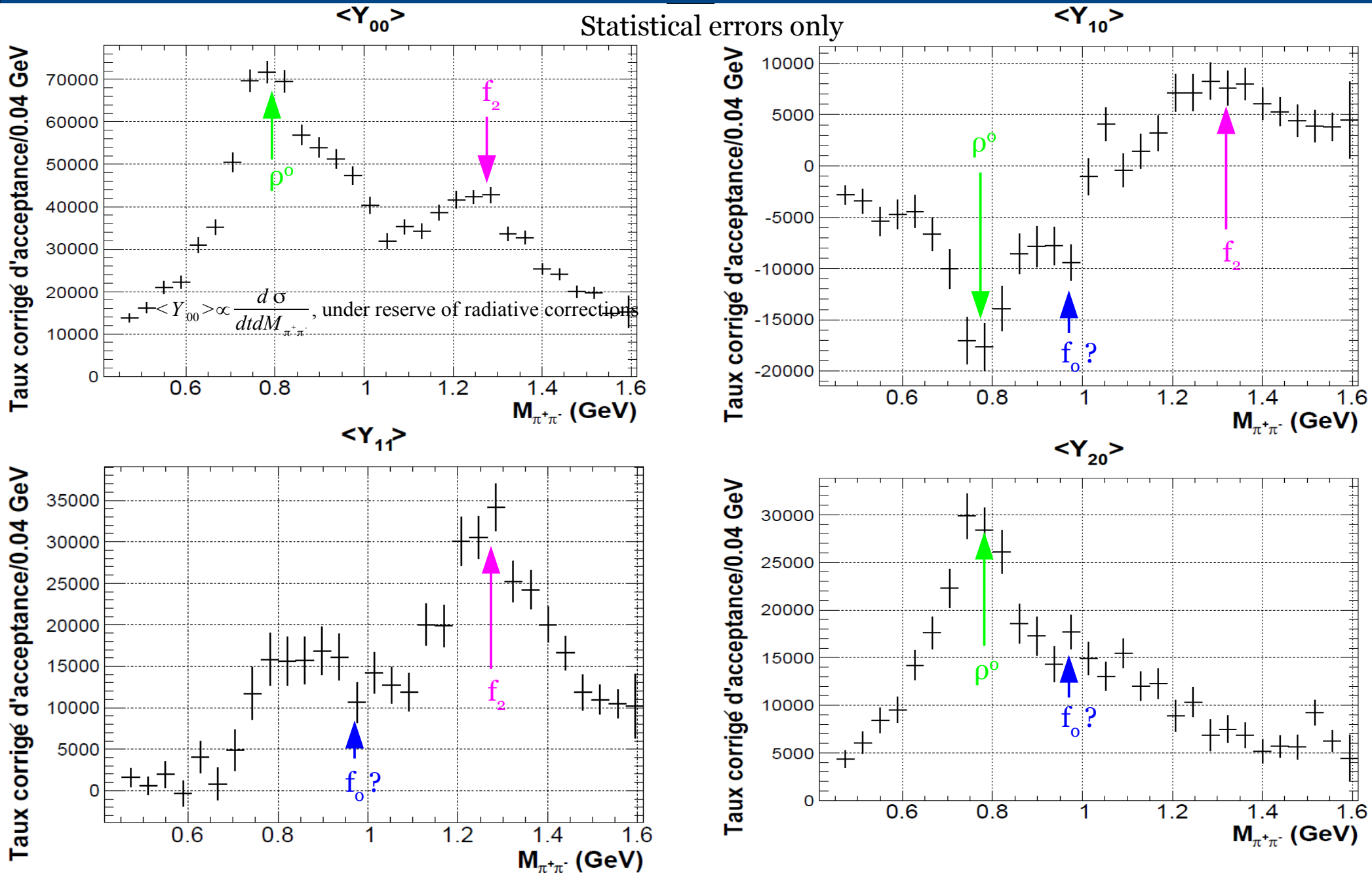


→ Data
→ Fitted intensity with CLAS acceptance



- **Mass independent fit.**
- Several **fit scenarios (8) tried**, 1 with parameters set to 0 and randomly initialised parameters for the others. Kept fit with the **best -ln L**.
- **Fit quality** checked by comparing π^+ angular distributions from the **data** with those predicted by the **intensity reconstructed by CLAS**.
- **Good agreement between the fit and the data.**

Moments of angular distributions: results



→ ρ^0 and f_2 resonances clearly visible. Possible hint of f_0 with a small width ($\Gamma \sim 40$ MeV).

1. Introduction and physics motivations

2. Experimental setup

3. Cross section for $f_0(980)$ and $f_2(1270)$

4. Moments Analysis of 2-pion electroproduction

5. PMT calibration for the Central Neutron Detector (CLAS12)

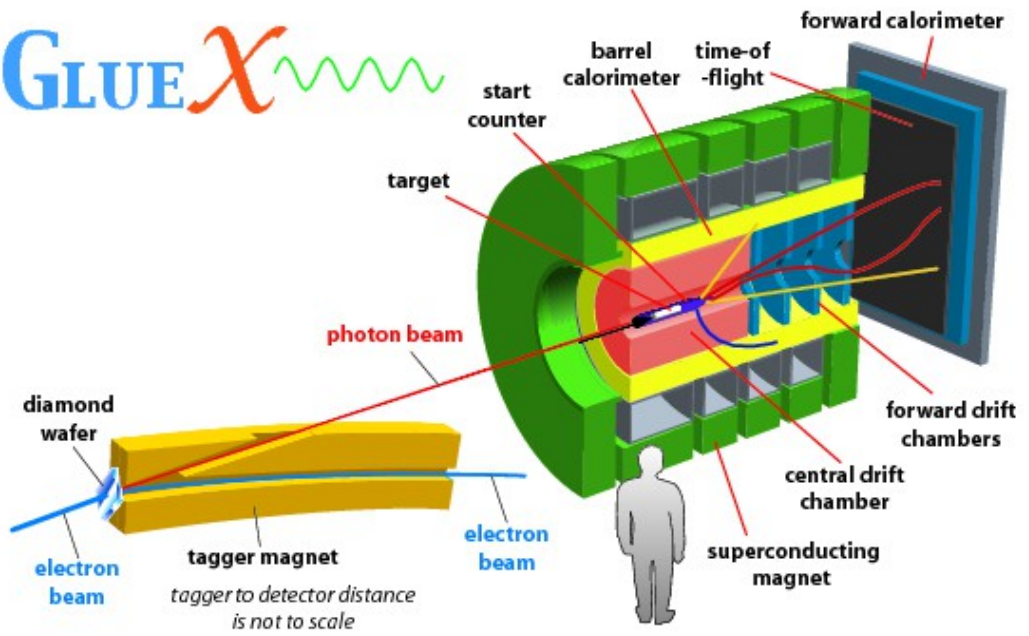
6. Conclusions

Conclusions

- **First cross section measurements** of exclusive $f_0(980)$ et $f_2(1270)$ electroproduction off the proton.
→ $-t$, Φ and $\cos \theta_{\text{HS}}$ -dependence studied.
- $f_0(980)$ and $f_2(1270)$ in a region **strongly contaminated by the background**.
→ Large systematic errors.
Limited by our knowledge of the background.
Analysis note is ongoing.
- **First attempt of a partial waves analysis** on $ep \rightarrow e\pi^+\pi^-$. **(Work in progress)**
→ Underconstrained fit : partial waves decomposition to be worked out (parity conservation?)
→ Statistics is currently limited, forbidding a fully differential extraction of partial waves amplitudes.
→ How to deal with radiative corrections?
- Alternative analysis by determining **moments of decay angular distributions**.
→ f_2 resonance visible. f_0 to be confirmed with larger statistics
Analysis limited by the statistics
(With higher luminosity, analysis with large Q^2 , x_B intervals and fine t , Φ , M bins might be possible)
- Central Neutron Detector (CLAS12) : gain calibration of the PMTs

Future prospects

GLUE X



- GlueX detector :
 - High intensity polarized photon beam
 - Uniform acceptance (azimuthal especially)
 - Commissioning under completion

- **Light meson spectroscopy → $f_0(980)$**

$\gamma p \rightarrow p\pi^+\pi^-$
 → 6 GeV done (first measurement of f_0)
 → Complete the analysis at 12 GeV (achievable with GlueX I ?)

$\gamma p \rightarrow pK^+K^-$
 → f_0 at threshold
 → K identification improved by addition of DIRC in Hall D(2018)

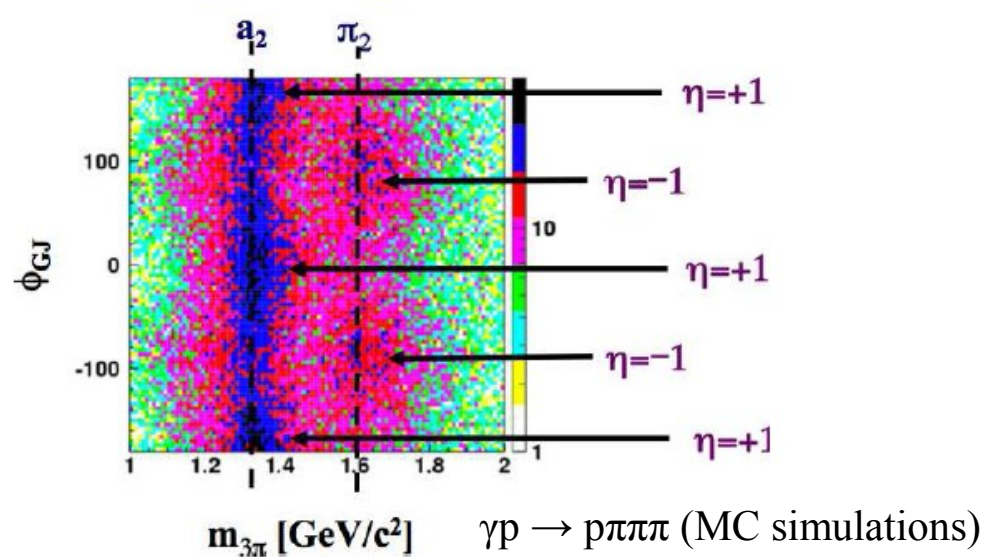
$f_0(1500)$ glueball?

- **Search for exotic excitations**

- Early physics expected in 2016:
 - Beam asymmetries
 - Cross sections measurements of known mesons (possibly in PWA)

Polarized photon beam
 → Filter on the naturality of exchanged particle.

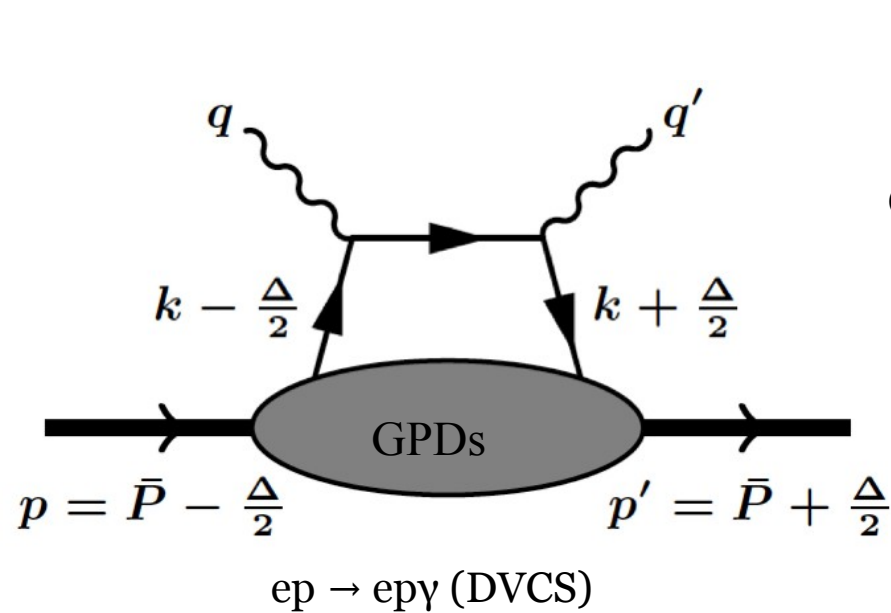
2^{++} 2^{-+}



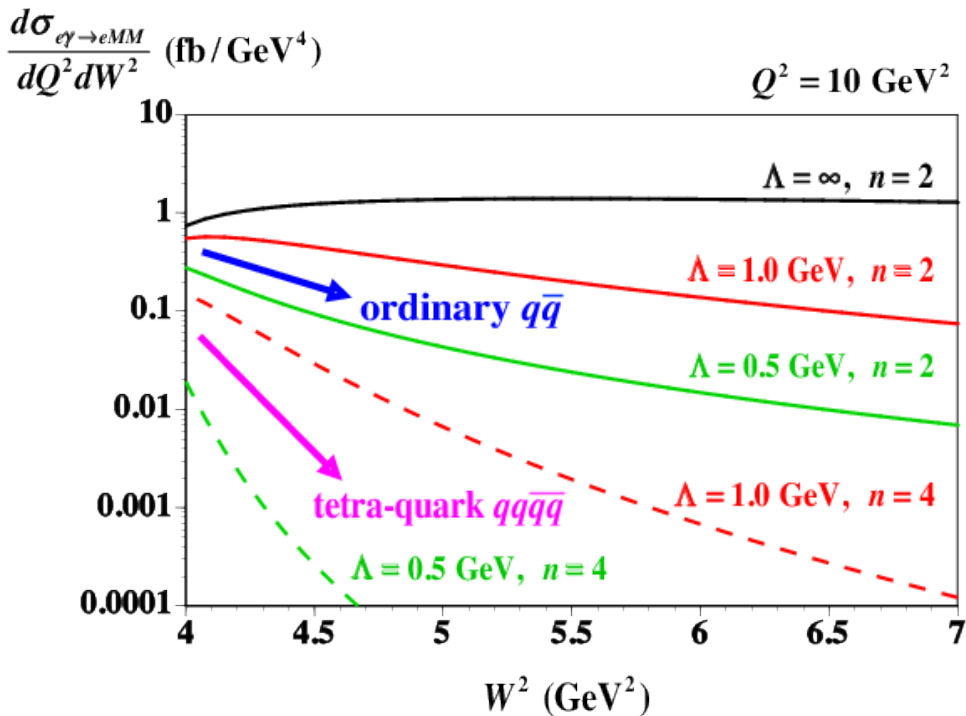
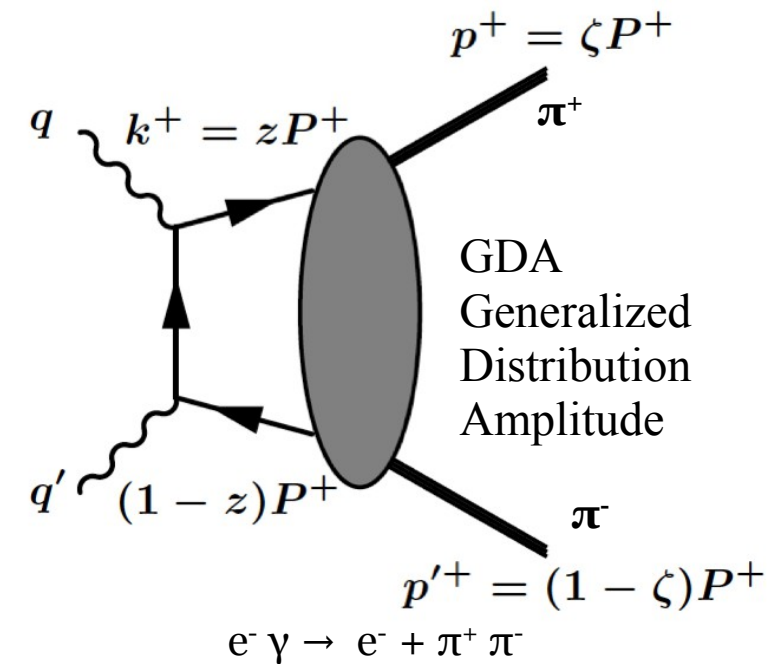
Thanks for your attention.

Backup slides

Generalized Distribution Amplitude (GDA)



Crossed diagram

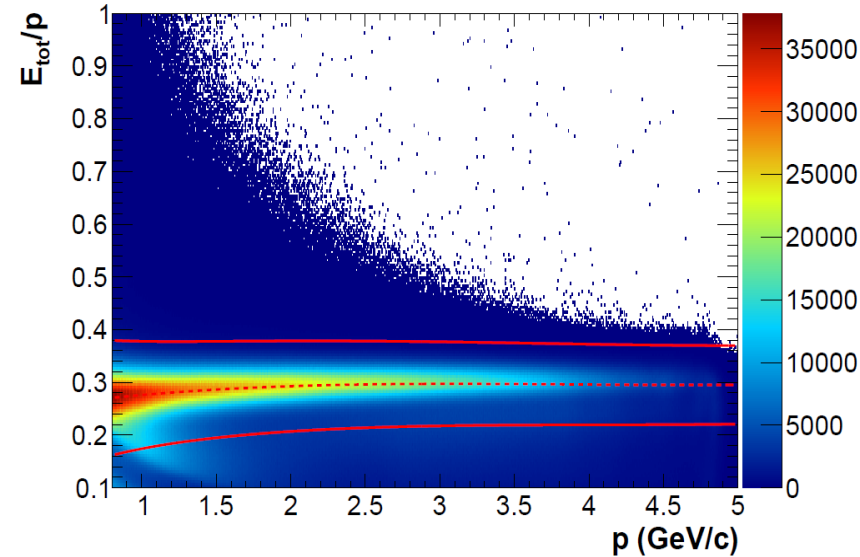


- GDA described **production of hadrons** in a **partonic picture**.
- GDA \rightarrow Different form factor according to the object's nature ($q\bar{q}$, tetraquark...)
- **Cross sections** depends on the object's **nature** described by the GDA.

Electron identification

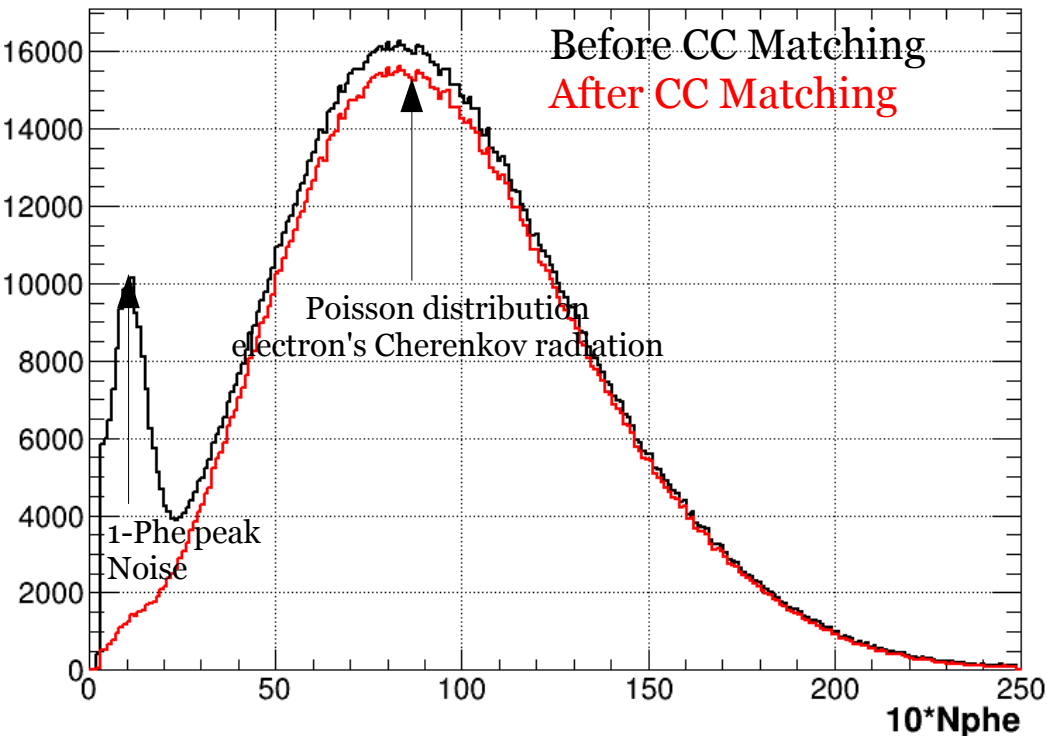
Among negative charged tracks ($q < 0$) :

- $p > 0.8$ GeV/c
- Vertex selection within the LH2 target.
- EC and CC fiducial cuts.
- Energy sampling fraction :
 - Total energy deposited/p.
 - Deposited energy fraction in Inner and Outer part of the EC.



“CC Matching”

- Photoelectron emission spectra from CC show a large number of track (**pic 1-Phe**) which are misidentified as e^- .
- Geometrical cuts on the tracks between CC and SC.
- Cuts on the time-of-flight between CC and SC.
- Significant reduction of e^-/π^- contamination



Photoelectron emission spectrum from the 2 photomultipliers in module #7 sector 3

Proton and π^+ identification

Among e-X selected events:

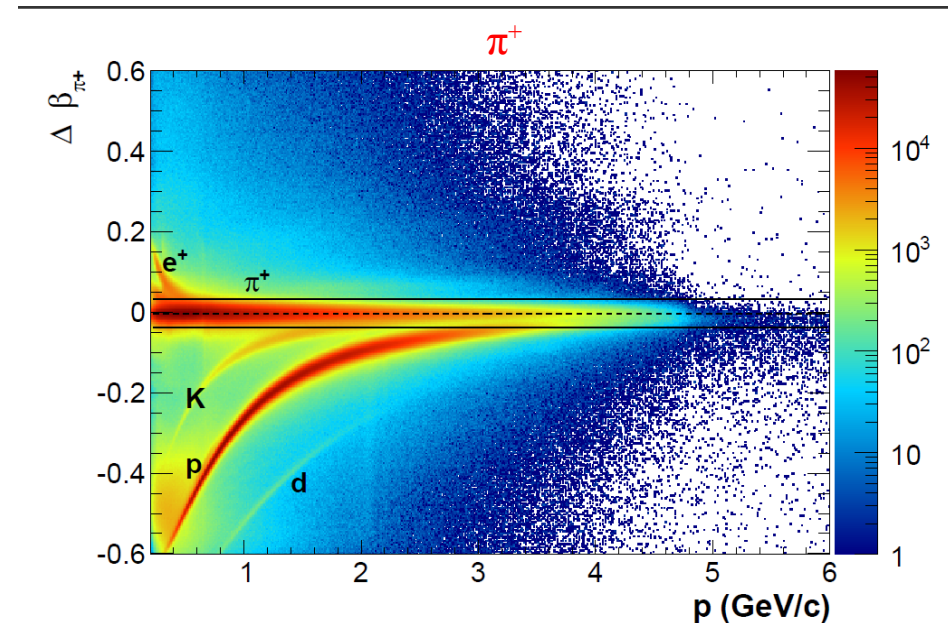
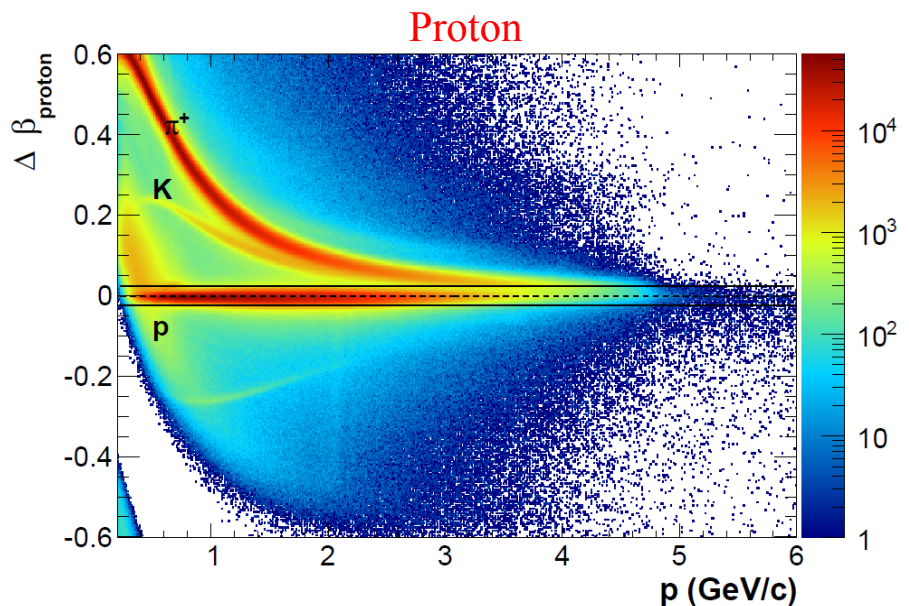
- $q < 0$ and $p > 0.2$ GeV/c
- Fiducial cuts in θ and φ .
- Vertex selection within the target volume.
- **Proton and π^+ identified by time-of-flight measurements :**

Predicted velocity for a particle with given mass m

$$\Delta\beta_m = \beta_{mes} - \beta_{calc}(m) = \frac{l}{ct} - \frac{p}{\sqrt{p^2 + m^2}}$$

Measured velocity \rightarrow β_{mes}
 Target-SC distance \rightarrow l
 Momentum (DC) \rightarrow p
 Time of flight (SC) \rightarrow ct

\rightarrow 2.5 σ cuts on $\Delta\beta_p$ and $\Delta\beta_{\pi^+}$



Exclusive $e p \rightarrow e' p' \pi^+ \pi^-$

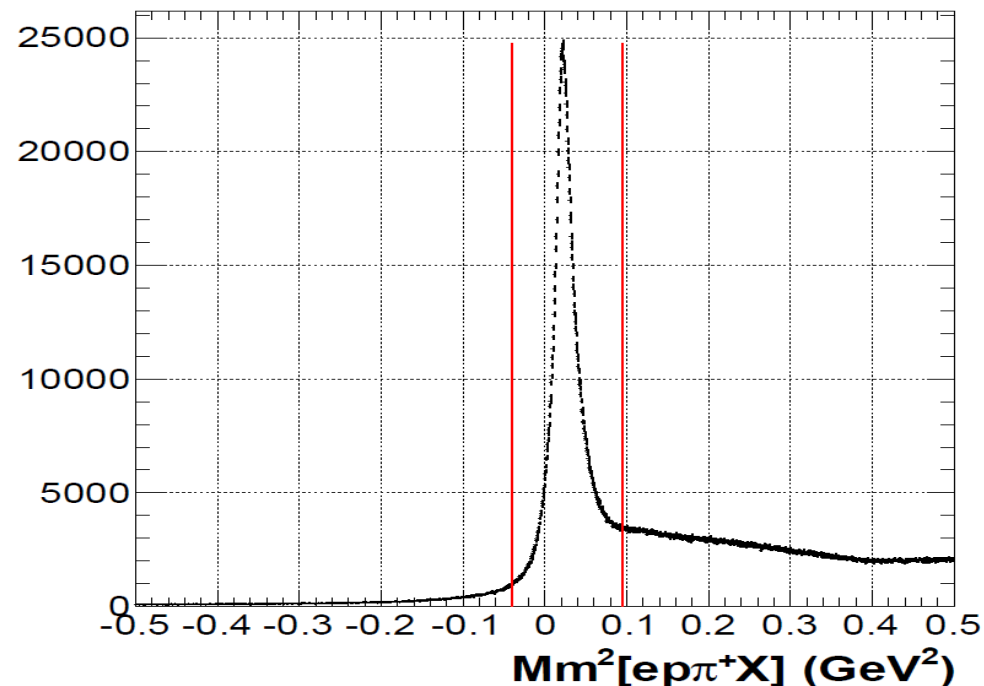
Among $e p \pi^+ X$ selected events :

- Selection on the missing mass $Mm[e p \pi^+ X]$:

$$p_X = p_p + p_e - (p_{e'} + p_{p'} + p_{\pi^+})$$

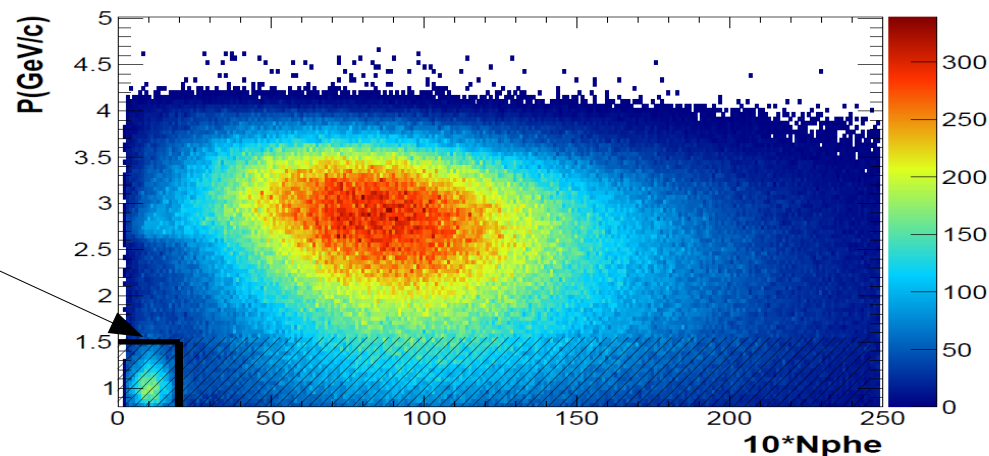
Cuts around the π -peak:

$$-0.05 \leq Mm^2[e p \pi^+ X] \leq 0.08 \text{ GeV}^2$$



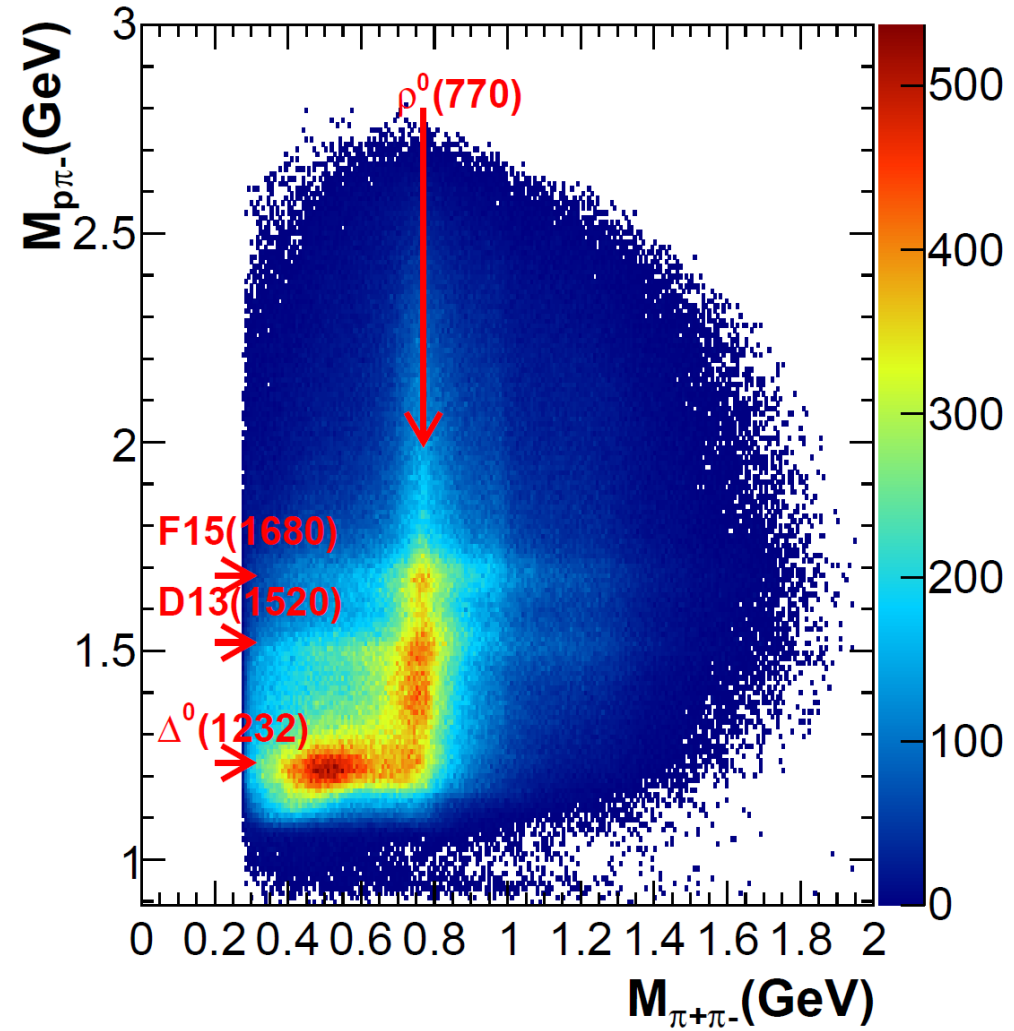
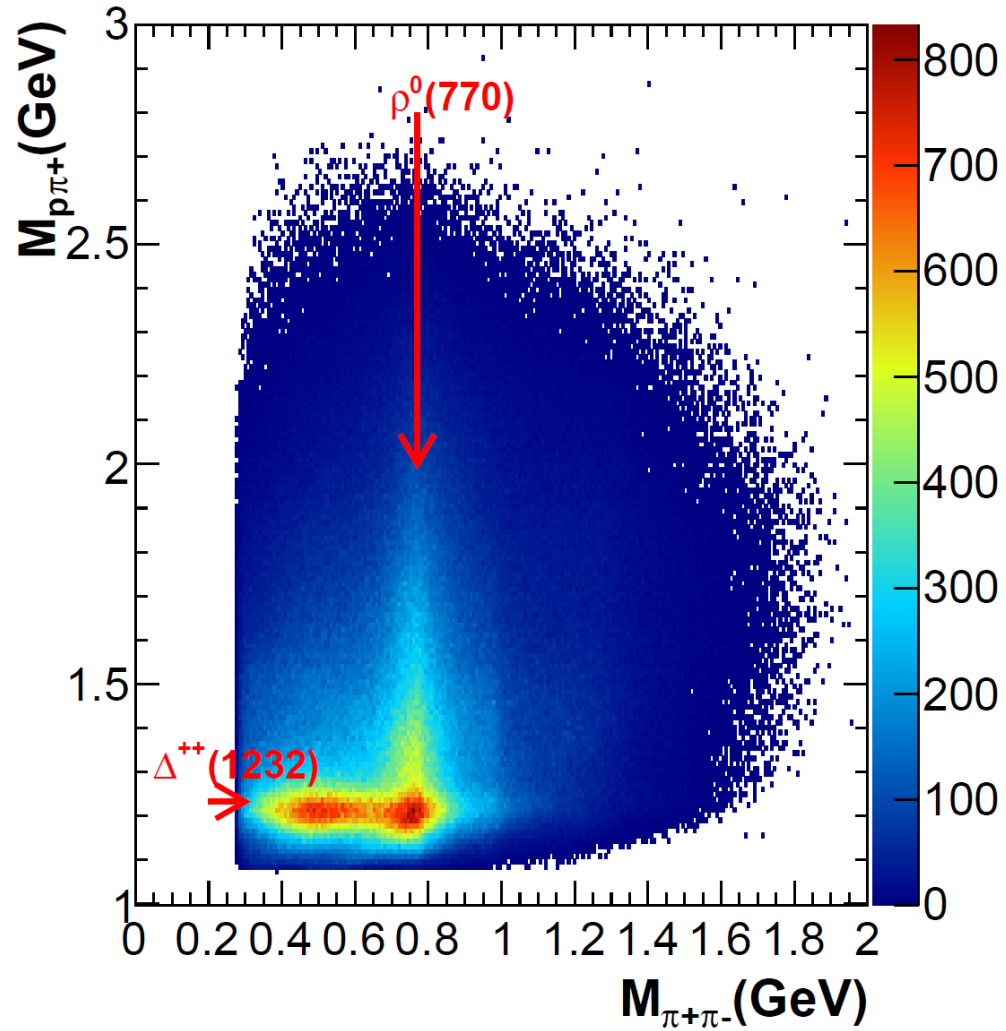
- 1-Phe peak (CC) remains after the missing mass cut for $p_{e^-} < 1.5 \text{ GeV}/c$.

→ $(p_{e^-}, N_{phe}) = [0.8; 1.5] \times [0, 300]$ region excluded

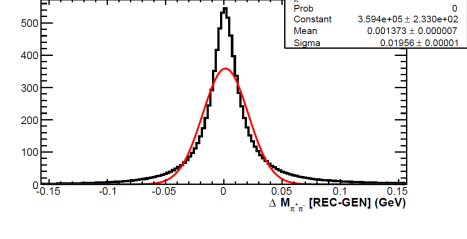
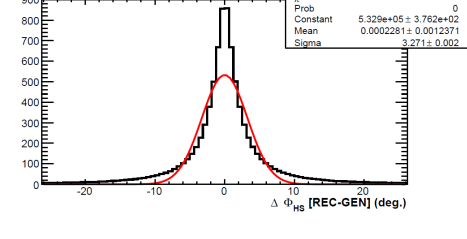
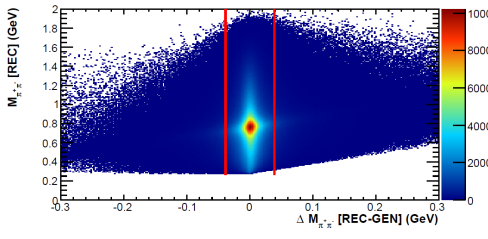
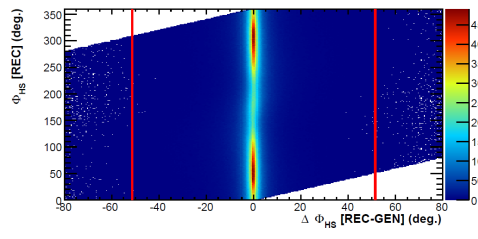
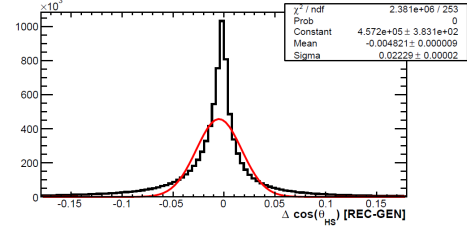
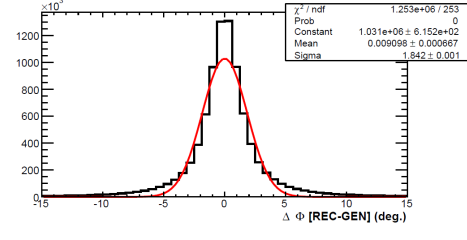
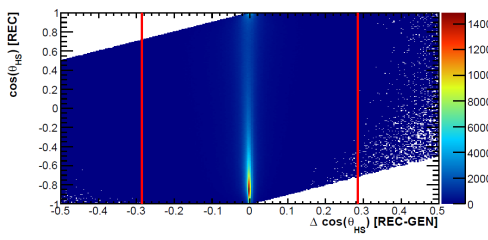
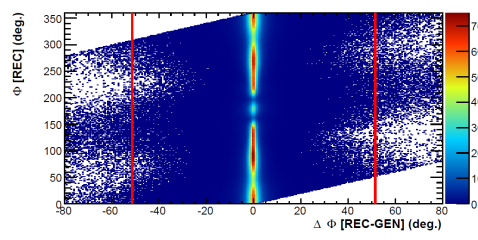
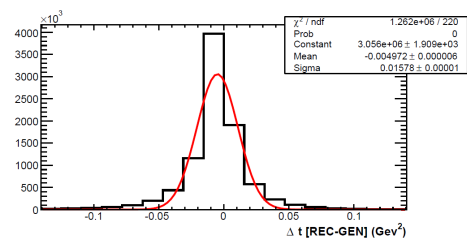
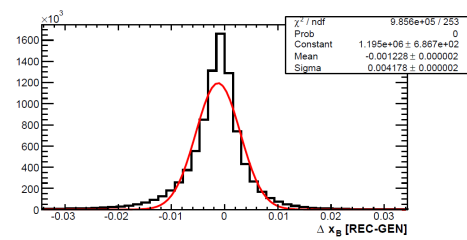
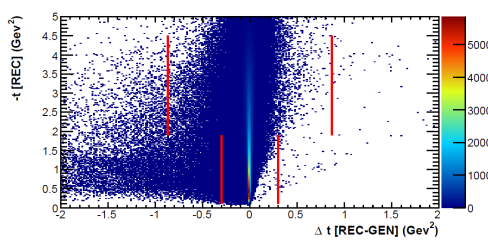
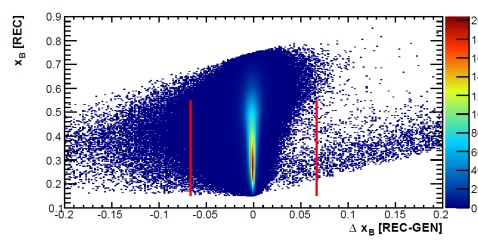
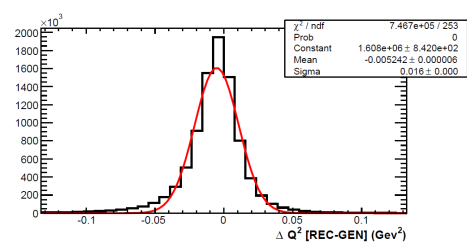
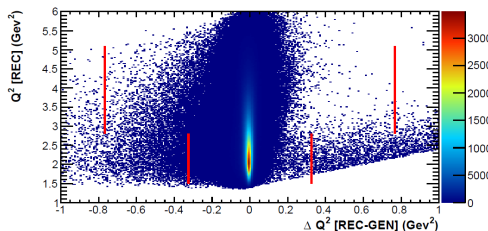
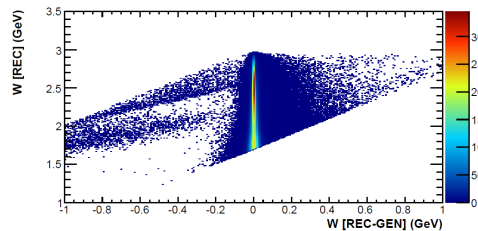


- Cuts on Z vertex difference between the proton and electron, the pion and the electron.

Dalitz plots



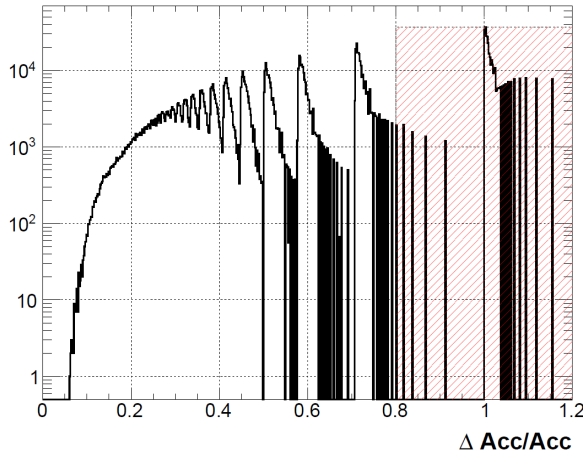
Kinematic resolutions



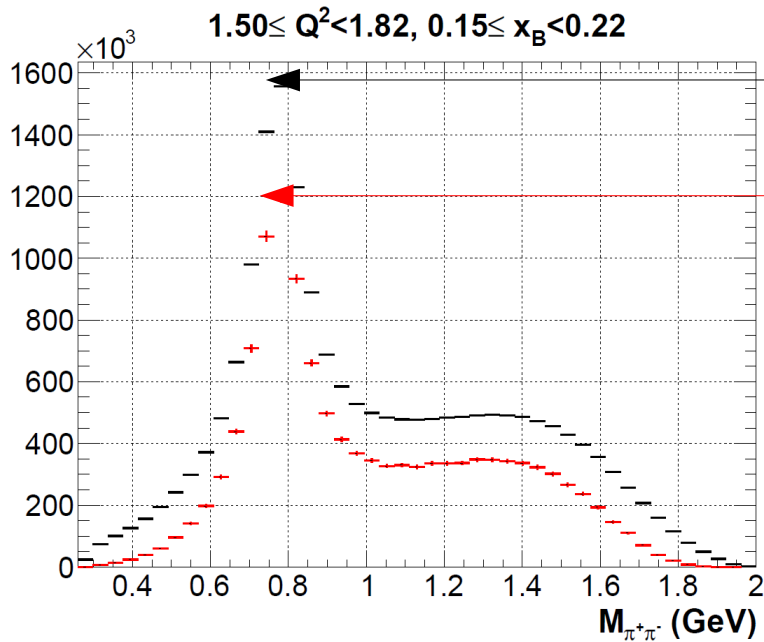
Acceptance correction

- $Acc_{\text{Corr Rad}}$ computed for each $(Q^2, x_B, t, \Phi, \cos \theta_{\text{HS}}, \Phi_{\text{HS}}, M_{\pi\pi})$ 7D bin and applied as an event-by-event weight.

- 7D bins with large relative error **rejected** :



$$\frac{\Delta Acc}{Acc} < 80\%$$



Generated Monte Carlo without radiative effects

Monte Carlo events accepted by CLAS (w/ rad. Effects) , corrected by the 7D acceptance

- 7D acceptance correction on reconstructed MCis not able to retrieve all generated events

→ Hole factor correction F_h

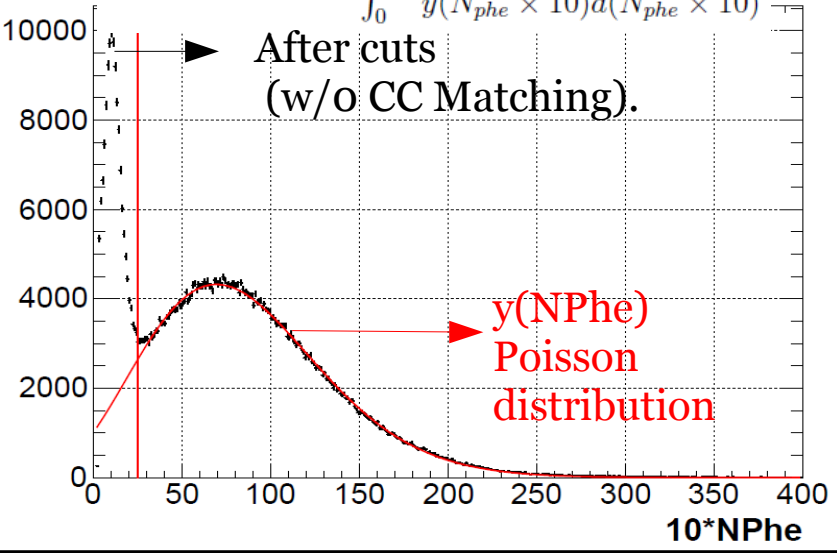
$$F_h(Q^2, x_B, \nu, M_{\pi^+\pi^-}) = \frac{h_{\text{Gen non rad}}(Q^2, x_B, \nu, M_{\pi^+\pi^-})}{h_{\text{Corr Acc 7D}}(Q^2, x_B, \nu, M_{\pi^+\pi^-})}$$

- (Q^2, x_B, ν) bins with a strong hole factor correction are **rejected** :

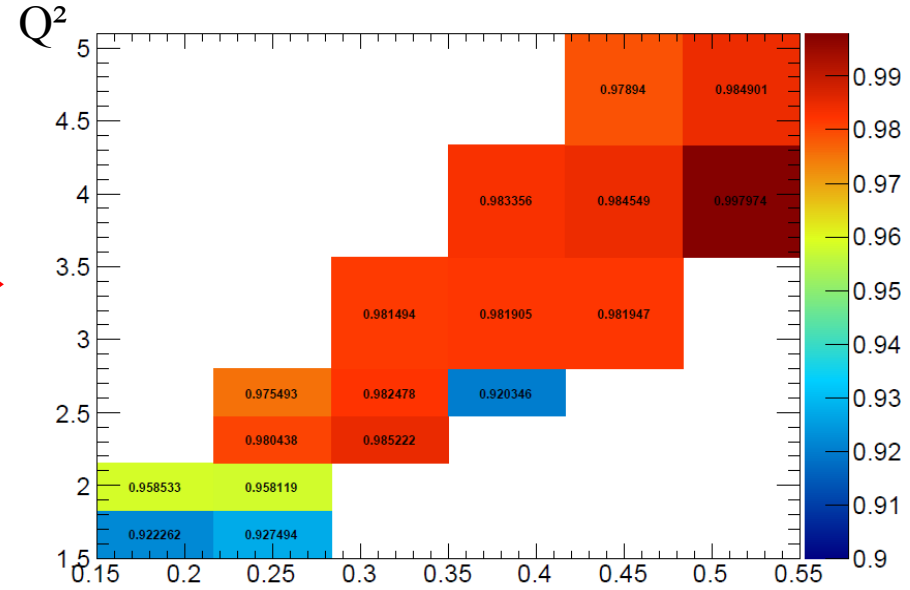
$$\bar{F}_h(Q^2, x_B, \nu) > 30\%$$

CC selection cuts are applied only to the data
 → Need to estimate the good electrons rejected by these cuts

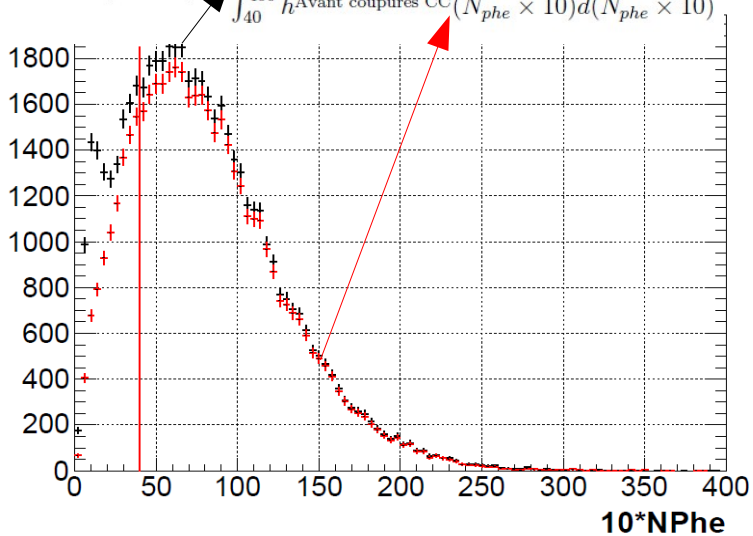
$$Eff_{CC}(Q^2, x_B) = \frac{\int_{25}^{250} y(N_{phe} \times 10) d(N_{phe} \times 10)}{\int_0^{250} y(N_{phe} \times 10) d(N_{phe} \times 10)}$$



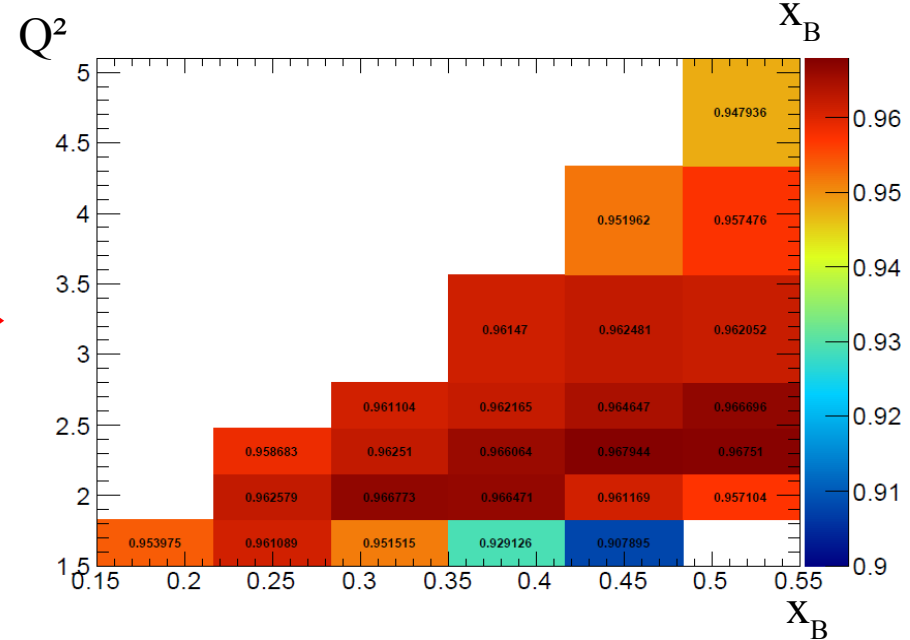
e-X
 $1.82 < Q^2 < 2.15$
 $0.15 < x_B < 0.22$
 $p_{e^-} < 1.5 \text{ GeV}/c$



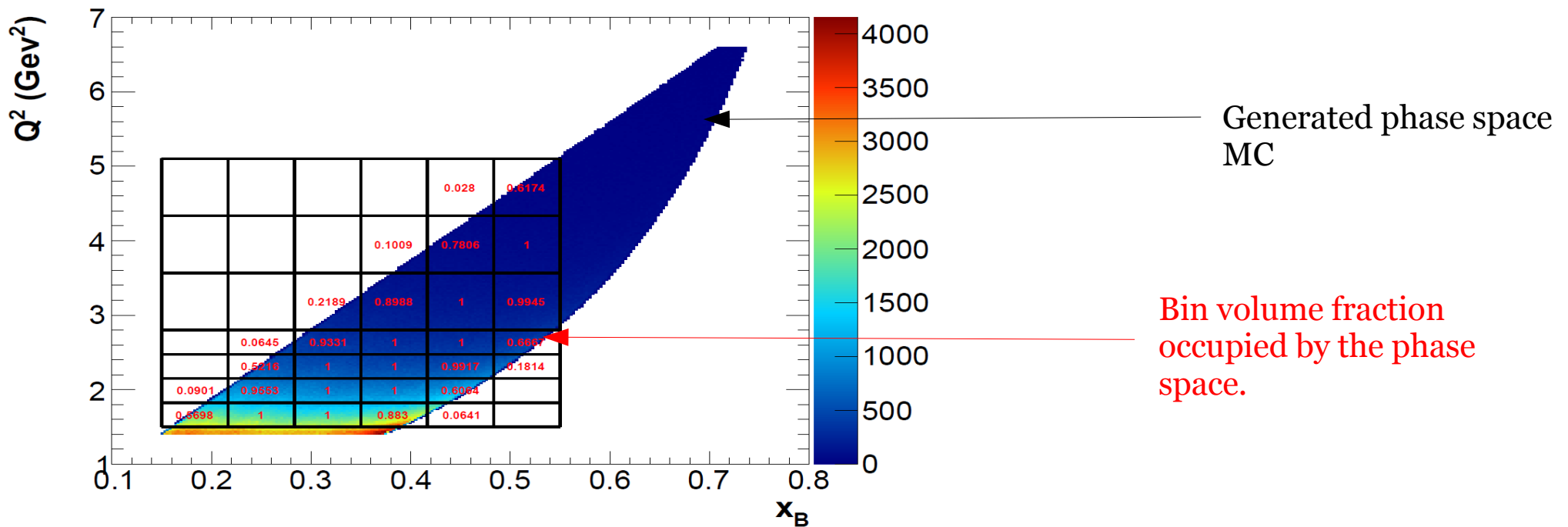
$$Eff_{CC}(Q^2, x_B) = \frac{\int_{40}^{400} h^{\text{Après coupures CC}}(N_{phe} \times 10) d(N_{phe} \times 10)}{\int_{40}^{400} h^{\text{Avant coupures CC}}(N_{phe} \times 10) d(N_{phe} \times 10)}$$



e-X
 $1.82 < Q^2 < 2.15$
 $0.15 < x_B < 0.22$
 $p_{e^-} \geq 1.5 \text{ GeV}/c$



Bin volume correction



- Most (Q^2, x_B) and (Q^2, x_B, t) cells are not fully filled by the phase space.
- Each cell is **subdivided into 100x100 subcells**.
- Bin volume fraction :

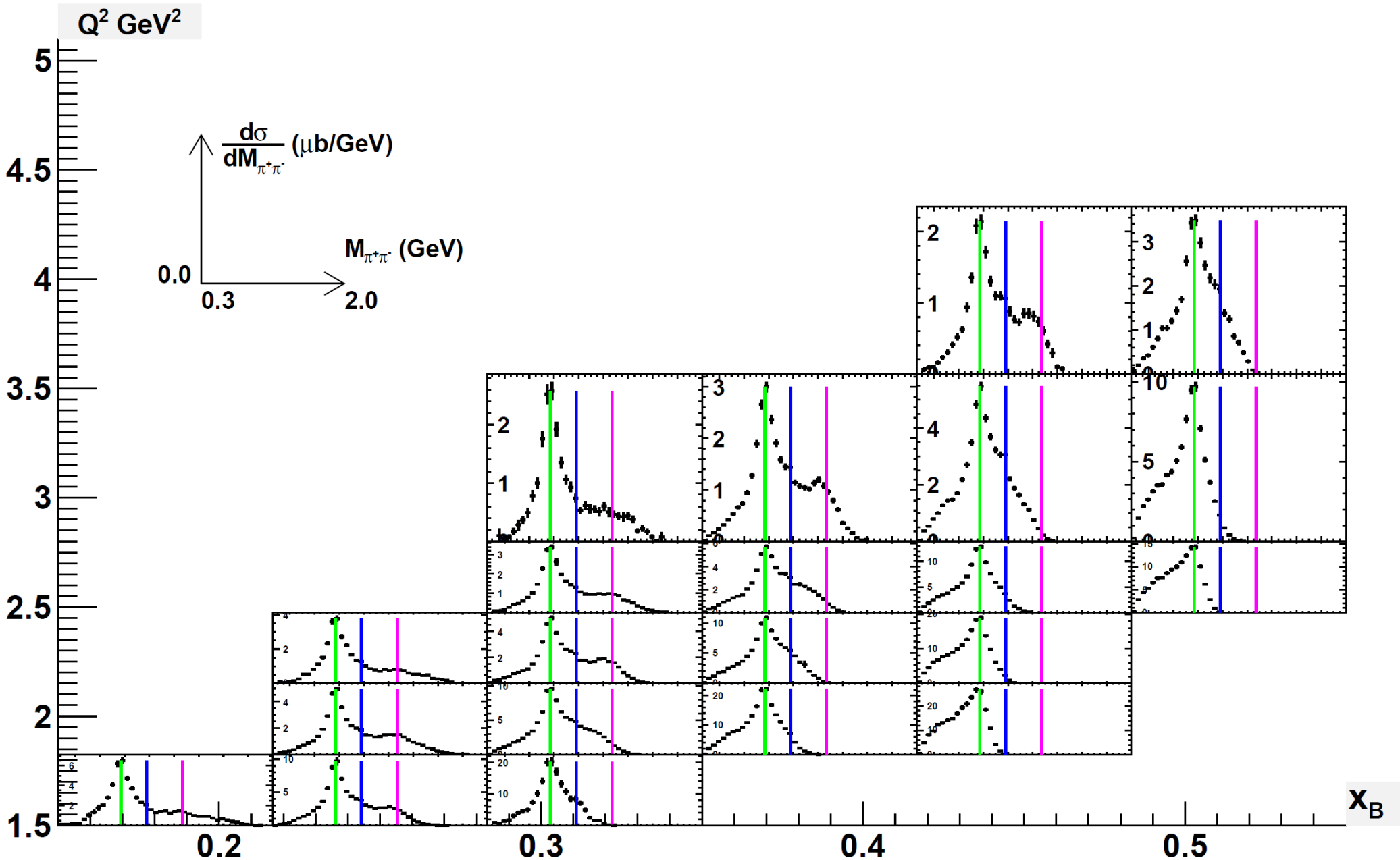
Total number of subcells

$$F_{\text{Corr Vol}} = \frac{V'}{V}$$

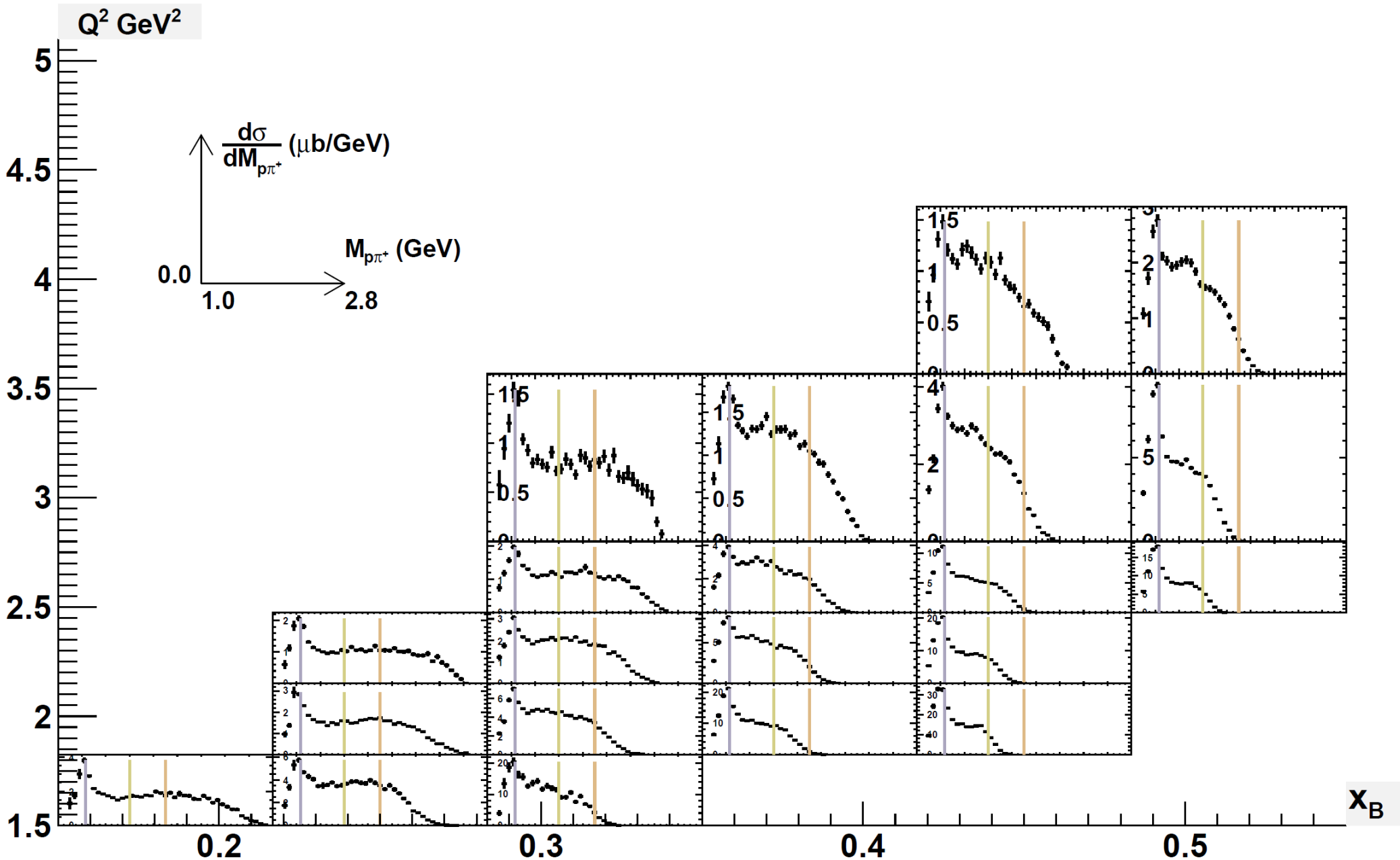
Number of subcells satisfying the cuts :

$$\begin{aligned}
 E_{\text{faisceau}} &= 5.75 \text{ GeV}, \\
 W &> 1.8 \text{ GeV}, \\
 p_{e^-} &> 0.8 \text{ GeV}/c, \quad 10^\circ < \theta_{e^-} < 90^\circ, \\
 0.1 &< \frac{v}{E_{\text{faisceau}}} < 0.95
 \end{aligned}$$

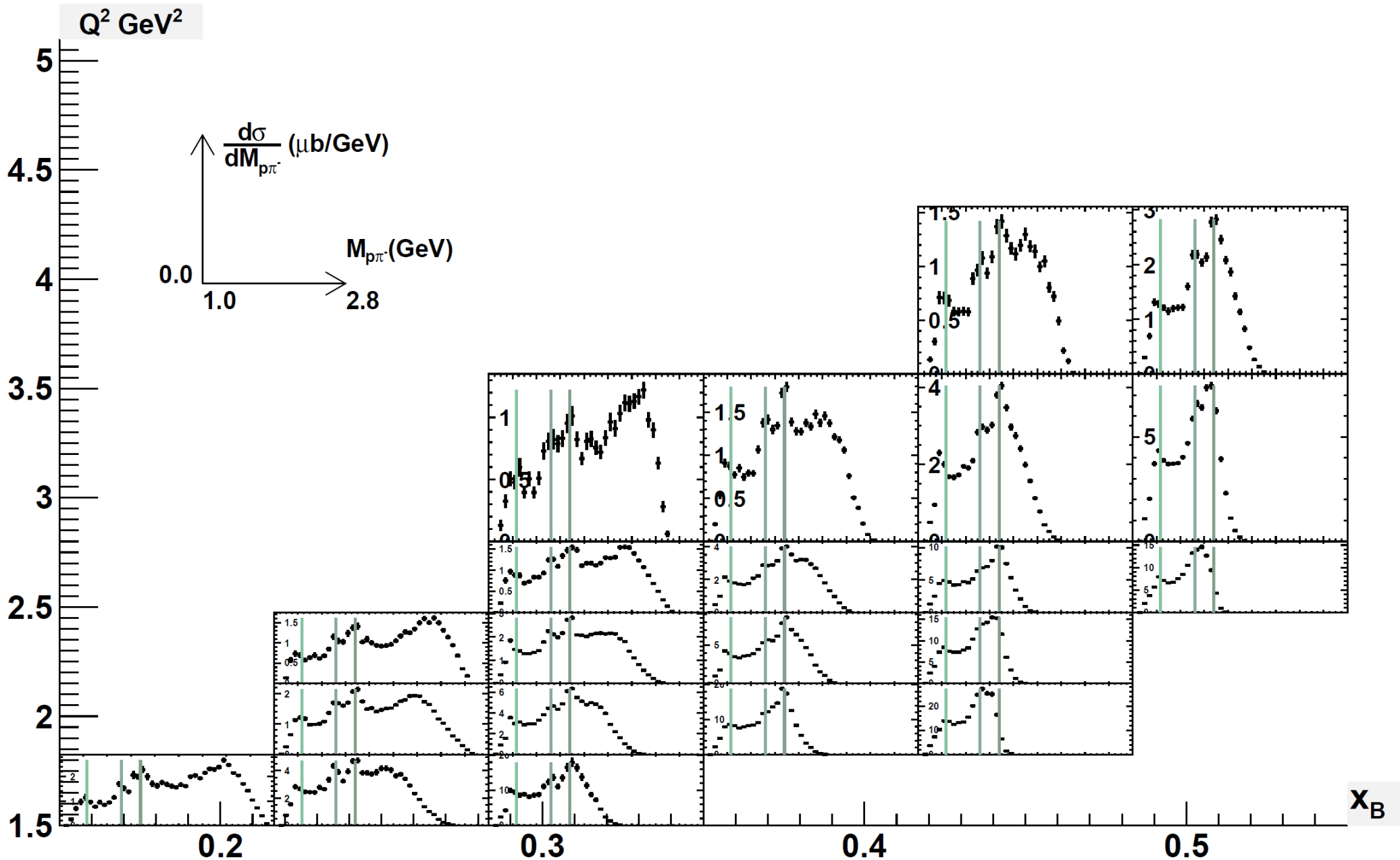
$M_{\pi^+\pi^-}$ cross sections in (Q^2, x_B)



$M_{p\pi^+}$ cross sections in (Q^2, x_B)



$M_{p\pi^-}$ cross sections in (Q^2, x_B)



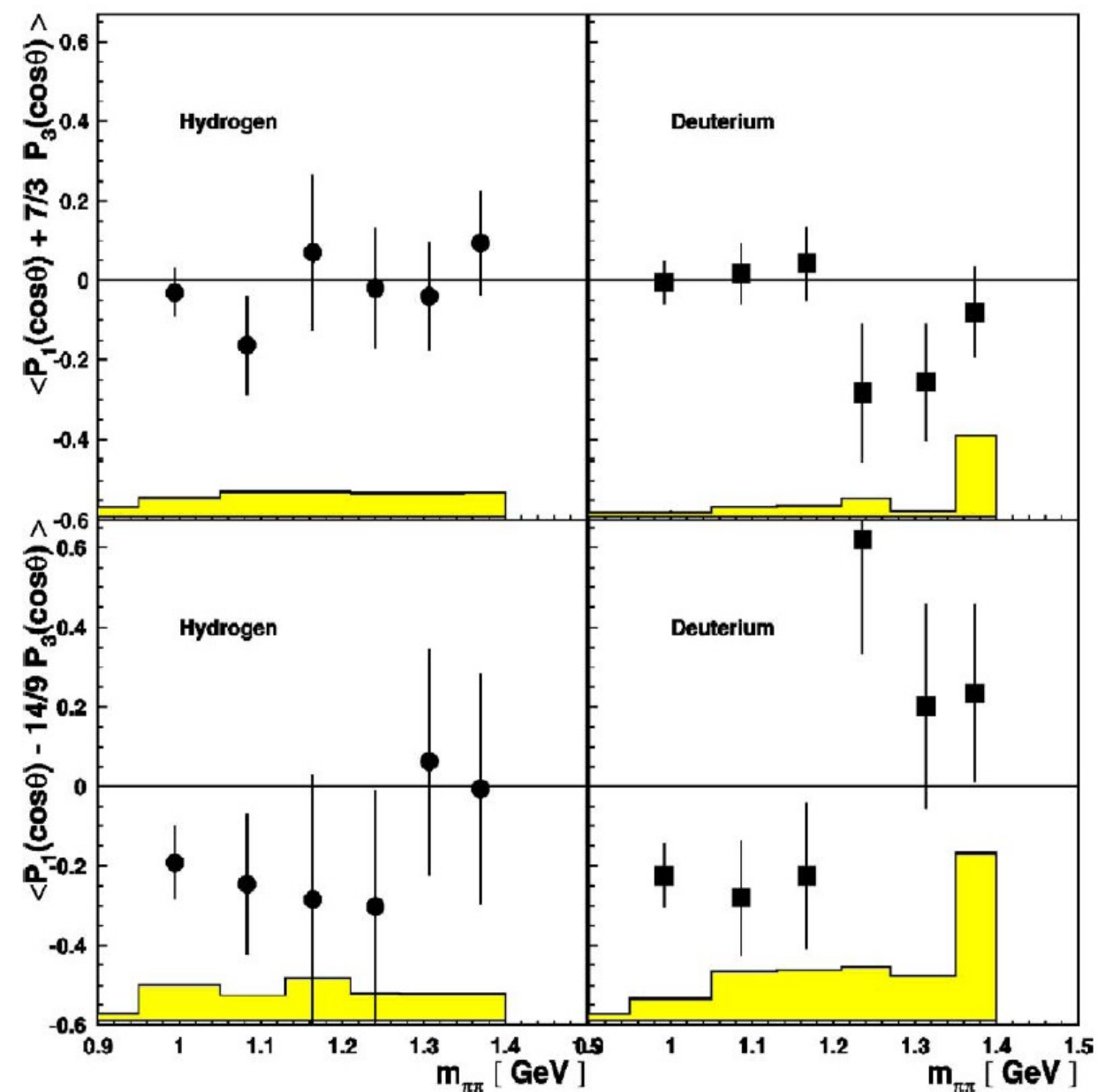
Legendre Moment (HERMES)

Airapetian et al. (Collaboration HERMES)
Phys. Lett. B 599, 212 (2004)

$$\langle Q^2 \rangle = 3.2 \text{ GeV}^2$$

$$\langle X_B \rangle = 0.16$$

$$\langle -t \rangle = 0.43 \text{ GeV}^2$$



→ Longitudinally polarised photon

→ Transversely polarized photon

Partial Waves Analysis

Parametrization¹

For each $e p \pi^+ \pi^-$ event,

$$I(\Theta, \Phi) = \sum_{L=0}^{L_{max}} \sum_{M=-L}^L V_{LM} Y_{LM}(\Theta, \Phi), \quad L_{max}=2, \quad |M| \leq 1$$

Intensity

Amplitudes (free complex parametre)

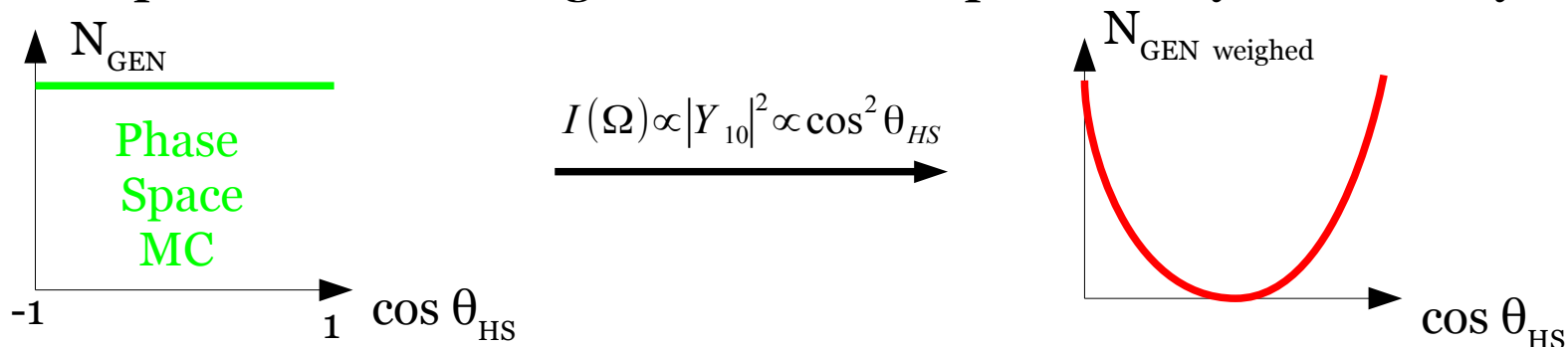
Spherical Harmonics

Fit of the intensity (AmpTools)²

Minimisation of $-\ln L = \underbrace{-\left(\sum_i^n \ln(I(\tau_i, \vec{x}))\right)}_{\text{Experimental data}} + \underbrace{\frac{1}{N^{GEN}} \sum_{k=1}^{NREC} I(\tau_i)}_{\text{ep}\pi^+\pi^- \text{ Monte Carlo accepted by CLAS (Acceptance correction term)}}$

$\tau_i = (\theta, \Phi)$
 $\vec{x} = \langle Y_{LM} \rangle$

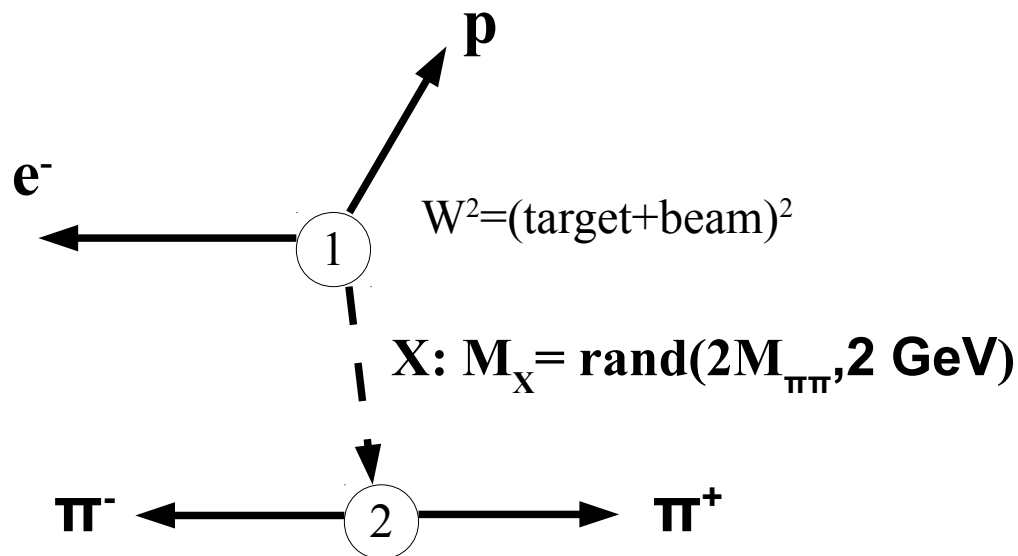
Acceptance corrected angular distribution predicted by the intensity



¹ M. Battaglieri *et al*, Phys.Rev. D80 (2009) 072005

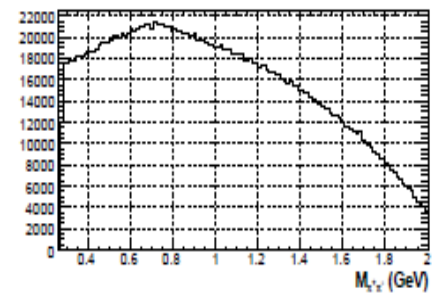
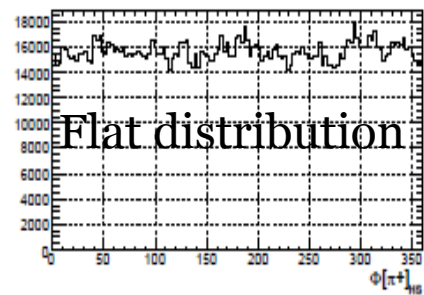
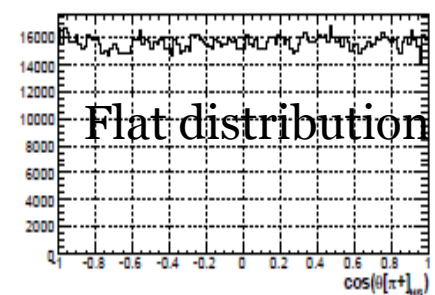
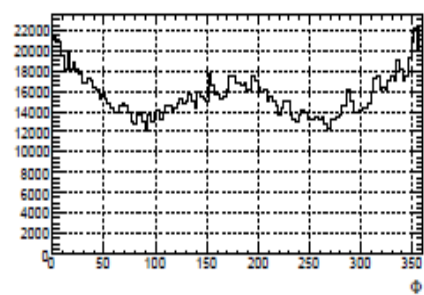
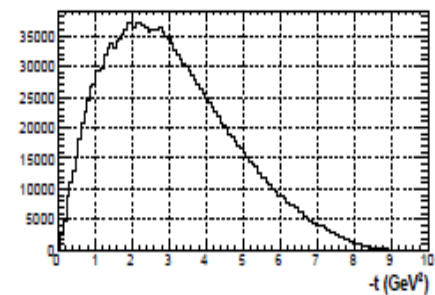
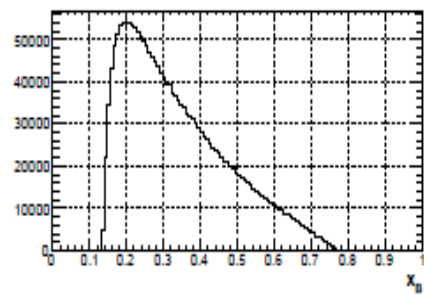
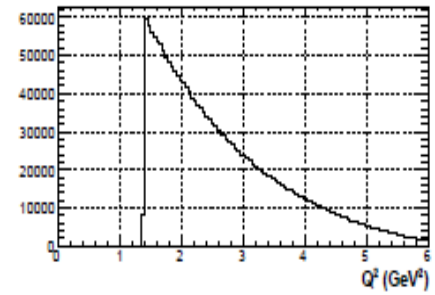
² <http://sourceforge.net/projects/amptools/>

Phase Space MC Generator

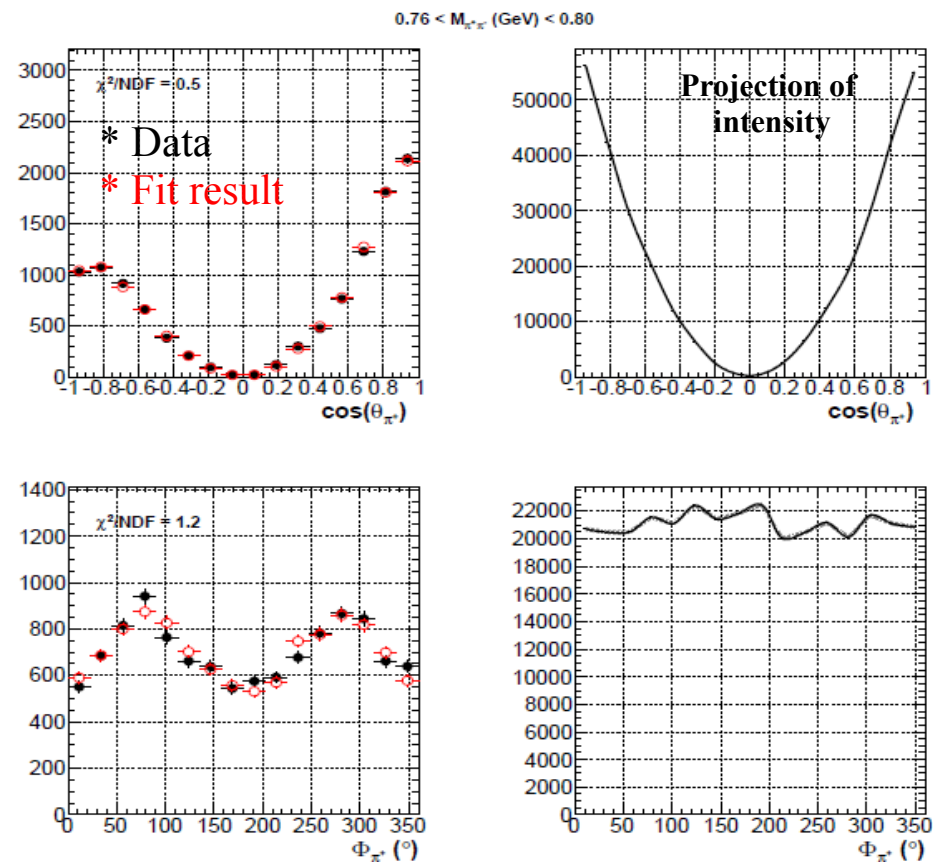
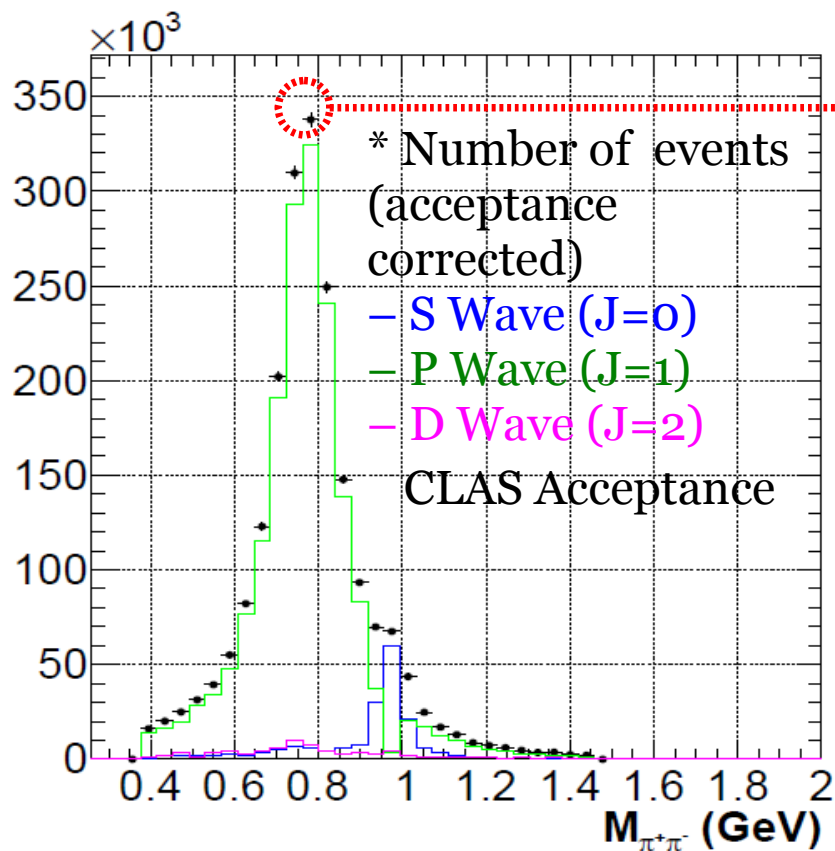


- 3 requirements :
 - Whole phase space covered
 - Uniform decay angular distribution for pion in 2 pion rest frame.
 - Particles generated according to phase space only.
- (Genbod routine).

$Q^2 > 1.4 \text{ GeV}^2$
 $W > 1.7 \text{ GeV}$



PWA on pseudo-data



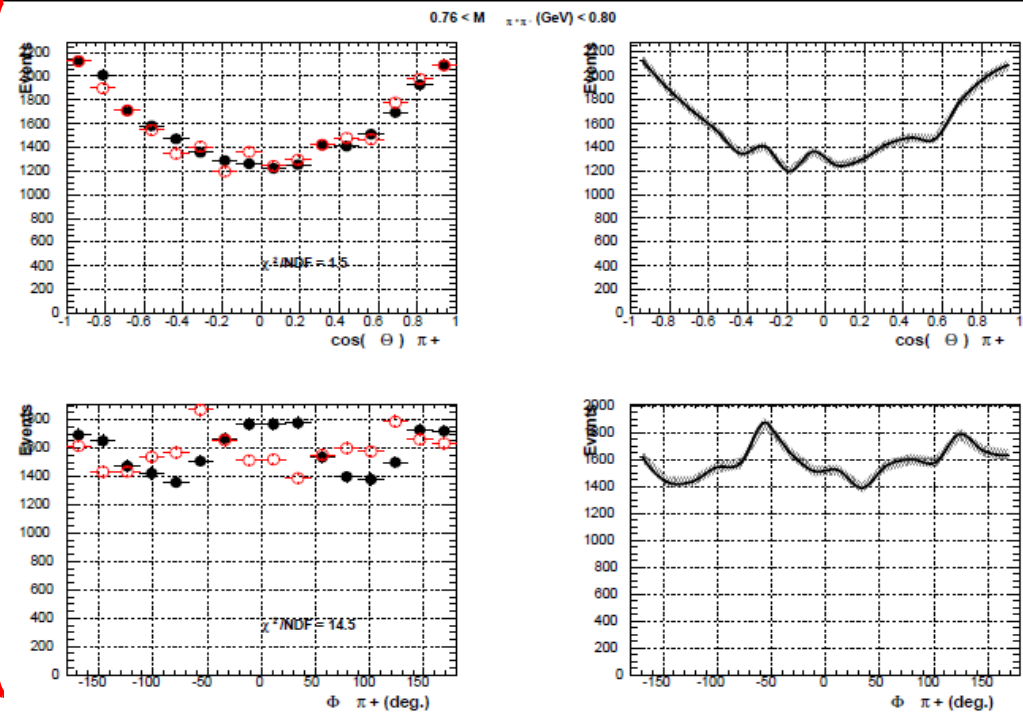
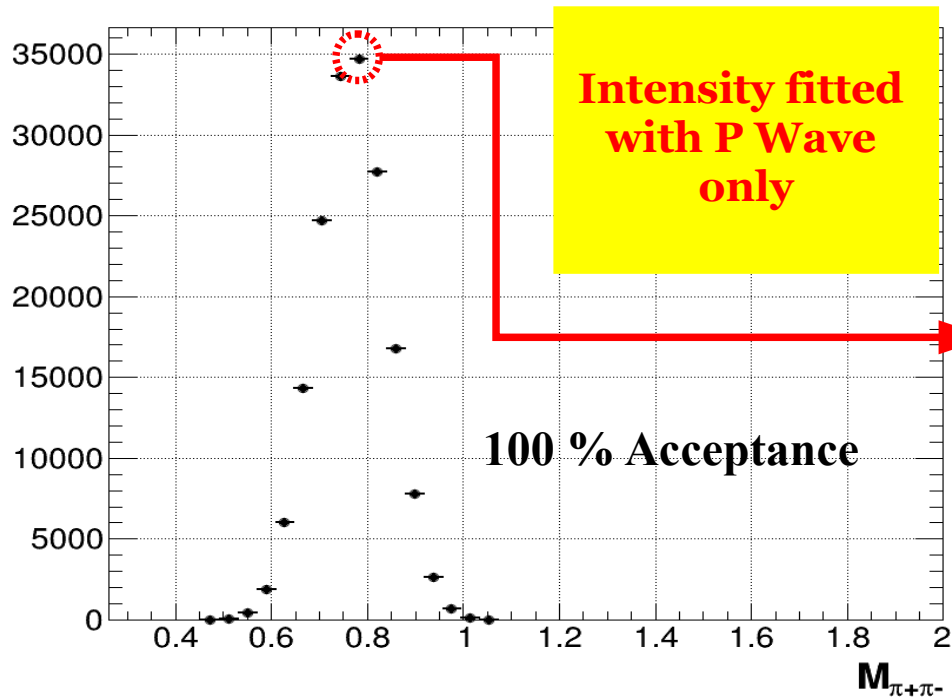
- 85K pseudo-data events extracted from accepted phase space MC with the following intensity :

$$I(\theta_{HS}, \phi_{HS}, M_{\pi^+\pi^-}) = |BW_{\rho^0}(M_{\pi^+\pi^-}) \cdot V_{10} Y_{10}(\theta_{HS}, \phi_{HS}) + BW_{f_0}(M_{\pi^+\pi^-}) \cdot V_{00} Y_{00}(\theta_{HS}, \phi_{HS})|^2$$

$\rho(770)$ Breit Wigner Amplitude 85

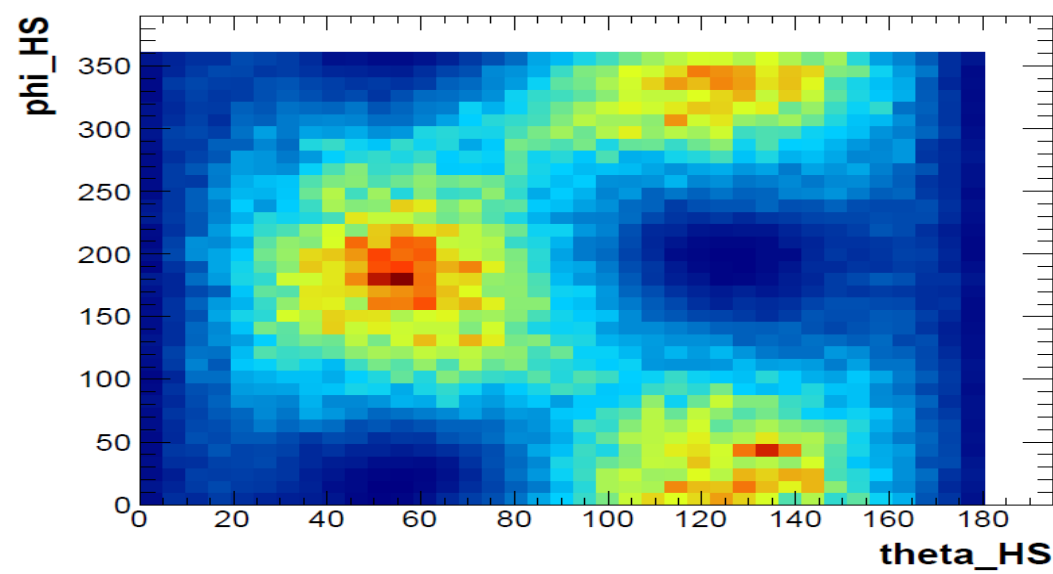
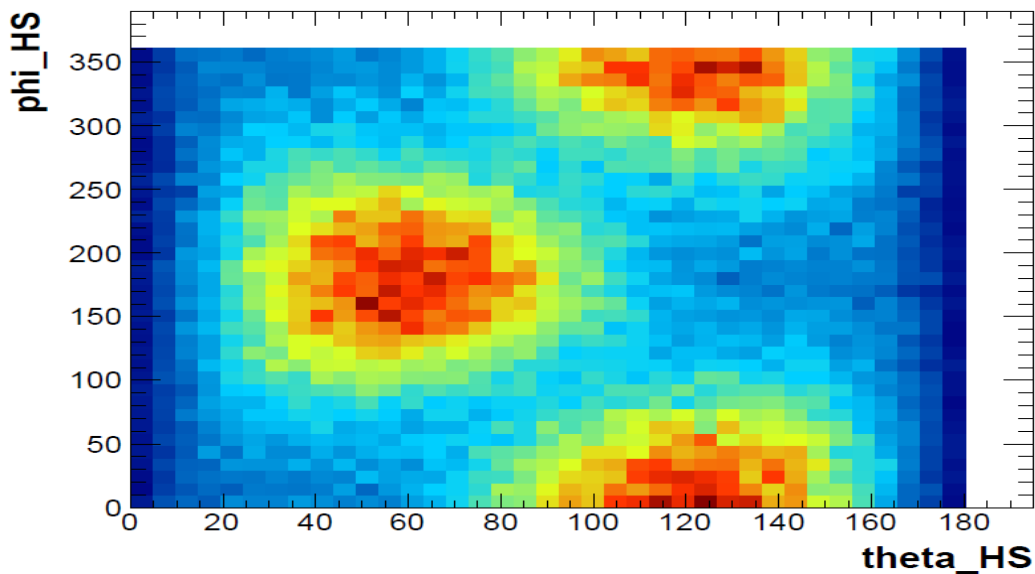
f_0 Breit Wigner Amplitude 15
 $\Gamma = 70$ MeV

- Good agreement between the fit and the data.
- Fit returns the right contributions of S and P Wave.
- PWA fit procedure in CLAS allows to separate S and P Wave in a simple case.



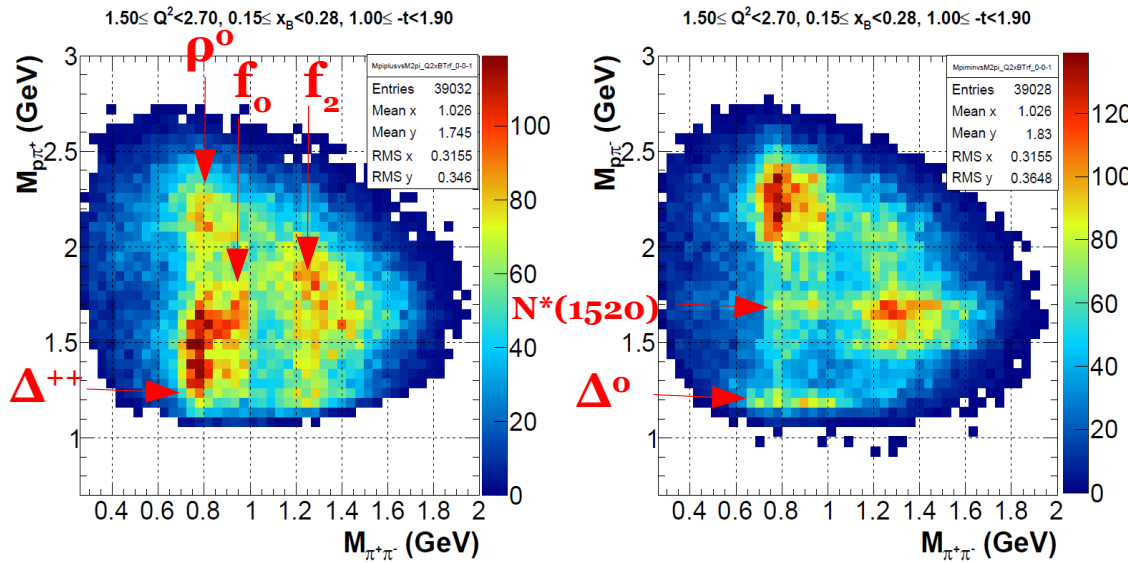
Genev ρ pseudo-data (full mass range)

Phase space weighted by the fitted intensity

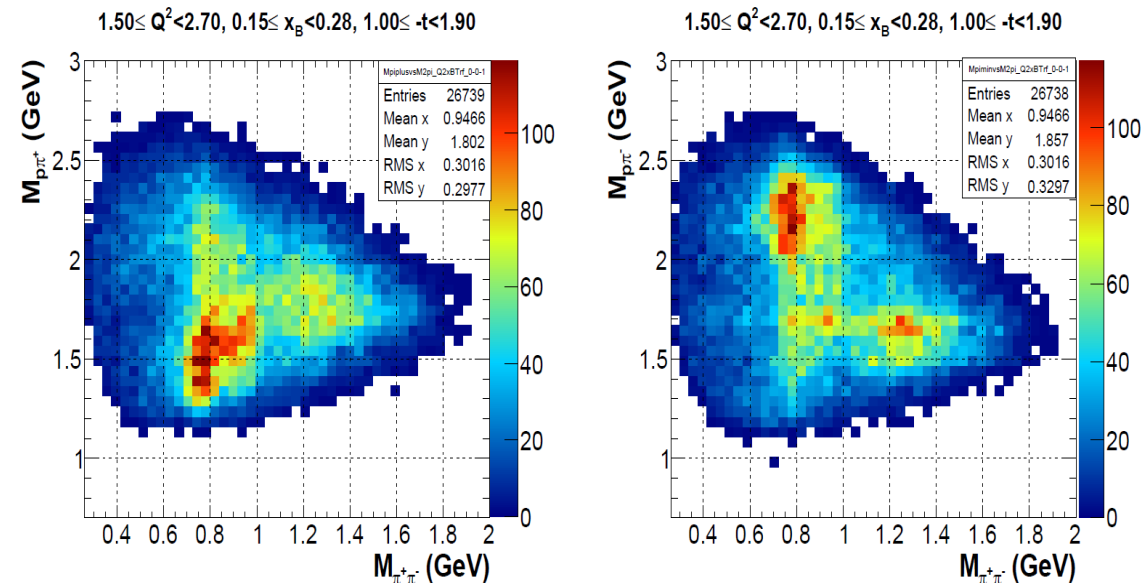


Baryon suppression

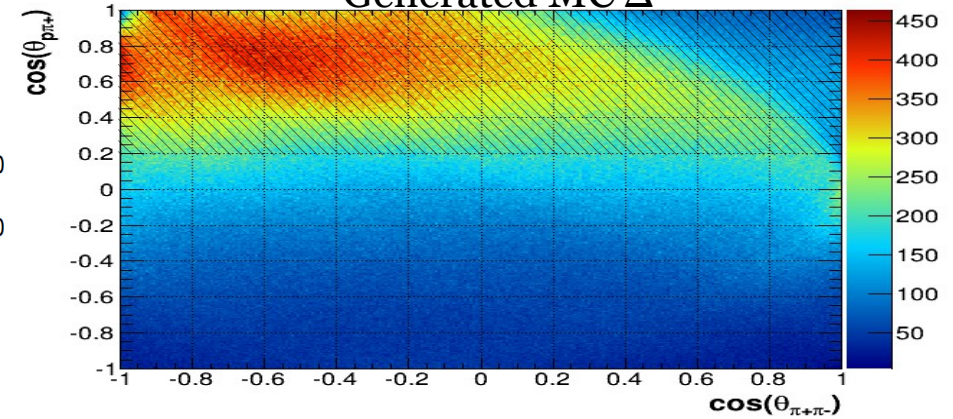
Before cuts



After cuts

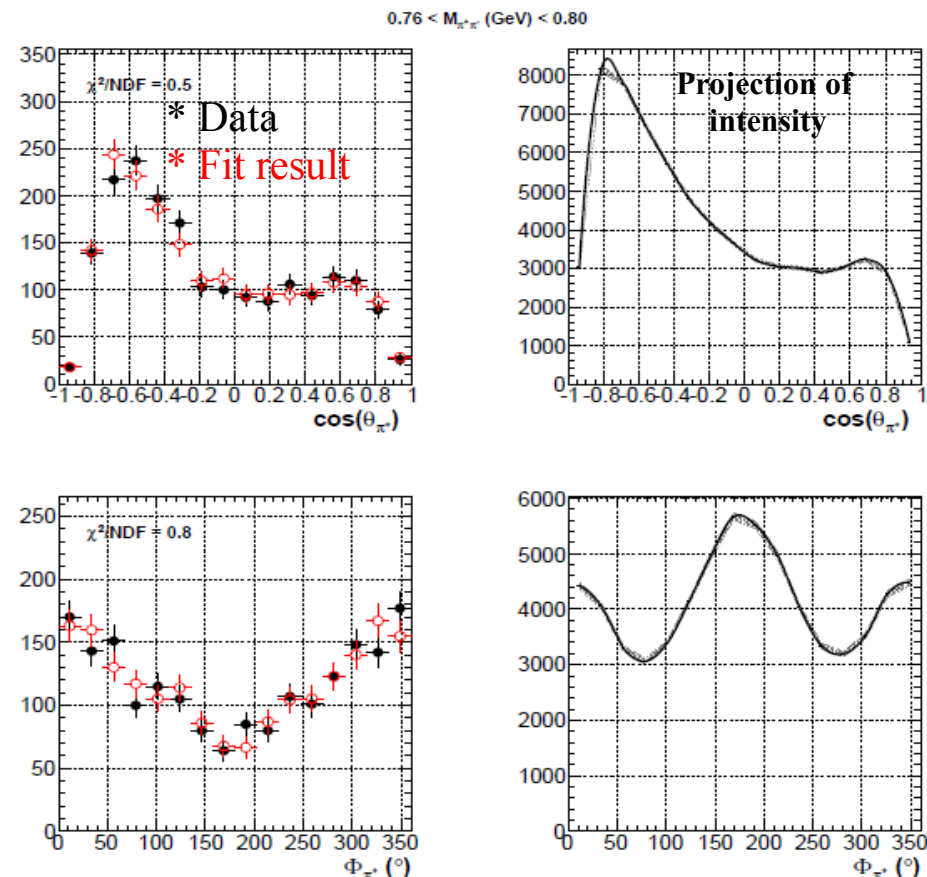
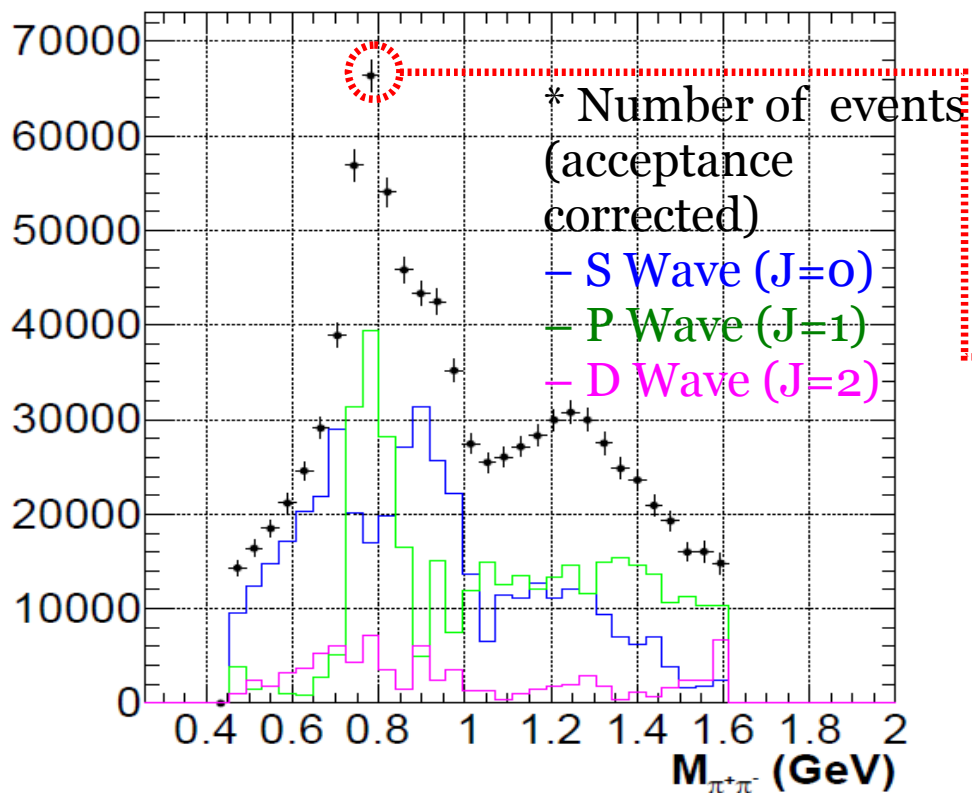


Generated MC Δ⁺⁺



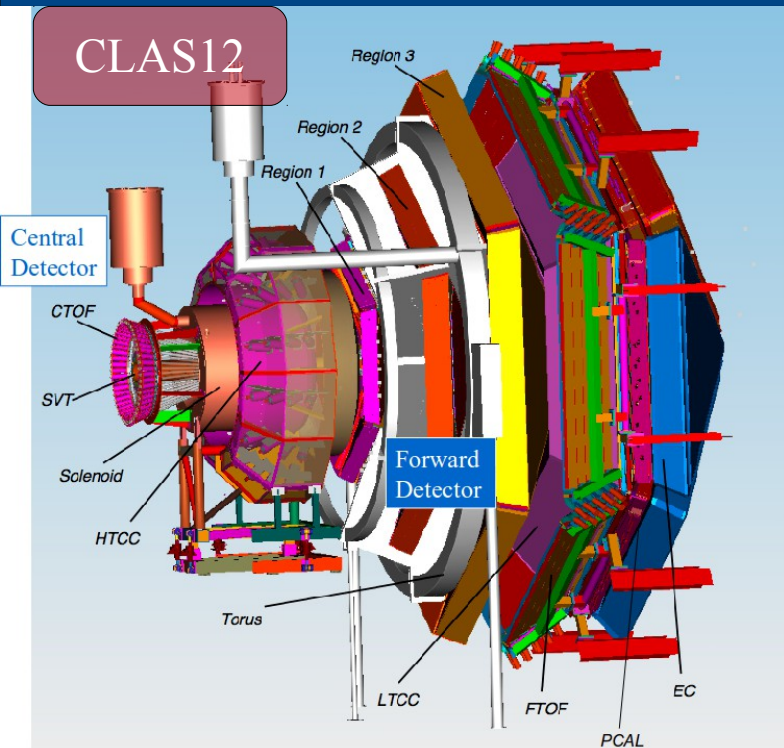
- The π⁺ from ep → eπN* → eππ projects onto an infinite set of spherical harmonics.
→ Kinematical cut to remove baryonic resonances
- In a first approximation, proton and π from baryon are collinear (cos(θ_{proton-π})=1), while ππ from meson are collinear.
cos(θ[proton-π⁺]) > 0.2
cos(θ[proton-π⁻]) > 0.2
- **Slight reduction of Δ⁰ and Δ⁺⁺ in the kinematical range considered**

PWA : results



- **Good agreement between 1D angular distribution from the fit and from the data**
- **Unsatisfying results :**
 - Not able to establish f_2 resonance in D-Wave.
 - Peak does appear in ρ (f_0) region in the P (S) wave, but does not have the proper resonance characteristics (mass, FWHM).
- Use of parity conserved amplitude basis may help ?

The Central Neutron Detector (CLAS12)



$$40^\circ < \theta < 120^\circ$$

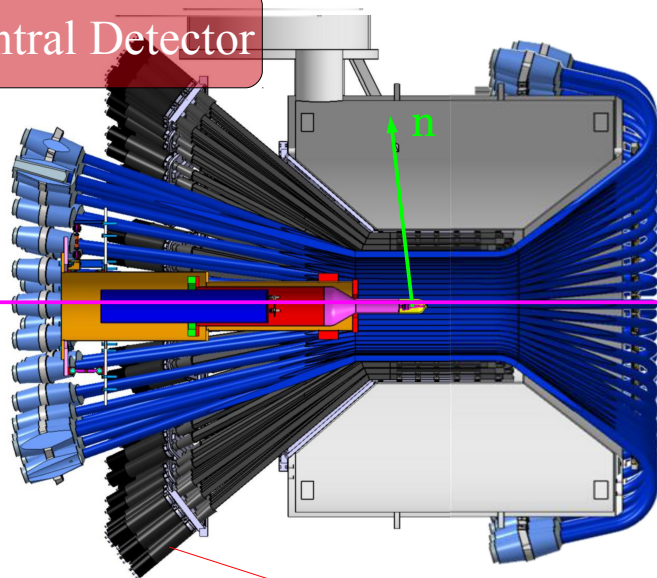
3 radial layers

48 azimuthal segments

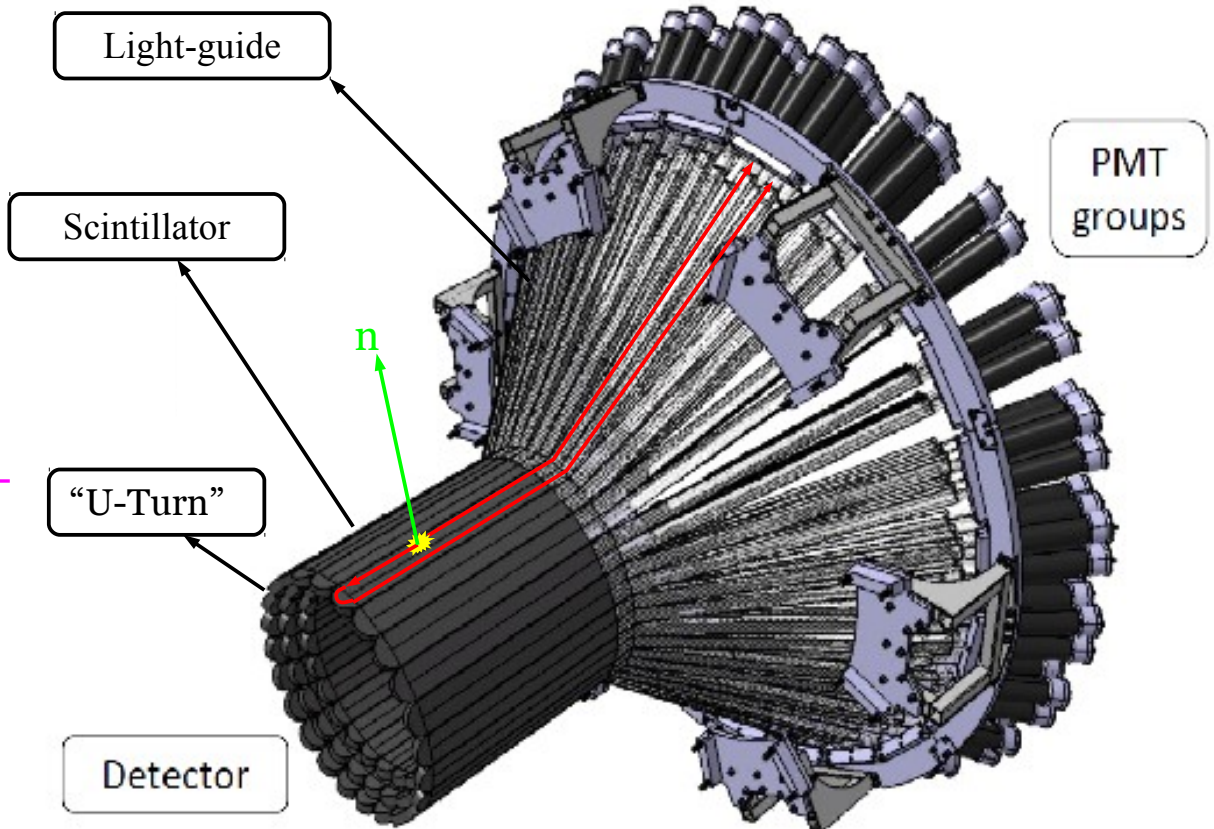
Read-out : 144 Hamamatsu R10533 PMTs

Time resolution ~ 130 ps (n/γ separation for $0.2 < p_N < 1$ GeV/c)

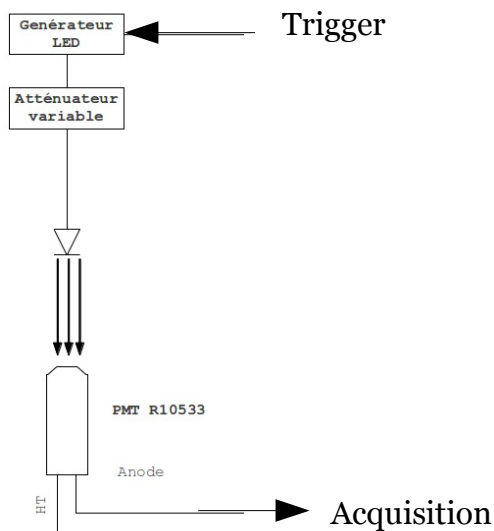
Central Detector



CND



PMT calibration



$$\text{Gain} \leftarrow G = \frac{I_k}{I_a}$$

I_k → Current of photoelectrons produced at the photocathode
 I_a → Anode current

- Gain measured from photoelectron emission spectrum:

$$G(V) = \frac{(\text{peak} - \text{ped}) \cdot \text{charge} / \text{ADC channel}}{G_{\text{preamp}} \cdot e \cdot N_{\text{phe}}}$$

V → Voltage
 $1.6 \cdot 10^{-19} \text{ C}$ → e
 N_{phe} → Nb. of emitted photoelectron at photocathode

- 144 PMTs calibrated.

